NASA TECHNICAL MEMORANDUM NASA TM-77558

METEORITE BOMBARDMENT AND DATING OF PLANETARY SURFACES

G. Neukum

Translation of: "Meteoritenbombardement und Datierung Planetarer Oberflaechen", (Dissertation on attaining Venia Legendi (tenure) in the Geophysics Department in the Faculty of Geological Sciences of the Ludwig-Maximilians University, Munich, West Germany, February, 1983, pp. 1-186.

NATIONAL AERONAUTICS AND SPACE ADMINISTRATION
WASHINGTON, D.C. 20546 SEPTEMBER 1984

STANDARD TITLE PAGE

1. Report No. NASA TM-77558	2. Government Accession No.	3. Recipient's Catalog No.
4. Title and Subtitle METEORITE BOMBARDMENT AND DATING OF PLANETARY SURFACES		5. Report Date September 1984 6. Performing Organization Code
7. Author(s) G. Neukum		8. Performing Organization Report No. 10. Work Unit No.
9. Performing Organization Name and Address Leo Kanner Associates, Redwood City, California 94063		11. Contract or Grant No. NASw-3541 13. Type of Report and Period Covered Translation
12. Sponsoring Agency Name and Address NATIONAL AERONAUTICS AND SPACE ADMINISTRATION, WASHINGTON, D.C. 20546		14. Sponsoring Agency Code

15. Supplementary Notes

Translation of: "Meteoritenbombardement und Datierung Planetarer Oberflaechen", (Dissertation on attaining Venia Legendi (tenure) in the Geophysics Department in the Faculty of Geological Sciences of the Ludwig-Maximilians University, Munich, West Germany, February, 1983, pp. 1-186

16. Abstract

The dating by measurement of impact crater frequencies is described, developed in the past 15 years primarily on the basis of the data from the missions to the Moon and Mars. The method allows us to obtain a good relative dating of surface structures of the Moon, planet Mercury and Mars, and the moons of Jupiter and Saturn through photographic analyses. A cratering chronology was obtained for the period between the oldest Moon crust (4.3 to 4.4 billion years) to the present time which gives a good absolute dating of any areas of the Moon's surface.

17. Key Words (Selected by Author(s))	18. Distribution Statement Unclassified-Unlimited		
19. Security Classif. (of this report) Unclassified	20. Security Classif. (of this page) Unclassified	21. No. of Pages 153	22. Price

Foreword

The first great contribution to the topic of this study came while I was employed at the Max Planck Institute for Nuclear Physics in Heidelberg in Professor-Doctor Gechtig's group. I should like to thank him for the support which he gave me and the working group, particularly the time of my transfer to Munich (in 1976/1977) to the Insitute for General and Applied Geology. There the planetological studies were continued under the direction of Professor Doctor Bodechtel, with considerable support from the German Research Association. I would like to thank Mr. Bodechtel particularly here for the encouragement which the planetology working group and I, myself, received in his Department for Photogeology and Remote Exploration and the Central Department of Geophotogrammetry and Remote Exploration. It was at that time that the main studies on the chronology of the development of the planet Mars were carried out by me in close collaboration with Doctor Hiller.

My transfer and that of the planetology work group (1981/1982) to the German Aeronautic and Space Research and Experimental Institute (DFVLR) e. V., Oberpfaffenhofen Research Center, was closely connected with my committment to the camera experiment of the Galileo-Mission (Jupiter orbiter and probe mission) which will give further improved data on the Jupiter system by the end of the decade. Part of the investigations on meteorite bombardment of the Galileo satellite of Jupiter were conducted in the framework of the preliminary studies for this project. I should like to thank DFVLR for supporting the subject; I should mention particularly the generous encouragement of my studies by Professor Doctor Lanzl, Director of the Institute for Optoelectronics.

I have been connected for a long time with the Institute for General and Applied Geophysics, especially because of common interests in the field of impact processes. I would like to thank here Doctor Pohl for the support which he gave me in the establishment of the scaling laws and for the careful examination of the manuscript.

I must acknowledge here, in particular, the commitment of my colleagues Doctor Hiller, Doctor Horedt, Mr. Nagel and Mrs. Eixenberger, who assisted me greatly in the establishment and completion of the manuscript.

The planetological studies carried out here would not have been possible without the generous support from NASA (Office of Space Science), the Federal Ministry of Research and Technology (BMFT) and the German Research Association (DFG).

TABLE OF CONTENTS

METEORITE BOMBARDMENT AND DATING OF PLANETARY SURFACES

G. Neukum

I. INTRODUCTION /1*

1.1. Importance of the Determination of Age in the Study of the Physical State and the Geological Development of Planetary Bodies

The physical state of a planet or its geological development may be determined by a number of methods and measurement procedures. These include, for example, physical measurement data from the field of altimetry, gravimetry or magnetometry, which were obtained in the planetary missions of the last fifteen years usually from orbits, or data on the heat flow, on petrography, chemical composition, radiometric age, etc.; which could be obtained by landing on the planet and measurements of the soils brought back to the Earth (or on meteorites).

The remote exploration photogeological study of planets compared to each other and the Earth is particularly informative with regard to the general determination of the physical state of the geological development. The determination of the geomorphological and stratigraphic relationships takes place by a procedure absolutely similar to that used on the Earth: the appearance of certain geomorphological forms allows conclusions to be drawn on their genesis and stratigraphic position. For example, it is thus possible to identify the appearance of volcanism, water, wind, impact events and tectonic processes. The formation of individual geomorphological forms is naturally determined in many cases by the physical characteristics of the planet, such as mass, surface gravitation, temperature, chemism, or in planets with an atmosphere, by atmospheric pressure and wind velocity. The comparative study of the physical state and the geological development of planets requires therefore in addition to the data obtained by remote exploration and geology, as many more further measurement data /2 as possible from the indicated areas to make the interpretation certain.

A special position in these investigations is assumed by the question of the progress in time of the development of a planet and the formation of its surface structures visible today. It is only possible to understand individual planetary courses of

---

*Numbers in the margin indicate pagination in the foreign text.

evolution by dating. Moreover an absolute statement regarding the age allows the calibration in time of the stratigraphic systems of planets obtained by photogeological methods. Finally all models of theoretical development of a planet depend directly on data on the age.

The direct radiometric dating has been possible so far only for the Earth, the Earth's Moon and meteorites through the direct access to rock samples and their study in the laboratory. A dating for the other planets (and also for the Earth's Moon taken as a whole) could only be carried out up until now by the above indicated remote exploration and photogeological methods, by determining the geomorphological and stratigraphic relationships and in particular by the measurement and interpretation of impact crater frequency.

The relative and absolute dating through impact crater frequencies has, in the last ten years, proven to be an increasingly justified and improved new method. The method is always applicable successfully, if a statistically sufficient number of impact craters can be obtained by image data. The imagewise recording of the surfaces of the terrestrial planets and the moons of Jupiter and Saturn showed that unlike the Earth, most of the other planetary bodies indicated (including the Earth's Moon) are much less molded by endogenous and exogenous processes (except perhaps for Venus), and in most cases we can see much further into the past when the impact rates and therefore the number of craters formed were much higher. Thus, measurements of the crater frequencies on the planets allow us to obtain in many cases a good relative and absolute dating of structures, which are billions of years old, quite unlike the Earth, where because of the great dynamics of development for these times, the data on age is very sparse and contains gaps. /3

The study of the crater population of the Earth's Moon along with the determination of radiometric ages on rock samples from the American Apollo Moon landing and the Soviet Luna Missions have given us an insight into the early history of the Earth-Moon system, the time of the intense meteorite bombardment about 4.5 to 3.8 billion years ago and the chronology of the early geological development of the Moon. With these missions and the following missions to the internal terrestrial planets Mercury, Venus, Mars and the large external planets Jupiter and Saturn, we have learned that almost all these bodies have undergone an early phase of high exogeneous and endogeneous activity, whose traces can still be identified and analyzed by us even today in large areas on the surfaces. We owe this new surprising finding to a great extent to the data of the camera experiments of the American planetary missions and the subsequent determination of the chronology of the meteorite bombardment and the geological development by the remote exploration and photogeologic evaluation and dating. Since we will receive no soil samples from other planets in the foreseeable future, the remote exploration methods

for dating and the investigation of the physical state and the geological development of the planets assumes considerable importance in the next few decades.

1.2. Impact Crater Frequencies as Images of the Meteorite Populations /4

Studies of the crater frequencies and their size distribution on the terrestrial planet and the moons of Jupiter and Saturn allow, besides the use for dating geological structures, information to be obtained on the impact rate of meteorites and their size distribution in the neighborhood of a planetary body. This relationship is obtained by the fact that for given velocities and given target material of a particular planet, a meteorite with a certain mass m produces a crater diameter D, which is in the first order a function of m. Thus the undisturbed frequency distributions accumulated on a surface exposed at a certain time until today provide direct images of the mass-velocity distribution of the meteorite population (each crater produced must be still identifiable, undestroyed today).

Assuming an average velocity and taking into account the target and projectile densities and the effect of the surface gravitation of the planetary body on the dimensions of the crater, crater diameter-frequency distributions can be converted directly into mass-frequency distributions of the causal meteorites.

But even without obtaining direct relationships between crater diameter and mass of the meteorites, crater diameter-frequency distributions are the function of the relative or absolute age of the target surface of the planet on which they have been accumulated, and can be used to analyze the mass velocity range of the causal meteorite as the function of time.

On several planetary bodies (for example, the Earth's Moon, /5
Mars, Mercury, Ganymede, Callisto) crater populations remain from the time of intense bombardment, about 4.5 to 3.8 million years ago until today. An analysis of these crater populations is rendered possible to us by the impact rate, their dependence on time and the diameter and mass spectrum of the meteorite populations, which had remained from the accretion phase[1] of the planetary body. Thus we can at least draw indirect conclusions about the accretion populations (populations of planetesimals) of the planets.

In the case of the Earth-Moon system it is possible to follow by investigations of crater populations a very different

---

[1] Phase of the building up of the planets from smaller bodies (planetesimals) about 4.6 billion years ago at the time of the formation of the Solar System.

age combined with absolute radiometric data, the dependence on time of the meteorite bombardment and the development of the mass spectrum of the meteorite from the time of the post-accretion phase of the Earth and Moon until most recently (a few million years). These studies represent a very important foundation for understanding the sequence of the meteorite bombardments in the internal Solar System and for the moons of Jupiter and Saturn. They represent a necessary base to interpret the chronology of the meteorite bombardment and the absolute determination of these by crater statistics with regard to the other planetary bodies, since their impact history is connected through the at least partly common meteorite populations and thus conclusions can be obtained only on the basis of extrapolation of the lunar data.

An important factor in the relative and absolute determination of age through crater frequency and analyses is the knowledge of the crater size distribution over a very large diameter range /6
and the dependence of the distribution in this diameter range on time, since in most of the cases, to date structures of different age or different size, crater frequencies can only be measured in different and often not overlapping diameter ranges. A comparison of the frequencies can then be carried out only on empirically or theoretically obtained distribution functions.

It follows from the previous arguments that the determination of the age of planetary structures through impact crater frequencies is closely related with the analysis of the development in time of the meteorite populations and their images, the crater populations and their diameter-frequency distributions, and practically a mutually connected analysis is needed.

1.3. Purpose of the Study

The purpose of this study is, on one hand, to provide the technical and methodical development of the relative and absolute dating through remote exploration methods, in particular through the analysis of meteorite bombardment (impact chronology) of the terrestrial planets and the moons of Jupiter and Saturn; on the other hand, the method is used for the relative and absolute dating of geological structures primarily of the Earth's Moon and the planet Mars, and provides a survey of the important events and their position in time in the geological development of these bodies. The discussion of the approach to the subject is to a great extent carried out on the basis of our own investigations, but also together with and compared with studies of other authors.

The method of determination of age through crater frequencies seems to be simple: impact craters, which are formed by meteorites (asteroids of comets) accumulate on a planet's surface. /7
The number of craters on an undisturbed noneroded surface increases

with the age of the surface, that is, the older the surface (the longer it is exposed to the meteorite bombardment), the more craters we will find. Crater frequencies (number/surface) of a stratigraphic unit of a planet provide us with a criterion of the relative age of this stratigraphic unit, while the crater frequencies divided by the average production rate provide us basically with the absolute ages (for example, Hartmann, 1973, 1977; Neukum and Wise, 1976).

In reality the method is very complex, since a basic prerequisite is in most cases not obtained for formation of the geological unit which was rapid as compared to the impact accumulation, and its further state of nondisturbance by other exogeneous and endogeneous processes. An analysis of crater frequencies usually requires an extensive photogeological interpretation and elaborate methods of counting and interpretation.

Concentrations of crater populations of the Moon as impact crater populations have alrady been published (i.e. Gilbert, 1893; Wegener, 1920, 1921). Nevertheless, the question of whether we are dealing in Moon craters with impact craters or volcanic craters was disputed for a long time (compare Baldwin, 1949, 1963) and was only decided recently without any further doubt with the Apollo Moon Landing in favor of the impact hypothesis (compare Taylor, 1975; Guest and Greeley, 1977). In the following years, with the missions to other planets and the high resolution photos of their surfaces, it became quite apparent that most of the craters on Mercury, Mars and most of the moons of Jupiter and Saturn are also impact craters. The arguments in favor of this were furnished by photogeological studies of the morphology and primarily by studies of the crater size distribution.

The dating of planet surfaces by crater frequency analyses in /8
their modern form has been applied since the fundamental studies of Öpik (1960) and Shoemaker et al. (1962), who on the basis of crater counts and theoretical analysis of impact rates of the Apollo asteroids[2] and comets (Opik) and analyses of terrestrial fossil craters (Shoemaker) came to the conclusion that the lunar maria (the seep regions which appear dark) are nearly 4.5 billion years old (assuming constant impact rate). This conclusion was not far from the age of about 4 to 3 billion years known today from the Moon soil analyses. Baldwin (1964) and Hartmann (1965) who arrived at ages of 2 to 3 billion years and 3.6 billion years achieved even better estimates. Even before the Apollo landings (which took place in 1969 to 1972) Hartmann (1966a) had found that the pre-mare bombardment of the lunar highlands must have been caused by an impact rate which was much higher (up to several hundred times) than the formation of maria at a later time.

---

[2] Asteroids crossing the Earth's orbit.

Unfortunately the method of dating was temporarily disputed by some authors, who shortly before the time of the Apollo landings revised upward the lunar impact rates (on the basis of only partly understood and misinterpreted meteoric data) resulting in the fact that the lunar age determinations were revised downward by a factor of 10 shortly before the Apollo landings.

Chapter IV is devoted to the question of the impact rate on the Moon on the basis of the results of the Apollo and Luna missions. While the impact chronology is today very well determined for the Moon, the discussions regarding the rates on other planets have lost nothing of their importance, but were recently the object of scientific controversies (compare Neukum and Wise, 1976, Neukum and Hiller, 1981, Basaltic Volcanism Study Project, 1981). But meanwhile an approach of the results of different authors has been agreed upon. Discussion of the situation and the state of the art for the terrestrial planet and the Moon of Jupiter and Saturn is the object of Chapters V to VIII. /9

Chapter IV.3 deals with the application of the Moon-impact chronology and dating of lunar geological structures, and gives the sketch of the chronology and stratigraphy of the Moon. Chapter V.3 deals with a similar obligation of the Mars impact chronology with the development of this planet.

An important basis for the relative and absolute dating is the knowledge of the crater size distribution over a very large range, and the relationship between the distributions of individual planets with each other and between their impact rates. The knowledge of the undisturbed crater size distribution on influence by endogenous or exogenous processes (production distribution) is particularly important in deriving the impact chronology of crater frequencies from different diameter ranges and the application of dating, and in analyzing multiple stage developments (for example, erosion, sedimentation, tectonics) of the individual geological regions.

The proper application of the production distribution is of fundamental importance in the procedure of dating through crater frequency. Moreover, exaxt analyses of the production distributions as a function of the age provide information on the development of the meteorite populations. These aspects are discussed in detail in Chapter III.

Chapter IX provides a comparative analysis of the early meteorite bombardment of the terrestrial planets and the moons of the large planets, which then lead to a general survey of the basic results of this study in Chapter X. /10

The following Chapter, Chapter II, will allow the readers to become acquainted with the planetary bodies which are discussed within the framework of the study. To this end a short survey is given of their surface structures and development.

II. SURVEY OF THE SURFACE STRUCTURES AND DEVELOPMENT OF THE TERRESTRIAL PLANETS AND THE MOONS OF JUPITER AND SATURN

To understand this study a brief survey will be given about /11
the planetary bodies discussed here. They all have in common a solid surface. Their geological history includes a wide spectrum and is partly fixed in the shaping of their surface and accessible to interpretation. According to their structure they may be roughly subdivided into:

a) the terrestrial planets Mercury, Venus, Earth, Mars and the Earth's Moon with average densities >3.3 g/cm^3 and

b) the satellites of Jupiter and Saturn with average densities <2.0 g/cm^3.

The Jupiter moons Io and Europa assume an intermediate position.

In studying the surface structures of the planets we can look back into the past to different extents. The component of primary, hardly differentiated surface decreases in the sequence moon, Mercury, Mars, Earth (Head et al., 1977).

Terrestrial Planets

The Earth's Moon

As our nearest neighbor the Moon was the first extraterrestrial planetary object of study of the scientists and the object of the first space missions, which peaked finally in the manned Apollo Landing Missions (in 1969 to 1972). Therefore, besides the Earth, the Moon is the best studied planet of our Solar System. From the available data on isotope ratios, chemical composition and age relationships, it may be derived that the differentiation of the Moon ended already very early, specifically about 4.4 billion /12
years ago. According to the general representation a crust rich in plagioclases arose from a cooling magma ocean (Wood et al., 1970). The genesis of this magma ocean, which had a minimum depth of 400 km, is highly dependent on the model. According to the splitting theory (compare Ringwood, 1950; Wise, 1966; Binder, 1974; Ringwood, 1979), the Moon was detached in the hot state from Earth. Particular geochemical data (Wänke, 1981; Wänke et al., 1983) favor among others such a common development of the Earth and Moon by splitting or co-accretion. In the case of a separate formation by accretion, the heating must have occurred predominantly by impact energy (Safronov, 1969, Kaula, 1980) and radio isotopes (Runcorn, 1977).

The Moon crust was exposed during its production and up to about one hundred million years thereafter to a heavy meteorite bombardment (compare Guest and Greeley, 1977; Taylor, 1975, 1982). This led to a close covering of the surface with impact craters of the most different size (Figures 1, 2). In this connection the topmost kilometers were destroyed, broken up and agglomerated, and the so-called Megaregolith was created (Hartmann, 1973). After this period of "heavy bombardment", which lasted up to nearly 3.8. billion years ago, the Moon was particularly active under the volcanic aspect for nearly one billion years. During this time the impact basins measuring up to 2000 km which had been produced during the intensive early meteorite bombardment ("heavy bombardment") were filled with basaltic lava. These "maria" imprinted on the front side of the Moon (Figure 1) arise very clearly with their low albedo against the anorthositic rocks of the older Moon highland forming predominantly the rear side of the Moon and part of the southern front side. The so-called lunar grooves are found predominately in the maria, but also in the highland. This term is mostly used with descriptive adjectives such as "sinuous" (twisted) or "arcuate" (arc-shaped) and designates valleys shaped in the form of canyons. The origin may be attributed partly to the tectonic processes /15
(trench ruptures) connected with the deposit and cooling of the lava but predominatly through lava erosion (lava channels) (Hulme, 1973). A form specific to maria is represented by the mare ridges, which may be several kilometers long, several kilometers wide and up to a few hundred meters high. We are dealing here either with arched surface layers, to whose summit magmas rose (Strom, 1971) or slipping ejections (Howard and Mühlberger, 1973). Unlike the Earth, the Moon is a "single plate planet" (Solomon and Chaiken, 1976) so that there are no plate tectonic forms.

During the last 2.5 billion years the Moon's surface does not show any geological activities, apart from extremely slight erosion processes and meteorite impact.

The Moon's surface has thus preserved the geological development during the early stage of the Solar System. As a result of the different Apollo and Luna Missions, we have very definite knowledge of the chemism and radiometric age of the soil samples taken from different points of the front side of the Moon. By remote exploration and statistical methods, these findings can also be extrapolated to the rest of the surface covered by photographs.

To determine a stratigraphic sequence, the large basins and some younger impact craters are suitable. Their ejecta are distributed over wide surfaces because of the low gravitation of the Moon and allow the classification in time through crater statistics. The Moon sequence contains the following eras, arranged from young to old, each time named for impact craters (Shoemaker and Hackman, 1962; Mutch, 1972; Wilhelms, 1983):

/13

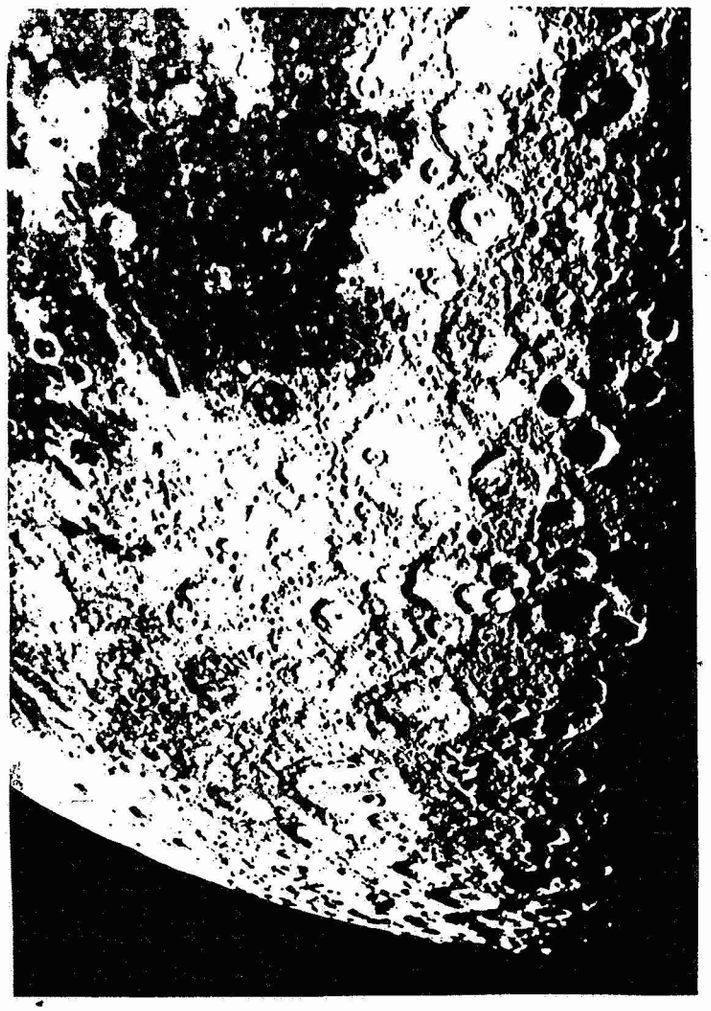

Figure 1a. Telescopic photograph of a part of the southern Moon highland of the front side and bordering (darker) mare region. In the central lower portion of the highland, the young radiating crater Tycho (D=85 km) may be seen.

Figure 1b. Telescopic photograph of a part of the front side of the Moon with extended (darker) mare surfaces. The top shows the edge of the Imbrium Basin; right underneath (on the left) the young craters Eratosthenes (D=60 km) and Copernicus (D=90 km) may be seen.

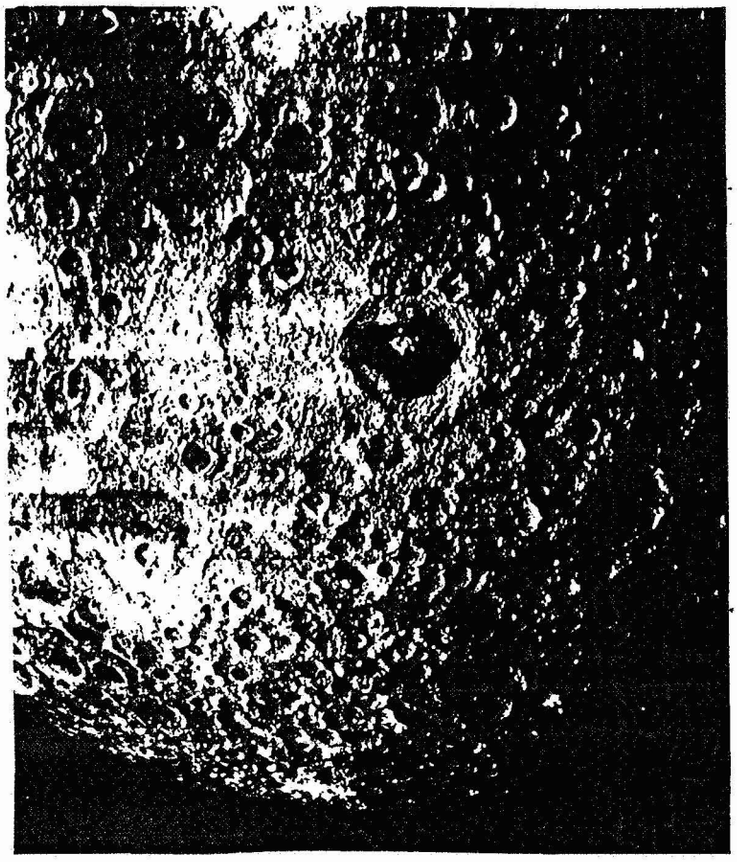

Figure 2a. Lunar orbital photograph of the Moon highland (southern portion) of the rear side of the Moon. Only very few of the younger large craters such as the Tsiolkovskiy Crater (center of the picture, D=160 km) are filled with mare basalt.

Figure 2b. Eastern basin of the Moon (D=1000 km, outermost prominant ring) and part of the dark mare filling of the Procellarum Ocean.

Copernican--Eratosthenian--Imbrian--Nectarian--Pre-Nectarian. /18

The exact classification in time of these ages is one of the topics of this study.

Mercury

The surface of Mercury is known about 40% from the photographs transmitted by Mariner 10. The planet seems to be very similar to the Moon (Figure 3a) which is surprising, since its size is between the Moon and Mars, and it has an average density comparable with that of the Earth of 5.4 g/cm^3. Naturally detailed investigations show that this impression is only caused by the dense crater layer (Strom, 1979). Thus extensive, probably volcanic levels between the impact craters lead to the conclusion that the planet was clearly more active during the "heavy bombardment" than the Moon. The several hundred kilometer long slips, which allow the conclusion of regional, probably also overall compression as a result of the contraction of the planet's circumference (Figure 3b) (Strom, 1979) are particularly important. The Caloris Basin (Figure 3c), an impact basin of about 1500 km diameter, seems to be filled with lava just like the lunar mare, and shows polygonally attached trench breaks and mare ridges.

Mars

As compared with the Moon and Mercury, Mars (Figure 4) shows a widespread diversity of geological formations (Arvidson et al., 1980; Carr, 1981). These results are partly from the presence of an atmosphere (95% CO_2, about 7 mbar surface pressure), which at the time when it was denser than today with more than or ≅ 30 mbar (McElroy et al., 1977) allowed water and thus erosion and deposition, as well as permafrost processes, partly from the much more /22
diversified and longer preserved volcanism and more intensive tectonic deformation of the crust (Wise et al., 1979; Greeley and Spudis, 1981). The most striking is a clear division into two (dichotomy) of the geological units in the rocks belonging to the early crust of the southern hemisphere and the younger volcanic layers of the northern hemisphere. They can be compared with highland and maria of the Moon. Here too the consequences of early heavy meteorite bombardment are maintained in the form of some impact basins such as the Hellas Basin and Argyre Basin (Figure 5a). In the transition zone, regressive erosion occurs over thousands of kilometers. Erosion valleys (Figure 6b) which start mostly from collapsed structures, or tectonic trenches, followed the route from the highland to the northern deep plains. The erosion causes are mainly flowing water, occasionally also ice/dust mixtures. Wind erosion on the other hand is mainly involved in the region of the polar caps.

/16

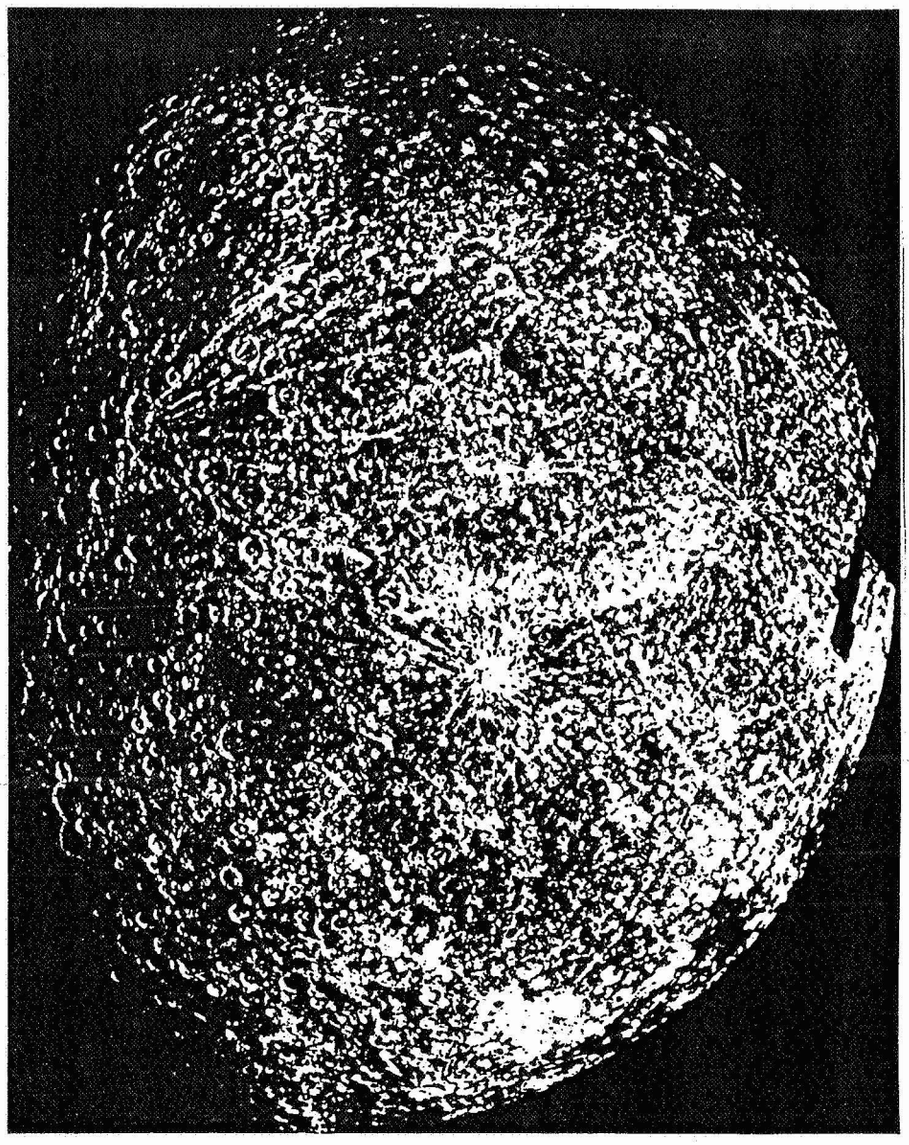

Figure 3a. Photomosaic of the Southern Pole region of the planet Mercury (Mariner 10 photograph).

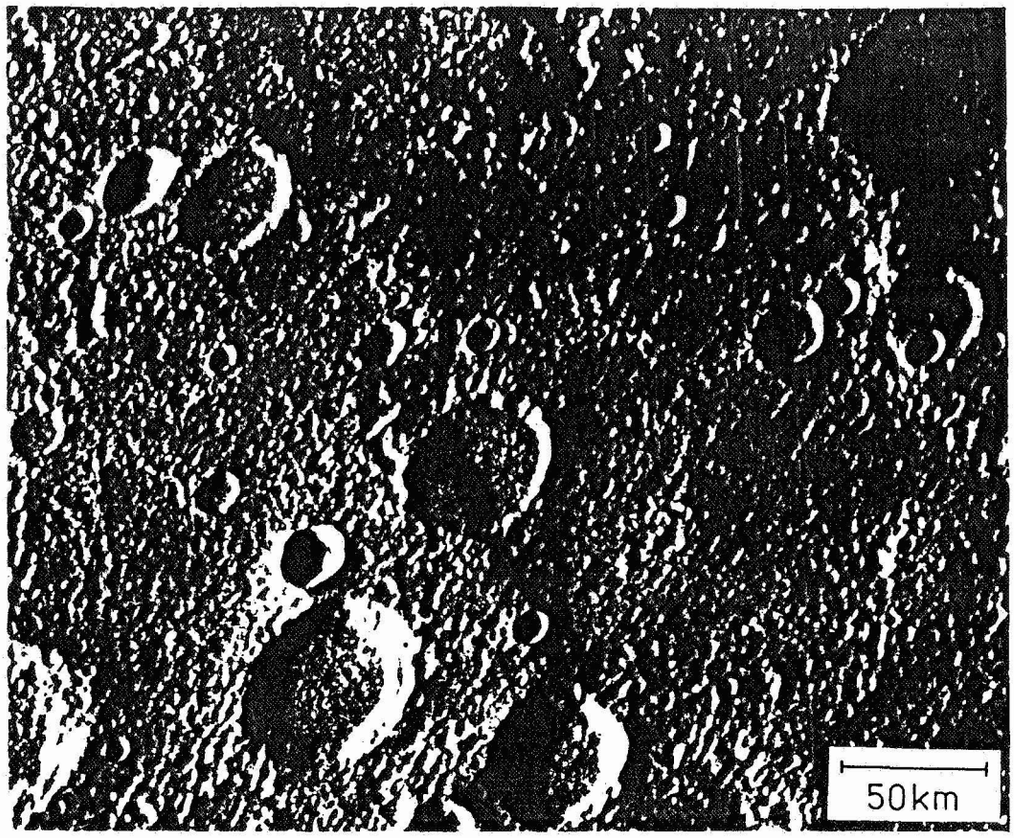

/17

Figure 3b. Part of the old Mercury highland with tectonic slip (Mariner 10 photograph).

At all degrees of latitude, especially the higher ones, so far no observed crater forms have been found on other planets, the so-called "splosh crater" and "pedestal crater" (Figure 5b). The ejecta layers of this crater seem to be formed in the shape of large flows, probably as a result of the meteorite impact in a permafrost soil. /22

A special diversity in geological formations is found in the Tharsis region. Twelve shield volcanoes, of which the highest one (Olympus Mons, Figure 6a) has an altitude of 20 km for a base diameter of 600 km, the largest (Alba Patera) several thousands of kilometers base diameter for only a few kilometers of altitude, stand in causal connection with a crust arching measuring about 10,000 km in diameter. Tharsis is also the center of the tectonic activity on Mars. Besides countless number of smaller break structures, we should mention particularly the Valles Marineris. This system of parallely running trench breaks connected with each other by transversal structures has a total length of about 5000 km for a maximum width of 160 km and a depth of up to 7 km. /23 The tectonically laid out Valles Marineris are transferred into the northern deep plains through a marked connecting alluvial

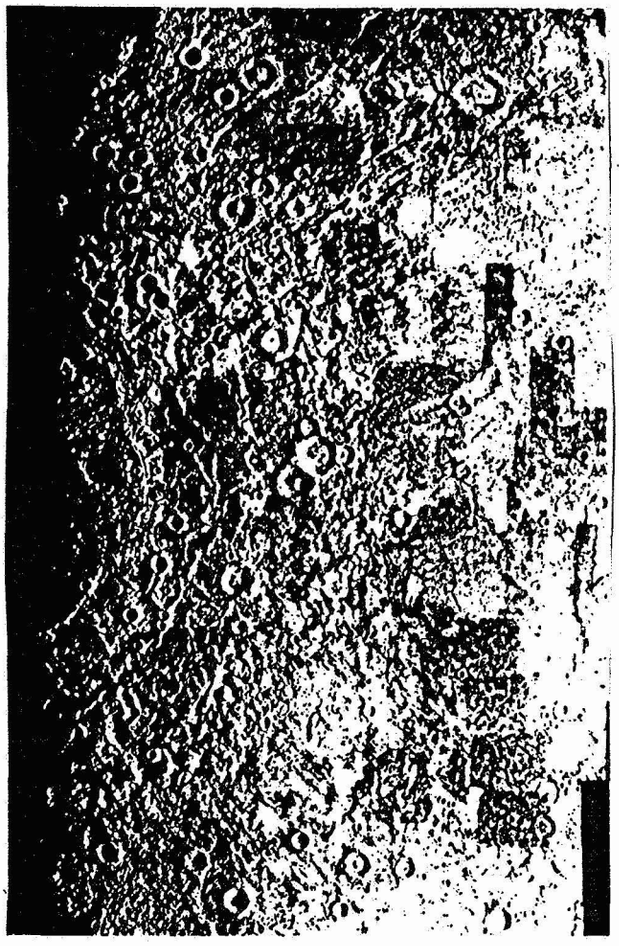

Figure 3c. Caloris Basin of Mercury (D=1300 km) with (probable) basaltic filling (Mariner 10 photograph).

system of valleys, the Tiu Valles.

A central problem for the classification of the different types of geological activities lies in the deduction of the age relationships. According to Mariner 9, 1972, in particular for deep plains, shield volcanoes and erosion valleys were considered very young formations (Hartmann, 1973; Soderblom et al., 1974). Later publications (Neukum and Wise, 1976; Hiller, 1979; Neukum and Hiller, 1981) show however that almost all the geological processes fall in one varying but limited period according to the age model. An exception is found in the Tharsis volcanoes, which apart from a few rest times, were active from the early history up till probably about one hundred million years ago (Neukum and Hiller, 1981; Hiller et al., 1982.

Venus

Venus is very similar to the Earth in size, density and orbit. Naturally apart from four point landings which have taken place up to now, because of the thick cloud layers of its atmosphere (CO_2, ≅90 bars pressure on the surface) it is accessible only by means of radar methods. At present only Earthbound radar pictures and conversions of the altitude radar of Pioneer Venus with very poor resolution (about 100 km), are available. It may be derived from the data that Venus has a very monotonous relief as compared with the Earth (Masursky et al., 1980). 70% of the surface is covered by hilly terrain, 20% deep plain (-2 km) and 10% highlands (+2 to +12 km) (Figure 7). Highland similar to the Earth's continents, Aphrodite Terra and Ishtar Terra project, and have their peak at Maxwell Montes (12 km in height).

It was impossible to answer up to now finally the question about the presence of a kind of plate tectonic, although a large number of arguments would favor it (compare Solomon and Head, 1982; Meissner, 1983). It is only apparent from existing /25

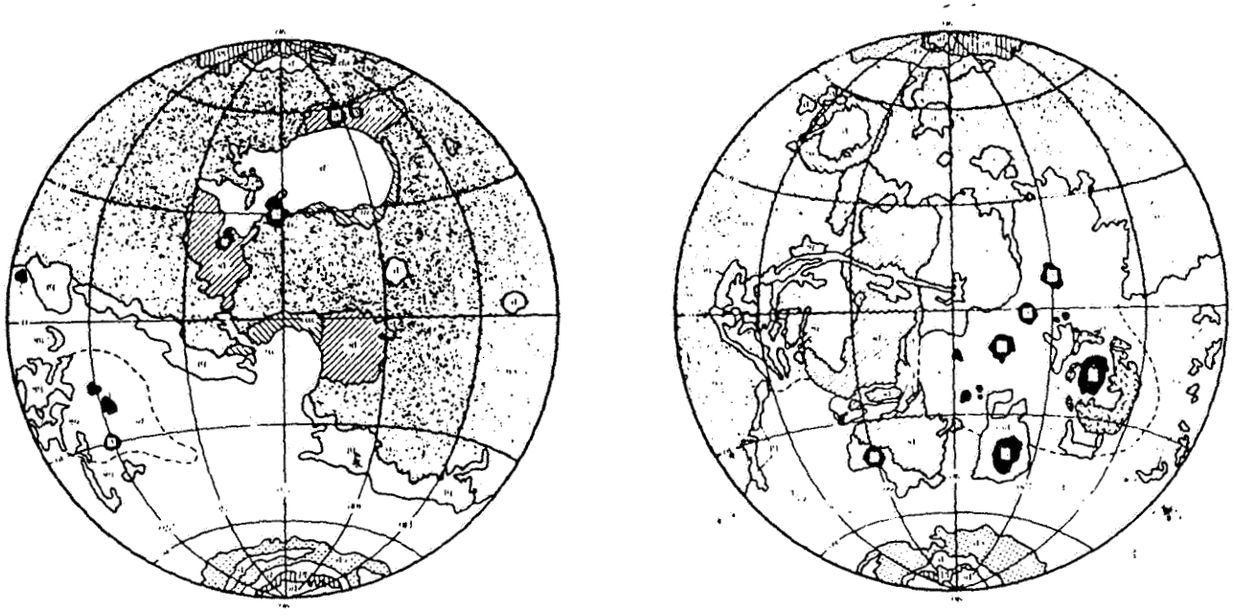

Figure 4. Simplified geological map of the planet Mars (Mutch et al., 1976)

Polar geological units:	pi(permanent ice); ld (layered deposits); ep (etched plains).
Volcanic geological units:	v (volcanic constructs); pv (volcanic plains); pm (moderately cratered plains); pc (cratered plains).
Modified geological units:	hc (hummocky terrain, chaotic); hf (hummocky terrain, fretted); hk (hummocky terrain, knobby); c (channel deposits); p (plains, undivided) g (grooved terrain).
Old geological units:	cu (cratered terrain, undivided; m (mountainous terrain).

/20

Figure 5a. Argyre Basin of the planet Mars (D=750 km) (Viking photograph).

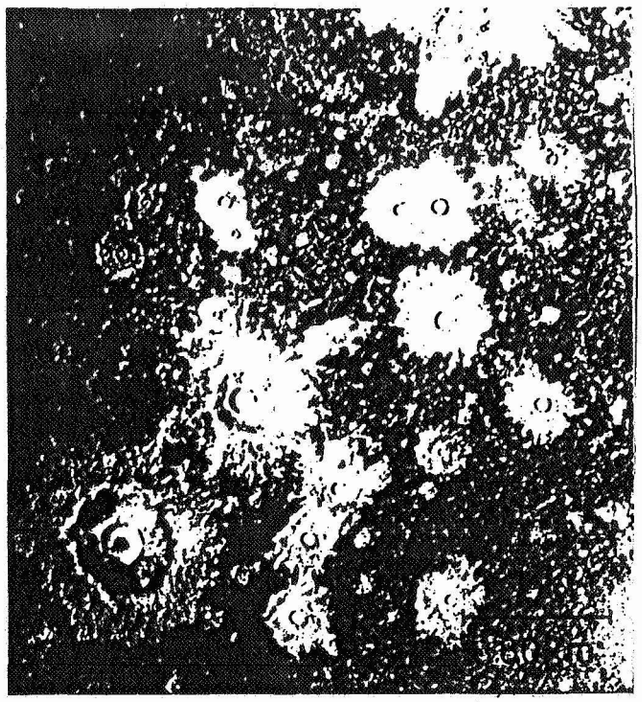

Figure 5b. "Pedestal" and "splosh" craters (Viking photograph).

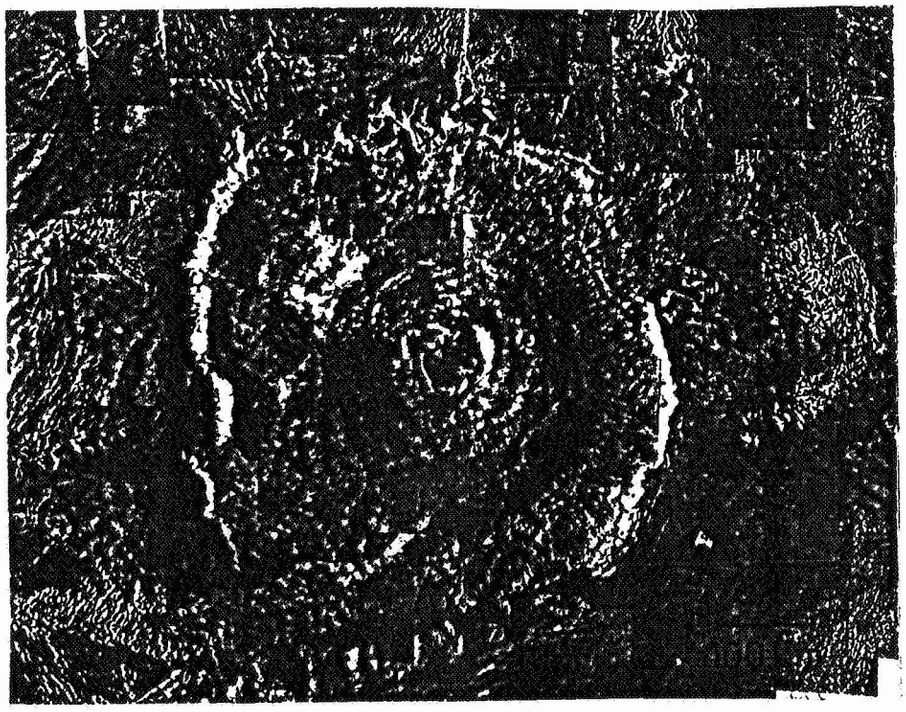

/21

Figure 6a. Mars--shield volcano Olympus Mons (Viking photomosaic).

Figure 6b. Kaser Valleys (erosion valley) of Mars (Viking photomosaic).

Figure 7. Radar map of Venus: (Pioneer Venus Mission) Mercator projection, 1:50 million at equator. The colored stages correspond to 1 kilometer difference in altitude in the region between 5 and 12 km and 0.5 km difference in altitude in the region between -2.5 and 5 km.

data material that Venus was or still is tectonically or volcanically active and has a complex geological history (Masursky et al., 1980). Round hollow shapes are interpreted as impact craters (Schaber and Boyce, 1977) but have not been confirmed. Within the framework of this study therefore these possible existing crater populations were not discussed. /25

Earth

We will not discuss further the geology of the Earth within the framework of this study. It should only be indicated that the planetary geology must work very strongly with photographic interpretations and conclusion by analogy. A basis for this is the knowledge acquired with field geology and classical photogeology.

A strong interrelationship with the Earth's geology and geophysics is found in particular in the exploration of meteorite impact on planetary surfaces. On the Earth as a result of intensive superimposition of the crust only a few craters have been preserved, especially on the high shields, mostly in poor state (Grieve and Robertson, 1979; Grieve and Dence, 1979). Detailed investigations could therefore be carried out in particular on some young and therfore hardly deformed craters. From the abundance of studies, we may select as representative the publications of Shoemaker (1963) on the Arizona-meteorite crater and Pohl et al., (1977) on the Nördlinger Ries. These results fit into the interpretation of the impact process from the other planets and represent an important data basis for the comparative analysis.

Galileo Moons /29

The four largest moons of Jupiter discovered already in 1610 by Galileo (Figures 8a--d, Table 1) reflect in a certain way the conditions in the Solar System (Smith et al., 1979). Just the average density of 3.5 g/cm^3 is found in Io with the "terrestrial" structure, over 3.0 g/cm^3 for the ice covered Europa, up to 1.9 and 1.8 g/cm^3 respectively for the "ice" satellites Ganymede and Callisto.

Io (Figure 8a, 9a) is the only geologically active satellite of the Solar System known so far with a countless number of volcanoes, of which eight were active at the time of the flight which passed by them. Sulphur and SO_2 droplets emerge at velocities of 300 to 1000 m/s and form fountains reaching up to 280 km height. The total surface is covered with a layer of sulphur and SO_2 snow. The color scale includes zones from black, red to orange and yellow up to white. The energy required for heating the body is produced probably through an orbital resonance

TABLE 1. PHYSICAL DATA ON THE INTERNAL SATELLITES OF JUPITER AND SATURN (Smith et al., 1979, 1982). /26

	Orbit (10^3 km)	Radius (km)	Mass (kg)	Average Density (g/cm^3)	Maximum image resolution (km/line pairs)
Jupiter Satellites					
Amalthea	181	270x165x150	?	?	8
Io	422	1816	8.9×10^{22}	3.5	0.5-1
Europa	671	1563	4.9×10^{22}	3.0	4
Ganymede	1070	2638	1.5×10^{23}	1.9	1
Callisto	1880	2410	1.1×10^{23}	1.8	3
Saturn Satellites			(10^{20} kg)		
Mimas	186	196	3.8	1.44 ± 0.18	2
Enceladus	238	250	7.4	1.2 ± 0.4	2
Tethys	295	530	63	1.21 ± 0.16	2
Dione	377	560	110	1.43 ± 0.06	3
Rhea	527	765	230	1.33 ± 0.09	1
Titan	1222	2575	1400	1.88 ± 0.01	1
Hyperion	1481	205x130x110	11	?	9
Iapetus	3560	730	190	1.16 ± 0.09	17
Phoebe	12954	110	?	?	38

/27

Figure 8a. Jupiter's moon Io (Voyager photograph) with active volcano (center of the figure).

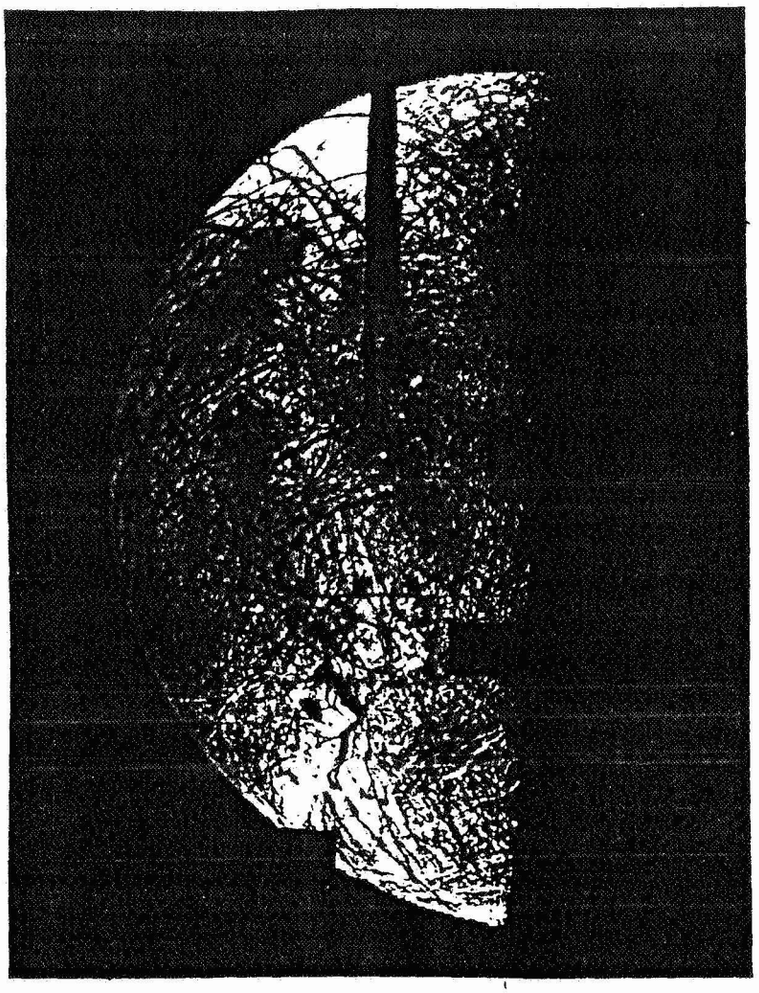

Figure 8b. Jupiter's moon Europa (Voyager photomosaic) with break structures.

/28

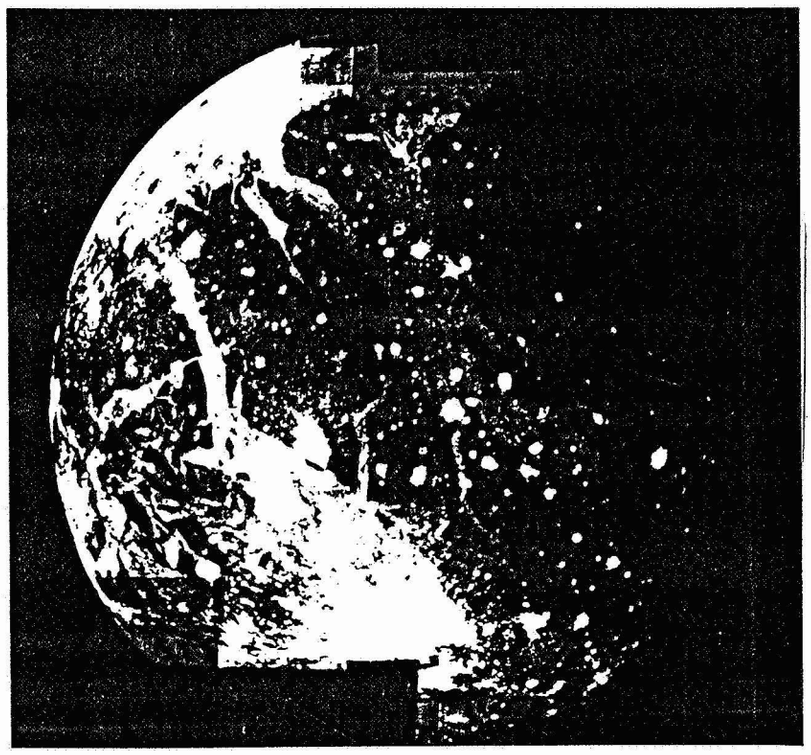

Figure 8c. Jupiter's moon Ganymede (Voyager photograph) with old (dark) and younger (bright) crusts.

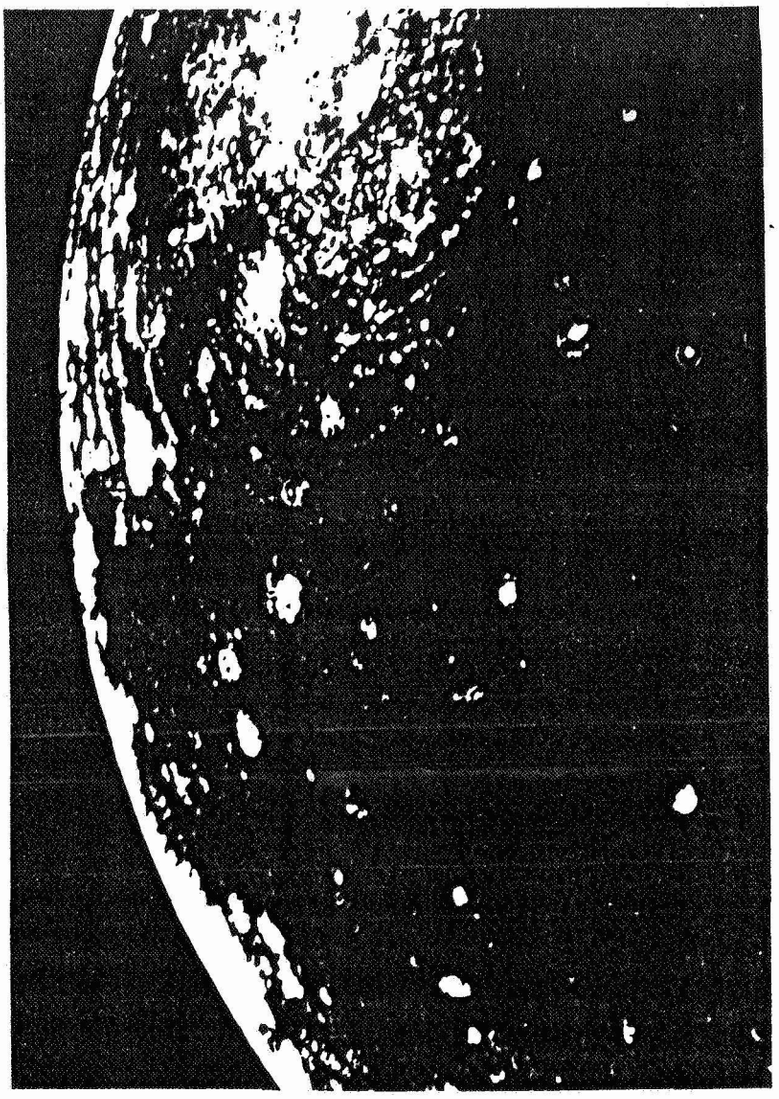

Figure 8d. Jupiter's moon Callisto (Voyager photograph) with Valhalla ring basin (D=600 km).

with the neighboring moon Europa, which leads to a slight orbital eccentricity of Io and a tidal friction arising because of it in the intense gravitation field of Jupiter (Peale et al., 1959). An alternative explanation of the heating of the moon Io was given by Ness et al. (1979): through electromagnetic interaction of Io with Jupiter's magnetosphere, currents of about $5 \cdot 10^6$ A flow between Jupiter and Io, which may lead to joule heating of the moon, of an order of magnitude of 10^{12} W.

Europa (Figure 8b, 9b) consists of silicate rocks with an ice mantel 20 to 150 km thick according to the model. The ice surface is characterized by a dense structure of rupture forms of the most different type and size. Probably we are dealing here with slip systems torn open by slight increase of volume in the satellite, and which are "healed" once again with the ascending water. Larger impact craters were not found at least on the part of the satellite accessible to interpretation. This leads to the conclusion of a relatively late stabilization of the ice crust.

/30

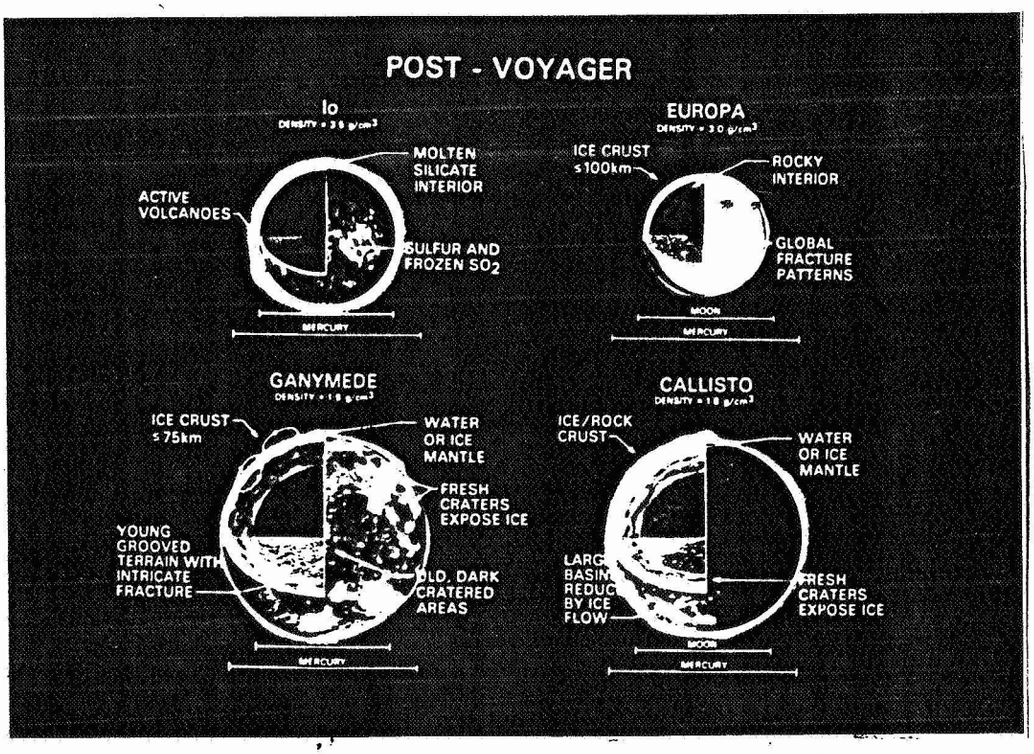

Figure 9a--d. Models of the internal structure of the Galileo satellites of Jupiter on the basis of Voyager results. (Figure: NASA--JPL).

Ganymede (Figure 8c, 9c) the largest of the Jupiter satellites, has just like its neighbor Callisto, a low density, which shows that it has a mixture of approximately half water ice and silicates. The surface is divided into dark areas densly covered with craters and brighter regions in between, broken up several times and split up. /31

In the old dark regions, so-called palimpsests appear as very large, bright, round surfaces. It is assumed that we are dealing here with very old impact craters, whose crater walls and bottoms were leveled by gravitational compensation in the plastic ice. The original crater diameter may generally be reconstructed and thus a crater distribution can be determined even for the oldest regions. The interior of Ganymede is assumed according to the model to be a silicate core and water or ice mantel and ice crust.

Callisto (Figure 8d, 9d) has a single-shape dark surface very densely covered with craters. Young impacts are mostly ejected star-shaped bright ice from the background. Except for a few impact basins (Valhalla, D=600 km diameter) all craters are <150 km in diameter. The interior of Callisto may be assumed according to the model to be identical to Ganymede, or consists of an undifferentiated mixture of ice and silicate.

Saturn's Moons

At present 17 moons of Saturn are known, which are partly in the region of the ring system (Figure 10 a-d, Table 1). All of them consist of a body of ice/silicate mixture with an average density, which is partly very close to that of pure water ice (Smith et al., 1981, 1982). They can be subdivided, leaving out Titan which is covered by a dense atmosphere, according to /32 their surface forms into a) undifferentiated ice/silicate bodies (Mimas (Figure 10a), Rhea (Figure 10b), Hyperion) and b) differentiated bodies (Tethys (Figure 10c), Enceladus (Figure 10d), Dione). Iapetus and Phoebe cannot be classified clearly here.

a) undifferentiated satellites: their surfaces are uniform and covered very densely by large impacts. Signs of endogenous activity such as tectonic formation or albedo differences, indicating geological units of different compositions, were not found. It may be derived from both observations, that in these satellites a differentiation if it had existed at all, ended very soon after formation.

b) differentiated satellites: the common characteristics are several surface units, which differ by different albedo and impact crater densities. Further indications of endogenous activities include mostly tectonically produced formations such as trough falls.

Enceladus may be mentioned as the geologically most interesting Saturn satellite.

Enceladus: 5 surface units may be clearly differentiated on the basis of crater density, texture and relief (Smith et al., 1982). Since the youngest geological unit has no impact crater at least with the maximum resolution of 2 km/line pair, the conclusion is drawn that there were several periods of activity in the development history of the moon. The energy required for the endogeneous activity is most probably obtained from a rarely occurring resonance with Io. A heating of the satellite by tidal friction would with this hypothesis not be a continuous process as the one in the Jupiter moon Io, but would take place only at very large intervals. Thus the vicinity of units of very different age on such a small body could be explained. /33

/34

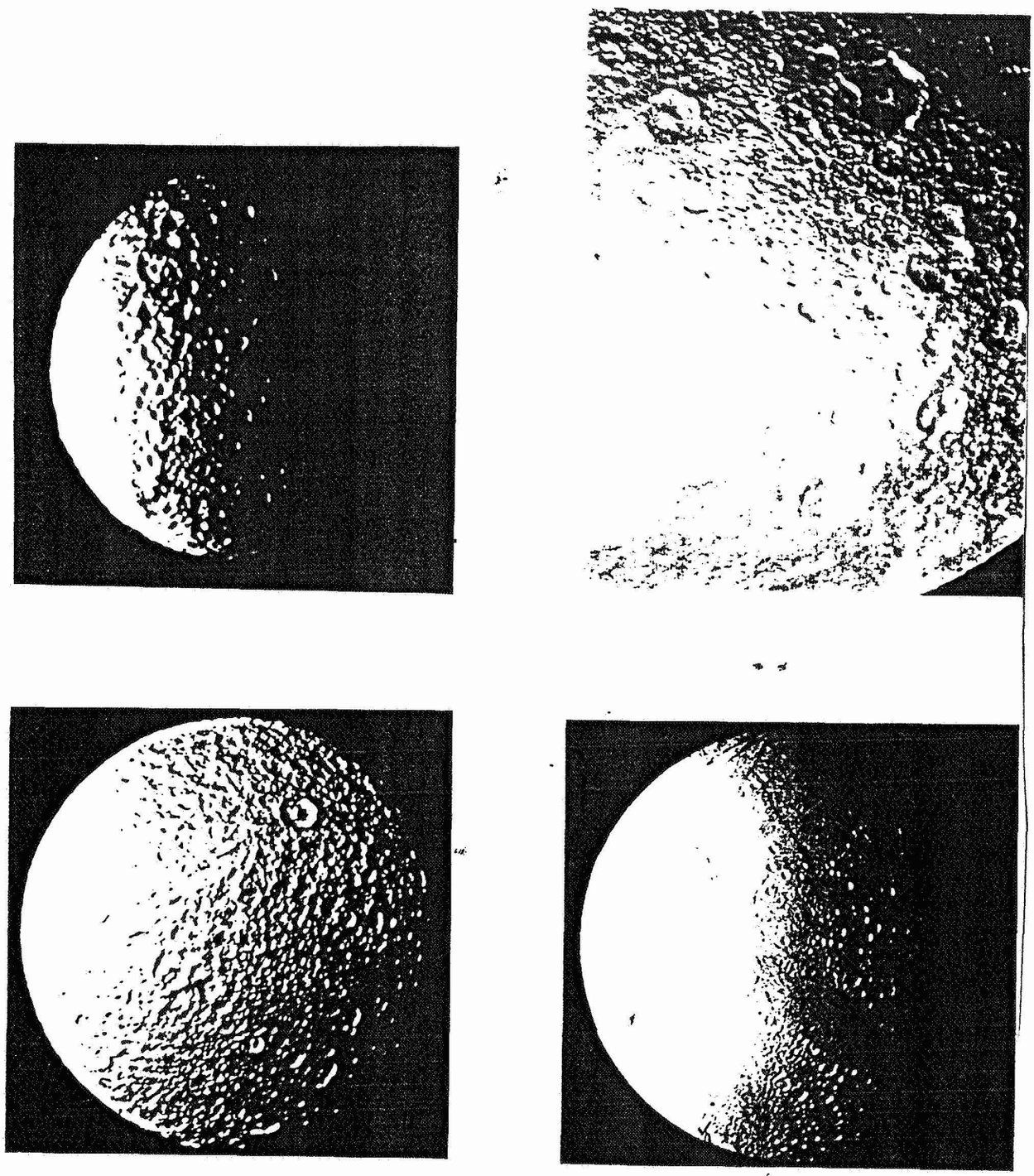

Figure 10. Saturn's moons, Mimas, Rhea, Tethys and Enceladus.

III. METHOD OF ANALYSIS OF IMPACT CRATER-FREQUENCY

III.1. Data Recording and Data Reduction

To analyze the impact crater populations, photographic and mapping material with sufficient spatial resolution is required, making it possible to obtain at least a rough photogeological interpretation and to measure statistically significant numbers of craters in the regions concerned. The photographic and map material available today is of very different type and quality and can be used only to a limited extent. /35

III.1.1. Type of Photographic Data and Map Material

The best spatial resolution and superficial coverage was obtained so far from the Earth's moon through the Lunar orbiter and Apollo Mission and on the planet Mars with the Mariner 9 and Viking Missions, since we have a planetary orbiter with long duration of the mission. In all other cases (planets Mercury, Jupiter's and Saturn's moon), up to now data were only obtained from flying past them (except for radar coverage through the Pioneer Venus Orbiter) with very different geometry, resolution, surface coverage and illumination. Therefore the main limitation is that the photogeological interpretation of the photographic data cannot be achieved with the same quality and crater populations can only be studied in different amateur regions and are thus not directly comparable. A summary of the planetary photographic and map material available today may be found in the study by Cameron and Vostrey (1982).

III.1.2. Image Data Processing /36

The planetary photographic material occurs in most cases as a rectified photo. In the case of the data on the Jupiter moon (Voyager Mission) however, rectification and mosaic formation (combination of individual images into photomaps) of the images had to be carried out. In addition in these cases usually image improvements were carried out, such as, for example, sharpening of the edges (high pass filtering).

To interpret the different geological units, increases in contrast and color extensions were carried out in part.

III.1.3. Image Analysis and Data Reduction

To achieve usable results, these data must be obtained on surfaces which have at least been roughly mapped under the photogeological aspect. The basic prerequisites are (compare

Neukum et al., 1975a; Hiller, 1979; Neukum and Hiller, 1981):

--selection of the most homogeneous possible regions (geological units), since mixed ages result in ambiguity of the crater size distribution;

--evaluation as to whether all craters are really located on the surface considered, that is, were formed during the exposure of this surface or must be assigned to an underlying and therefore older series;

--analysis of the erosion states of the region or the crater population (small craters can be eliminated);

--elimination of secondary and volcano craters; /37

--exact determination of the area to be covered;

--exact measurement of the edge diameter of the craters.

The data used in this study were obtained monoscopically or stereoscopically with digitization equipment and processed by computer. To compare with our own data and as a supplement data published in the literature by other authors were also partly analyzed. This took place in most cases by predigitalization of these data, if available in diverse form, or if in tabular form, by direct use and assignment to the size screen used as basis here, applying the suitable distribution function corresponding to the relevant studies.

III.2. Relationship Between Crater Production Distribution and Crater Retention Age

The crater populations on the planets are, in the first approximations, a reflection of the mass-velocity distribution of the meteorite populations causing craters[1]. Some quantitative relationships will be obtained below (compare Neukum et al., 1975).

Assuming a certain average velocity, a meteorite population of mass distribution n(m,t) produces in the mass interval (m,m+dm) a crater frequency distribution n(D,t) in the diameter range (D,D+dD) for a certain time of exposure t. The function n(D,t) will be called differential distribution (number per area per diameter at the time t). The relationship between the differential frequency and differential impact rate (number per area per /38

[1] The term meteorite is used hereafter generally for all impact bodies which can produce craters, independently of the size or nature (for example, asteroid, comet, etc.).

diameter per time at the time t) is given by:

$$n(D,t) = \int_0^t \varphi(D,t')dt' \quad .$$

The time t gives the exposure time for the age of the crater population (t>0).

The cumulative crater frequency N(D,t) (number per area of all craters greater than or equal to the diameter D which have formed during the exposure time t) is given by

$$N(D,t) = \int_D^\infty n(D',t)dD' = \int_D^\infty \int_0^t \varphi(D',t')dD'dt'.$$

The cumulative impact rate $\phi(D,t)$ is given by

$$N(D,t) = \int_0^t \phi(D,t')dt'$$

or

$$\phi(D,t) = \partial N(D,t)/\partial t$$

The function $\phi(D,t)$ can be divided into the function g(D,t) which represents the basic size distribution law, which can also be variable in time, and the function f(t) representing the general dependence of time. Therefore, we may write

$$\varphi(D,t) = g(D,t) \cdot f(t)$$

or

$$\phi(D,t) = \int_D^\infty g(D',t)f(t)dD' = G(D,t) \cdot f(t)$$

If there is no direct dependence on time of the distribution law, the function $\phi(D,t)$ can be separated into $\phi(D,t) = g(D) \cdot f(t)$ /39

$$\varphi(D,t) = g(D) \cdot f(t)$$

and

$$n(D,t) = g(D) \int_0^t f(t')dt'$$

or

$$n(D,t) = g(D) \cdot F(t),$$

where $$F(t) = \int_0^t f(t')dt'.$$

The cumulative frequency is obtained as

$$N(D,t) = \int_D^\infty \int_0^t g(D')dD' \cdot f(t')dt'$$

$$= G(D) \cdot F(t).$$

Such crater populations which could have formed during the period of exposure of the surface in an undisturbed way as an image of the mass-velocity distribution of the meteorite and whose accumulation took place in such a way that no mutual superimposition of the craters with mutual elimination took place, are called population in the production state and their frequency distribution, distribution in production or for short "production distribution".

Assuming isotropic flow and disregarding a possible target effect and assuming the production state, the crater frequency $n(D,t)$ and $N(D,t)$ of surfaces of a planet exposed for an equally long time with the same diameter D are measured equal over the entire surface. The frequencies, which are measured on surfaces of a planet of different age with diameter D, are different with regard to the time functions, that is,

$$N_1(D,t_1)/N_2(D,t_2) = F(t_1)/F(t_2) = C. \qquad /40$$

Each cumulative crater frequency N_i of a planet differs from another crater frequency N_k only by factor C_{ik}, which depends only on the corresponding exposure ages t_i and t_k of the surfaces on which N_i and N_k accumulated and depending on the diameter only through the distribution function G(D). The same applies for the differential crater frequency.

From this relationship it is possible to indicate a mutual relative age position of the geological units on which the crater frequencies have been measured. The crater frequency $N \sim F(t)$ for a fixed D can be taken directly as the criterion for the age. This age is designated here as the relative crater retention age (compare Hartmann, 1966b; Neukum and Hiller, 1981) and refers generally to a certain diameter. Here, usually, relative crater retention ages are indicated equivalent to the frequency N(D=1 km) or N(D=10 km) per km^2.

The designation crater retention age was used by some authors (compare Hartmann, 1966b; Basaltic Volcanism Project, 1981) as a synonym for all the absolute ages t obtained from crater measurements using the known relationship $N=G(D) \cdot (F(t)$, while in this case we speak of an absolute crater retention age or crater model age ("cratering model age").

III.3. Different Representations of the Crater Frequency Size Distribution

Crater frequencies may be found in the literature in different representation, specifically in the discussed cumulative and differential representations as well as in the form of incremental or relative frequency (see 3.3 and 3.4). This use of different /41
methods made it difficult in the past to compare with each other data from different authors. This problem was acknowledged and discussed by the scientific community, with the result that for different applications certain methods are recommended (Arvidson et al., 1978). It may be stated generally that cumulative representation offers advantages for determining age, rate of distribution for study of the distribution law, and the differential distribution to study the crater populations disturbed by multiple stage development or other processes. The incremental distribution was not recommended. A summary of the relationships and reasons is given below.

III.3.1. Cumulative Distribution

The cumulative distribution $N(D,t)$ given already in the previous paragraph was discussed by Öpik (1960) as the distribution which is particularly suitable for use in the problem of comparing two crater frequencies, especially for the purpose of determination of the relative age (= crater retention age). The advantage of the cumulative distribution is in particular that even for small numbers of craters it is quickly stabilized in its statistical area, since through the integration over the diameter

$$N(D,t) = \int_D^\infty n(D',t)dD' = \int_D^\infty g(D')dD' \cdot F(t)$$

all craters of diameters larger than D are included in the counting.

The cumulative presentation of the data naturally has a drawback, that it includes all the errors or numerical fluctuations for large craters because of summation. The exponential nature of the distribution however, attenuates quickly enough the effect of the large crater on the frequencies of the lower limit D toward smaller diameters. It is shown practically that even for /42
highly disturbed distribution fluctuations for large craters

come out mostly to not more than 20 to 30% at the lower limit. The cumulative distribution is naturally relatively insensitive as compared with the differential distribution n(D,t) with regard to a variation of the diameter-distribution law. When using the crater frequencies for dating purposes, however, the known already measured production distribution is taken as basis, which is approximated as calibration or standard distribution (compare Neukum and Wise, 1976) of the data, and through which the measured crater frequencies are refered to a crater diameter suitable for relative age comparison. The cumulative distribution of a relatively undisturbed crater population is shown in Figure 11a. The statistical error ($\sqrt{N}$) becomes quickly smaller by summation over all the large craters and through the exponential nature of the distribution.

The stage width of the lower limit is chosen here and in the entire study in such a manner (compare Neukum and Miller, 1981), that 18 intervals in D are inserted per decade (1; 1.1; 1.2; 1.3; 1.4; 1.5; 1.7; 2.0; 2.5; 3.0; 3.5; 4.0; 4.5; 5.0; 6.0; 7.0; 8.0; 9.0). The quasi-logarithmic occupation was found to be dense enough for the nature of these distributions. The stage width can basically be chosen arbitrarily, but must be taken dense enough to be able to resove insufficiently variations in N. Even an interval width of (D, $\sqrt{2}$ D), which is often chosen, is not sufficient to be able to record the sharp increase of distribution in the region around D=1 km.

III.3.2. Differential Distribution /43

The differential distribution is given as a continuous function by $n(D,t)=\partial N/\partial D$. A discrete approximation is usually obtained by $n=\Delta N/\Delta D$, while the stage width of the interval must be chosen suitably. An interval with not more than (D, $\sqrt{2}$ D) is recommended.

A cumulative distribution shown in Figure 11a is represented in Figure 11b in the differential representation. The stage widths are identical. These two variations show that we are dealing with a distribution which was developed almost undisturbed as an image of meteorite distribution, therefore approximately in the production state.

Figure 12 shows a mare surface of the Moon, which has undergone lava flooding with destruction of small craters and subsequent accumulation of other craters. Figure 13 shows the differential distribution of this population, in which the irregularities of the distribution for D=1.3 km indicate the destruction of smaller craters by lava flooding.

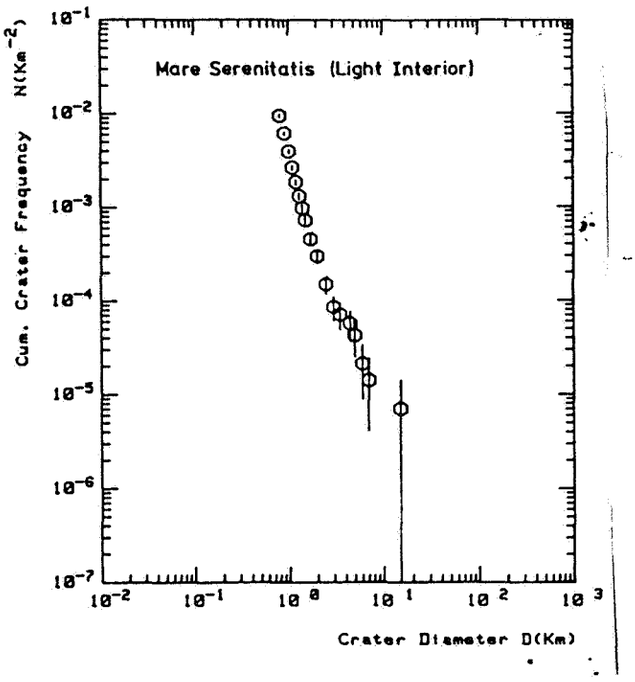

Figure 11a. A cumulative crater frequency distribution of the Serenitatis Mare (bright internal part) of the Earth's Moon. The distribution is almost a production distribution (Figure: Neukum et al., 1975a).

III.3.3. Incremental Distribution

One variant of the cumulative distribution is the incremental distribution. It was introduced by Hartmann (1966a). In this representation the crater frequency is usually measured progressively in intervals and plotted against the average diameter. The average diameter can be the geometrical or arithmetical average of the interval. Unfortunately this is often not defined in the literature. The size of the interval varies from author to author. Intervals of the size (D, 2D or (D, $\sqrt{2}$ D) are frequently used (compare Hartmann, 1966a).

The problem of the incremental distribution resides primarily in the fact that the frequencies depend on the size of the interval, which once again is not fixed. Mathematically, the following relationship exists between incremental and cumulative distribution for an interval choice (D, pD) (with p>1) for distributions corresponding to a power law of the type $n(D)=A \cdot D^{\alpha}$ ($\alpha<-1$) /46

$$N_{increm} = A \int_{D}^{pD} D'^{\alpha} \, dD' = (A/(1+\alpha))(p^{\alpha+1} - 1) \, D^{\alpha+1}$$

The cumulative distribution is

$$N = A \cdot \int_{D}^{\infty} D'^{\alpha} \, dD' = -(A/(\alpha+1))D^{\alpha+1}$$

It follows therefore that $N_{increm} = (1-p^{\alpha+1})N$

The incremental distribution is accordingly lower in its value by a factor $1-p^{\alpha+1} < 1$ below the value of the cumulative

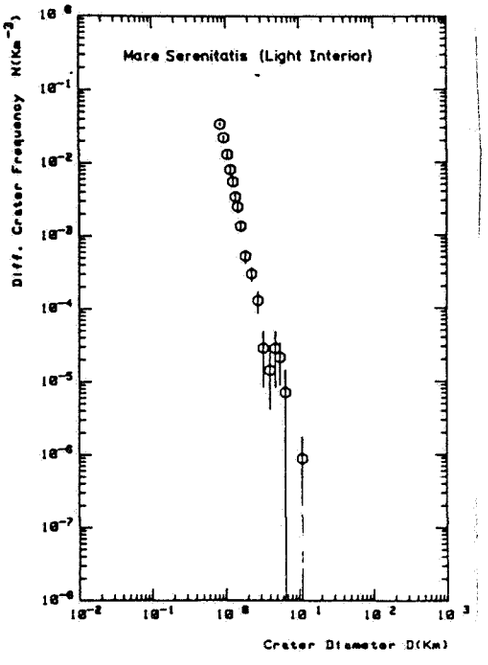

Figure 11b. Differential representation of the distribution of the crater population of the Mare Serenitatis.

distribution and has the same distribution characteristics, that is, the same distribution index $1+\alpha$.

The incremental distribution is not recommended because of the dependence of the numerical values on the choice of the interval sizes (compare Arvidson et al., 1978).

III.3.4. Relative Distribution

The relative distribution R is defined (Arvidson et al, 1978) as

$$R = n(D)/D^{-3} \quad \text{(for fixed t each time)}.$$

The standardization of the differential distribution n(D) to a distribution $\sim D^{-3}$ was chosen, because the populations of the large craters on the Moon and the other terrestrial planets show on the average distributions which fluctuate around $n(D) \sim D^{-3}$. Through standardization we obtain a representation which reacts very sensitively to deviations from /47
a differential distribution with distribution index (Exponent) -3, and is therefore very suitable for study of the fine structure of distributions.

Figure 14 shows an example of a relative distribution. Constant values of R over a very large range of diameters show a dependence $n(D) \sim D^{-3}$ or $N \sim D^{-2}$. For distribution laws $n(D) \sim D^{-2}$ we obtain in the log-log diagram of Figure 14 straight lines which have a slope of 45° with increase in D; for distribution laws $n(D) \sim D^{-4}$ we obtain straight lines, which have a slope of 45° with decreasing D.

III.4. Modification of Production Distribution by the Effect of Exogenous or Endogenous Processes

As a result of the effect of geological processes impact crater populations occur as production distribution only in extremely few cases. The different processes and their characteristic effect on the distributions will be discussed below (compare Neukum et al., 1974a; Neukum and Horn, 1976).

/45

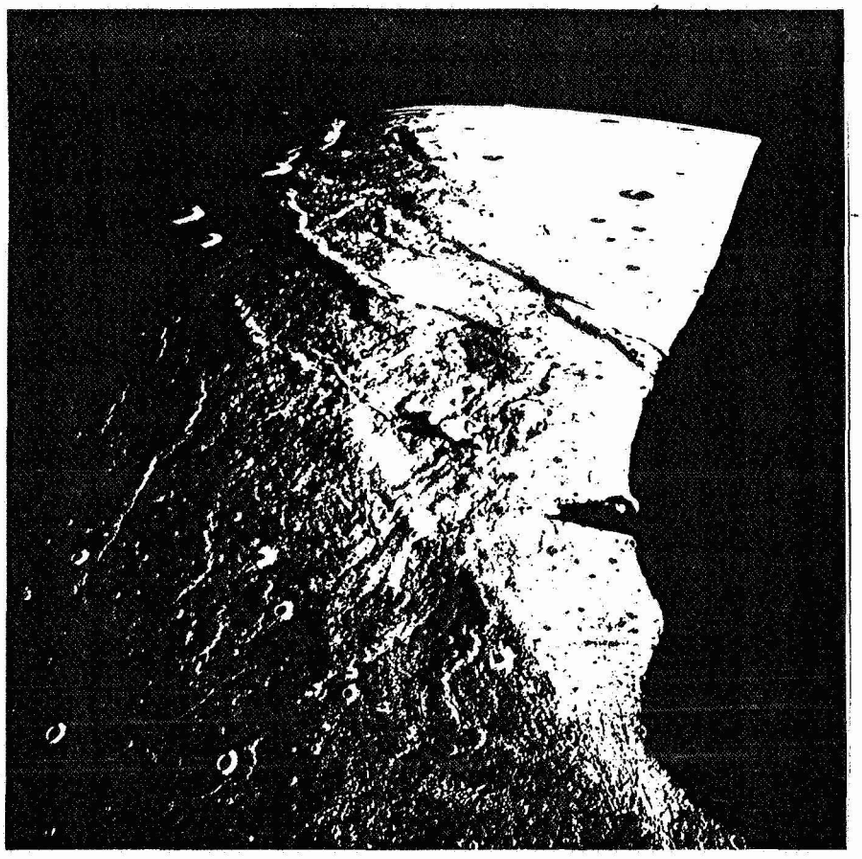

Figure 12. Apollo 15 photograph of a mare surface of the Earth's Moon with a view toward the north in the Mare Imbrium. Lava flows have erased more craters. These lava flows belong to the latest lava extrusions of the Earth's Moon.

III.4.1. Impact Superimposition and Equilibrium Distribution

After a long enough time of exposure of a geological unit, many craters are accumulated in such a way that new impacts can destroy the already existing craters. Gradual erosion of large craters by a large number of small impacts with accompanying filling by ejected material of the small impacts is another mechanism leading to the destruction of craters. The small craters of the population are first affected by such processes, since they are very numerous, can often overlap each other and can also be destroyed by a few large impacts. Moore (1964), Trask (1966) and /49
Shoemaker et al. (1970b) studied lunar crater populations, to investigate these processes. Gault (1970) simulated in laboratory experiments the crater destruction by impact superimposition. Various publications give a theoretical discussion of the development of the crater population under the effect of impact superimpositions, abrasion by small impacts and spilling by ejected material

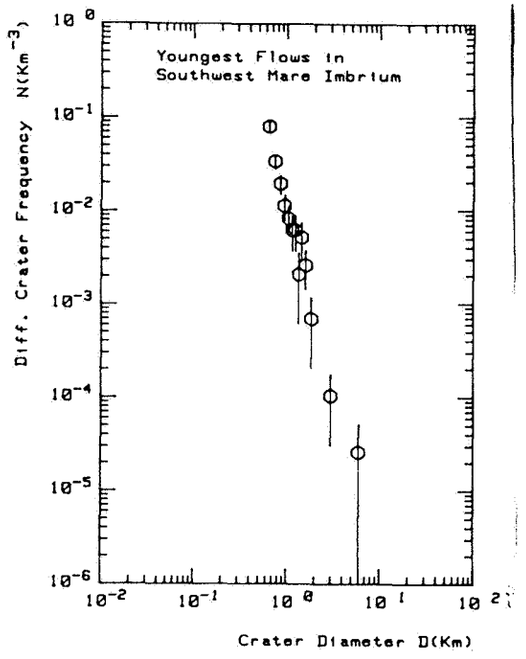

Figure 13. Differential distribution of crater population of a region, which is shown in Figure 12 (data from Neukum and Horn, 1976). The irregularity around D=1.3 km shows the elimination of smaller craters by covering with lava.

and other erosive processes (Marcus, 1964, 1966, 1970; Walker, 1967; Ross, 1968; Soderblom, 1970; Neukum and Dietzel, 1971; Woronow, 1977). All these studies lead to the result that the crater population under the above indicated destruction effect tends to a state of equilibrium, in which the number of the newly formed craters holds a balance with the number of destroyed ones on a statistical average. Results of the form $N_E = K \cdot D^{-2}$ are obtained (N_E = cumulative equilibrium distribution, K = constant) if the basic production distribution satisfies a power law $N \sim D^{\alpha}$ with $\alpha < -2$. Neukum and Dietzel (1971) give for K:

$$K = (-2\alpha - 4)/\pi b^{(2+\alpha)/\beta} .$$

α is a distribution index of the cumulative distribution; β is a quantity, which occurs in the relationship between crater diameter D and mass m of the causal meteorite ("Scaling law", compare Chapter IX.2), $D \cong m^{1/\beta}$; b is the parameter which describes the efficiency of the destruction by superimposition and covering with ejecta and is defined through the relationship $m_{min} = bm$, where m_{min} (equivalent D_{min}) is the smallest mass which can still destroy crater D, produced by the mass m.

In studies of equilibrium distribution of Moon craters in lunar mare regions, Trask (1966) found the relationship:

$$N = 10^{-1.1} \cdot D^{-2} \quad (D \text{ in km}, N \text{ pro km}^2), \qquad \text{/50}$$

consequently $K = 10^{-1.1}$ for post mare craters in the region $D \lesssim 100$ m.

For $K = 10^{-1.1} = (-2\alpha - 4)/\pi b^{(2+\alpha)/\beta}$, $\alpha = -3$ (compare Chapter IV.1.), $\beta = 3.4$ (compare Chapter IX.2.) we obtain

$$b = 8.5 \cdot 10^{-4}, \text{ d.h. } m_{min}/m = 8.5 \cdot 10^{-4}, \text{ or } D_{min}/D = 0.12.$$

This result shows that in the formation of the equilibrium population of the post-mare craters, the cumulative effect of

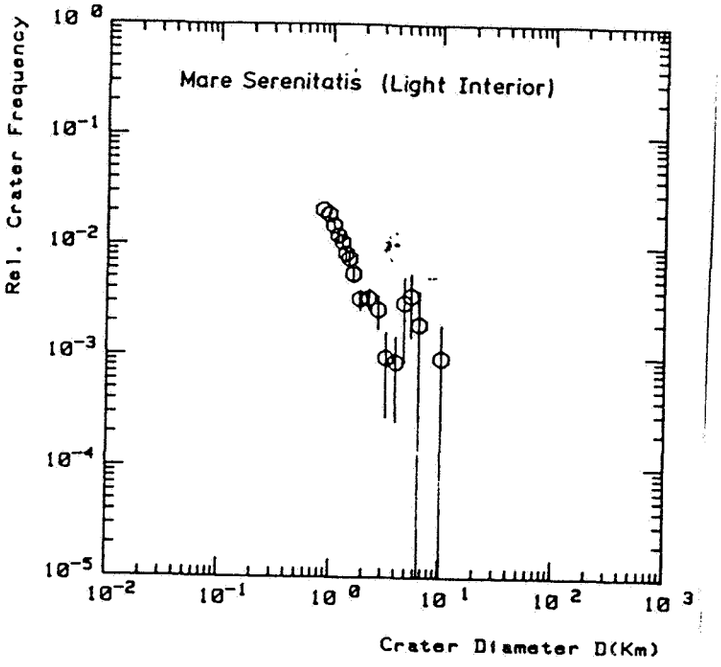

Figure 14. Relative distribution of population of Mare Serenitatis (from Figure 11).

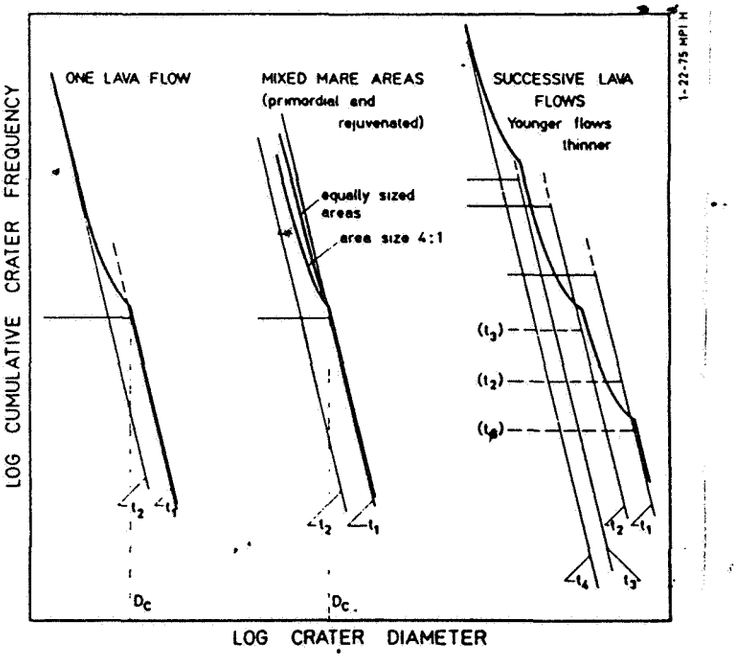

Figure 15. The effects of the consecutive lava flooding on a crater population with idealized crater frequency distribution $N \sim D^{\alpha}$ α=const. (Figure Neukum and Horn, 1976).

the destruction of very large craters by many small impacts plays a dominant role and not the direct superimposition of craters which are of comparative or larger size. This is consistent with the results of Soderblom (1970).

In the case of the distribution index of the cumulative distribution $\alpha>-2$, no equilibrium distribution occurs with $\alpha=-2$, but a distribution arises, which is similar to the production distribution, but with a greater frequency, which is reduced as compared with the production distribution by a factor which depends mainly on the age of exposure of the surface. For $\alpha=-2$, the distribution characteristic remains observed in a similar manner as in the case $\alpha>-2$ (Neukum and Dietzel, 1971).

In general, crater populations behave with the continuing meteorite bombardment in such a way that with increasing age and exposure the distributions reach equilibrium for increasingly large diameters D_E. Then two branches of the distribution may be observed: for $D>D_E$ the population is in production; for $D<D_E$ the distribution is in the state of equilibrium. For $\alpha<-2$, $D_E \sim F(t)^{-1/(2+\alpha)}$, where $F(t)$ is the time interval of the distribution (Neukum and Dietzel, 1971).

The crater populations of the land regions (highland) of the Moon show a very dense backing of large craters (D>10 km), which are frequently superimposed several times on each other. Whether in these populations we are dealing with those (almost) in the production state on in a state of equilibrium was for a long time the object of scientific controversy. The populations have a distribution with cumulative distribution index of nearly -2, which causes some authors (compare Hartmann and Wood, 1971; Gault, 1970) to come to the conclusion that we are dealing with equilibrium distribution. More detailed studies of distribution show however (Neukum, 1971; Strom and Whitaker, 1976; Woronow, 1978) that specifically in certain diameter regions, the cumulative distribution index is close to -2, but we are not dealing with distribution with constant cumulative distribution index, but that the distributions have a complex structure. Moreover, geological units of different stratigraphic age of the lunar terrae and the highlands of Mars and Mercury show that the absolute frequencies are different according to the differences in the stratigraphic age, but have the same diameter distributions. The consequence is that we must be dealing in highland populations with distributions which are at least approximately in the production state and not in the state of equilibrium (compare Chapter IV.1). /51

In the study of the highland frequencies and the interpretation of their distributions, the question as to how many craters of different size can be packed on a preassigned area has played a big role. These studies have led to the concept of "saturation". According to Gault (1970) "geometric saturation" is reached, when for the densest possible hexagonal packing of

craters of the same size on a surface, the cumulative area of all craters amounts to 90.5% of the surface. The relationship between the geometric saturation and the population, which has reached equilibrium with $N_E = A \cdot D^{-2}$, is such that "% saturation" =0.9 A (Neukum et al., 1973). The concept of "geometrical saturation" does not have much physical meaning, but is frequently used in literature as a relative criterion for crater frequency. /52

Unfortunately, the concept of "empirical saturation" has caused particular errors. This is a concept which is not defined exactly in terms of crater frequencies of distribution laws, but simply means that among all the erosive effects occurring in the nature in impact, a population has reached a state in which it no longer changes its diameter distribution (an exception is the erosion by endogenous effect, such as wind or lava extrusions).

The indefiniteness of the term has unfortunately led to the fact that it is used more and more in such a way that we often talk of saturation, when the subjective impression exists that a surface is so densely covered by craters that perhaps the densest possible packing is reached. This objective influence can however be very deceptive and has led to wrong interpretations (see Chapter IV.1).

III.4.2. Erosion and Sedimentation

Crater populations on all planets are frequently exposed to the effect of lava flooding, of large areas of superimposition with ejected material or erosion as a result of the effect of the wind, water or glaciers or by mass movements on mountain slopes. The effect of such erosion and sedimentation processes is generally that smaller craters are erased and larger ones can survive. The consequence is that the crater populations affected by erosion and sedimentation have a flatter distribution than their production population. In the case of flooding a population by lava, very frequent, especially on the Moon and Mars, the effects can be recorded quantitatively (compare Neukum and Horn, 1976; and Neukum and Hiller, 1981). /53

Figure 15 shows the effect of lava flooding on an idealized cumulative distribution $N \sim D^{\alpha}$ with α=const for different cases. At the time t_1 the geological unit (measurement surface) is flooded. Smaller craters are completely covered, larger ones survive. The original size distribution (indicated by the dashed line for the covered smaller craters) is changed in its characteristic manner. If no additional impacts take place, the distribution after the flooding will have a constant value for $D \leq D_C$. With further exposure, in the interval of time between t_1 and t_2, a new population of craters is built up (the distribution in Figure 15, indicated by t_2). If no differentiation is made between the

populations, we count at the time t_2 the sum of both populations, indicated by the solid curve. For $D>D_C$, the sum distribution runs parallely to the distribution of the population before the flooding, but with a value higher by the population accumulating after the flooding. For $D=D_C$, the distribution is abruptly flatter, because the contribution of the craters of the population before the distribution is zero (it corresponds to N=const and the cumulative distribution). For $D<D_C$, the sum distribution is once again sharper and asymptotically close to the distribution of populations which accumulated after the flooding. Figure 15 shows two more cases frequently occurring, specifically when in the study of a structure only part of the measurement surface is covered with lava of a later flooding, or several less powerful floodings have taken place.

In reality more complex flooding processes may have occurred on the Moon or the other terrestrial planets. All effects on the crater size distribution should, however, be similar to the three cases discussed or be constituted from them. If the flooding /54
took place only once, the irregularity at $D=D_C$ may be used in the determination of the thickness of the lava flows. According to Pike (1967), we have the relationship $T=0.048 \cdot D^{0.95}$ for the edge height T of a crater diameter D (when D<15 km). (The edge height is the height of the crater wall over the undisturbed surface). For flooding by lava with erasure of the smaller craters up to a certain size, T may be determined for $D=D_C$. The latest lava flows in the Mare Imbrium (Schaber, 1973; compare also Figures 12 and 13), for which we measure $D_C \approx 1.3$ km, have accordingly a thickness of about 60 m (Neukum and Horn, 1976).

Characteristic irregularities, arising from a repeated flooding, are often found in distributions of crater populations on mare surfaces of the Moon or the deep plains (Planitiae) of Mars. Detailed information can be obtained from this on the development structures and on the periods during which such multiple floodings have taken place. An example of a population which was affected by several lava floods is shown in Figure 16 (Apollo 11 landing area and surroundings). An example for the planet Mars (Elysium Planitia) is shown in Figure 17a, b in the form of cumulative and differential distributions. The comparison of the measured distribution with the population distribution shows deviation in the measurement values from the production distribution at about 4 km crater diameter and below. The differential distribution shows clearly that craters of less than 4 km in diameter were almost totally erased (decrease in the differential frequency), and that craters accumulated once again on the newly created surface (part of the curve which rises again toward smaller craters). The old crater population (which accumulated before the flooding) and the young population (after flooding) can be separated approximately, as shown in Figure 17c: the old population is measured for D>4 km. The young population is obtained by subtraction of the contribution of the old population. An approximation of the standard /57

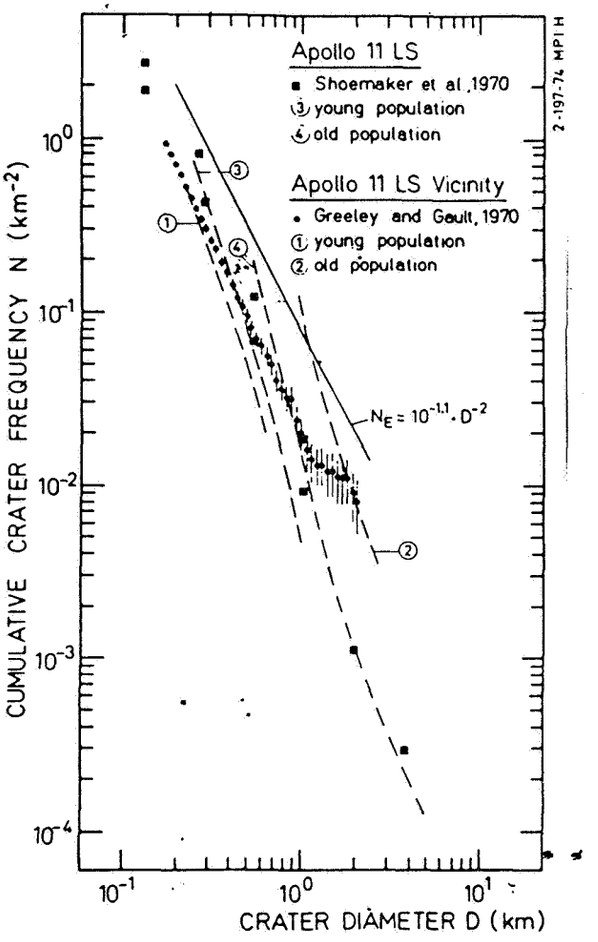

Figure 16. Crater frequency distributions of Apollo 11 landing area and its surroundings (data from Shoemaker et al., 1970, Greeley and Gault, 1970). These data were interpreted in such a way that the distributions were effected by successive lava flows. This conclusion is drawn for the flattening of the distributions towards smaller diameters, similarly to the model in Figure 15, and from a comparison with the lunar production distribution (standard distribution, dashed line curves). The frequency of the smallest craters can be associated with the latest endogenous activities, while the largest craters are interpreted as survivors of the population which had accumulated before the flood. The flattening of the distribution is not caused by impact erosion, which may be derived by comparison with the equilibrium distribution $N_E=10^{-1.1}D^{-2}$ (Trask, 1966), which is much higher.

distribution (that is, the crater production size distribution approximated by an algebraic expression, see Chapter IV.1) to the two separated distributions gives the corresponding relative crater retention age and the crater frequency for D=1 km.

(The bending of distributions in the region $D \lesssim 0.5$ km in Figure 17 is therefore due to the fact that the craters in the measurements are close to the limit of resolution and were not recorded quantitatively.)

Crater populations which were effected by other erosive processes, for example, of the fluvial or glacial type, show usually no such characteristic features as the populations influenced by lava flooding. Naturally in such processes smaller craters are preferably eliminated also, which is manifested in a flattening of the cumulative distributions for small craters (already a drop for the differential distribution).

Figure 18 shows the population of the terrestrial phanerozoic craters of North American and North Europe (Grieve and Dence, 1979) and compared with terrestrial standard distributions (production crater size distribution, see Chapter IV). Below 20 km crater diameter, the deviation of the measured distribution from the standard distribution shows the elimination of the smaller craters.

III.4.3. Contamination by Secondary Craters and By Volcanic Craters

The ballistic ejection of material during meteorite impact causes the formation of secondary craters, just as in the scattering field of ejection material (ejecta) around large fresh craters on the planet (compare Figure 19). Oberbeck and Morrison (1973) studied the formation of secondary craters in the laboratory and compared them with lunar forms. They found that secondary craters often form crater chains with craters /60
which are often deformed elliptically approximately radially in the direction to the primary crater, and are mostly flatter than comparably large primary craters. The best characteristic for identifying the secondary craters is the "herringbone pattern" which arises in the simultaneous multiple secondary impact (compare Figure 20).

On the basis of the study by Oberbeck and Morrison, secondary craters may be included in many cases. The differentiation between primary and secondary crater is, however, not clear in all cases, especially if secondary craters do not appear in chains, but in isolated individual units. Therefore, especially in the region of the discontinued ejections, large primary craters can contain a significant contribution from nonidentifiable secondary craters in measurements. It is therefore recommended to measure not in the vicinity of scattered fields of large primary craters (except on the continuous ejecta covers, where there are no isolated secondary craters) or to limit ourselves in the

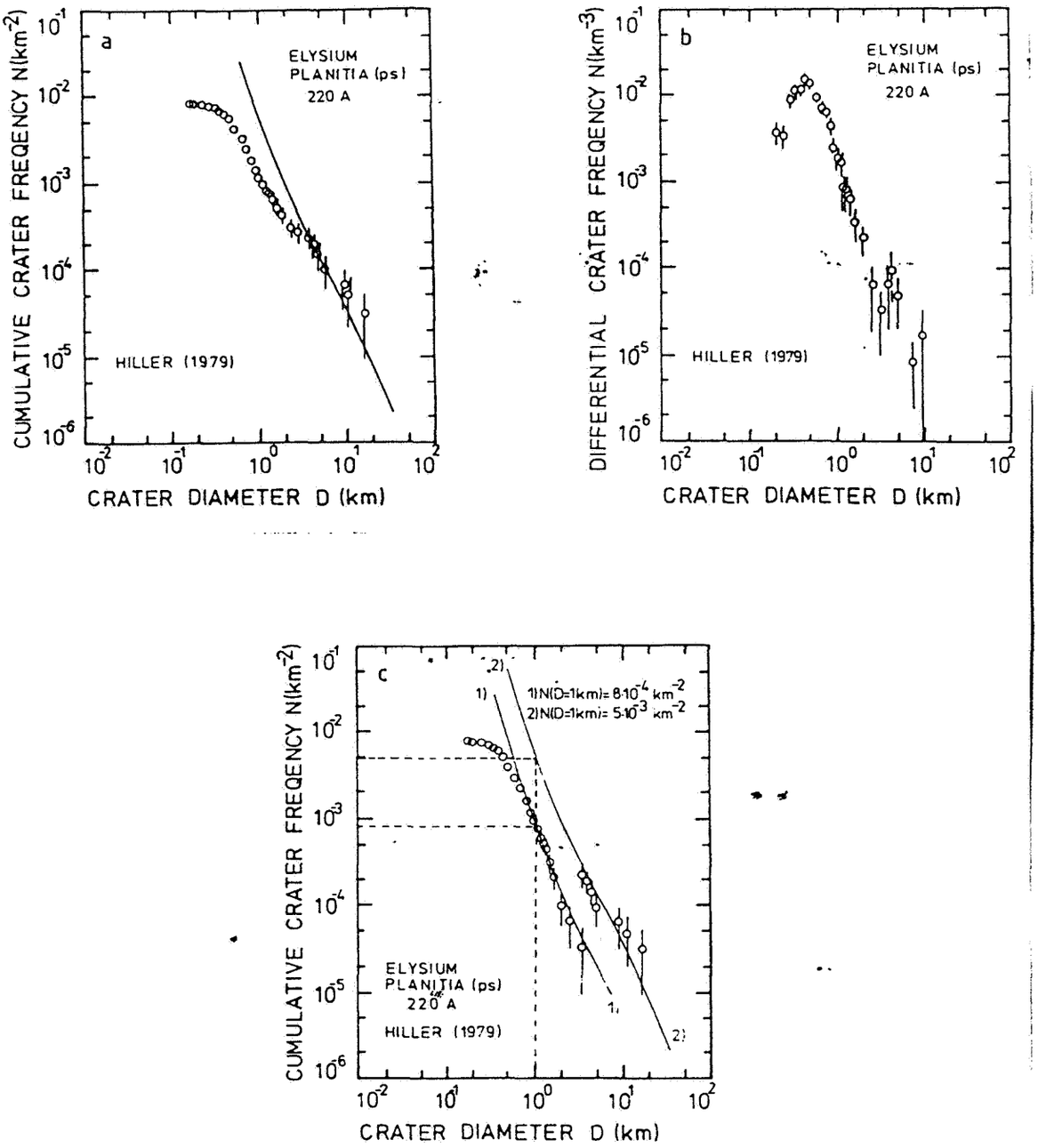

Figure 17a--c: Example of the effect of the influencing of the crater population of Mars in Elysium Planitia (p s = smooth plains) by lava flooding and extraction of relative ages (crater retention ages).

a) cumulative crater frequency distribution
b) differential crater frequency distribution
c) separation of populations which had accumulated before and after the flooding, and determination with corresponding crater retention age N(D=1 km).

(Figure Hiller, 1979 and Neukum and Hiller, 1981).

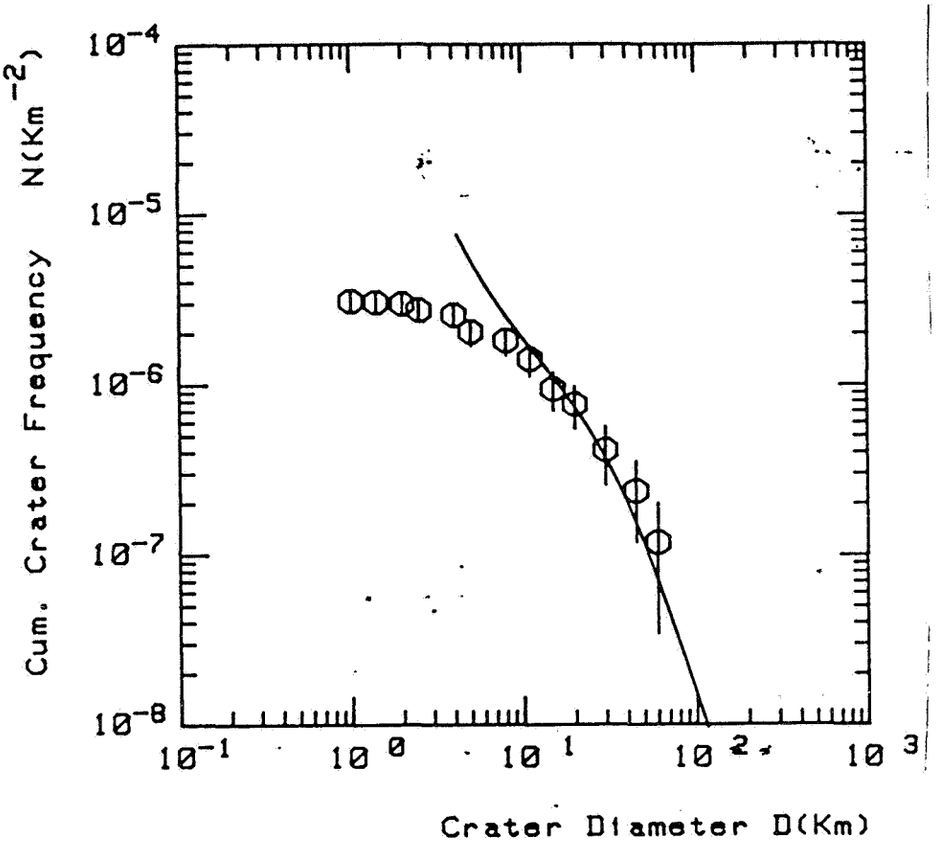

Figure 18. Frequency of the phanerozoic crater in North America and Northern Europe (data from Grieve and Dence, 1979). The population is affected in the region D<10 km by erosive processes (elimination of craters) as shown by the comparison with the production distribution (curve).

/59

Figure 19. Moon crater Copernicus with a scattered field of secondary craters.

Figure 20. Secondary crater chain of the Moon crater Aristarchus.

measurements to the largest possible craters, since above a certain size in proportion to the size of the primary crater, no secondary crater should occur (D(primary)/D(secondary) = 10-20 (Shoemaker, 1965).

Neukum et al. (1975a) have indicated in detail in the investigations that in general the contamination of the primary crater frequencies by secondary craters lies at a few percent of the population of the Earth's Moon. König (1977) showed that at least in individual cases with careful mapping of the measurement region, very reliable measurements can be carried out of primary crater frequencies even on secondary crater chains.

The problem of secondary craters and the problem of which components of the crater distributions of the terrestrial planets is primary or secondary was for a long time the object of controversies. In particular, the increase in lunar distribution for D≲1 km was considered by many authors as the contribution of secondary craters (compare Shoemaker, 1965). Similar /61
arguments were put forward for the distribution on other planets, especially for the distributions which were measured on Mars (Soderblom et al., 1974) where a similarly sharp increase is found for the distribution for D≲1 km as in the case of the Moon. In the present investigations it was found that the distributions for D≲1 km represent mainly primary crater distributions. This is discussed in Chapter IV.1.

In various studies of recent years, it was shown (compare Oberbeck and Aggarwal, 1977; Wilhelms et al., 1978) that for part of the larger craters (D>10 km) in the highland of the Moon, we have secondary craters. Wilhelm (1976) showed that with careful mapping and photogeological interpretation, the separation of the secondary craters from the highland primary population is possible in a satisfactory manner.

A small portion of the lunar craters is obviously of volcanic origin. Such craters are frequently found in lunar grooves or trenches (compare Grudewicz, 1973). By their morphology and their occurrence they may be excluded in most case from the countings.

Only in the case of the planet Mars, volcanic craters occur in larger numbers, and are of a type such that a separation in some cases proves to be difficult. These are craters which are comparable to the terrestrial mare type (Wormer et al., 1979) and were formed probably in a similar manner in the form of explosive volcanism. In such regions of Mars, which are naturally rare, it is impossible to determine any sure age by crater frequency measurements.

IV. PRODUCTION-CRATER SIZE DISTRIBUTION AND IMPACT CHRONOLOGY OF THE EARTH-MOON SYSTEM

/62

By an exact analysis of the crater population of the Earth's Moon and the dependence on time of the impact rate in the Earth-Moon system, we will lay the foundation for the dating methods with crater frequency, and give a sketch of the development of the Earth's Moon and interaction with the meteorite bombardment. These results represent thus the basis for the discussion for other terrestrial planets in the following Chapters.

IV.1. Analysis of the Production Crater Size Distribution of the Earth's Moon

The regions of very different age of the Moon show crater frequency in production over a very large age range. The mare region between about 3 and 3.8 billion years, the Moon highland (Terra or Plural Terrae) for ages more than 3.8 million years, and some young impact craters, allow the analysis of crater frequency over the last couple of hundred million years. The determination of the production size distribution and the effect rate as a function of time can be solved empirically by measuring the crater frequency $N(D,t)=G(D)\cdot F(t)$ and $n(D,t)=g(D)\cdot F(t)$ over the largest possible variation in D and t intervals (compare Chapter III.2.). (Here it was already assumed that $g\neq g(t)$ and $G\neq G(t)$; this is obtained finally from the studies described below).

IV.1.1. The Lunar Standard or Calibration Distribution

A detailed analysis of the function G(D) and N(D,t) for different fixed ages t each time was carried by out by many authors (while here only the most modern analyses are cited). Shoemaker et al., (1970) found $N\sim D^{-2.9}$ for D<3 km for mare surfaces of different age of the Moon. /63

Hartmann and Wood (1971) found $N\sim D^{-2}$ for craters with D>1 km and Baldwin (1951) found $N\sim D^{-1.8}$ for approximately the same region. What is common to these studies is that a variation in time of the diameter distribution was not established, that is we have $N(D,t)=G(D)\cdot F(t)$.

Chapman and Haefner (1967) argued for the first time that their measurements seemed to indicate that there is not a simple power law of the diameter-size distribution of the type $N\sim D^{\alpha}$, α=const, but that the power has a size dependence, that is $\alpha=\alpha(D)$. This would also follow from the previously indicated measurements by Shoemaker et al. and Hartmann and Wood or Baldwin, as an explanation compatible with all analyses.

A detailed analysis of the distribution law was carried out by Neukum et al. (1975a) and thereafter by Neukum and Königq (1976) and König (1977). Crater populations on the surface of the Moon as homogeneous as possible and of very different age, with undisturbed crater distribution were analyzed over the maximum possible diameter range.

The measurement regions and their crater population are selected in such a way that the frequency of different measurement regions overlaps with the other regions in their minimum and maximum diameters. Thus different frequencies could be compared with each other for the same diameter ranges. Consequently the ratio $N_i/N_k=C_{ik}$ of different populations is formed, or in other words, the frequencies can be standardized with each other by "slipping" in logN direction. The result in Figure 21 shows that in the standardization of the frequencies with each other a smooth curve is obtained. The following conclusions may be drawn therefore for:

1. The distributions in the region 20 m$\leq$D$\leq$1 km on regions 0.1 to 3 billion years old are consistent and the total data may be combined into an overall distribution. The fact alone that this is possible without difficulty, that is, by successful standardization of the individual distribution with each other a smooth variation of the function is obtained, showed that the crater size distribution was not subject to any significant variations. The corresponding applies therefore also to the size and velocity distribution of the crater producing body. /65

2. In the region D$\gtrsim$1 km, the distributions of regions with ages between 3 and more than 4 billion years are consistent. This means that in the period between about 4 billion years and about 1 billion years, the greatest size distribution did not undergo any significant changes in this size range. The corresponding also applies for the size and velocity distribution of the crater producing body.

The lower time limit of about 1 million years shows therefore that the crater populations have built up over the entire period of exposure ($\geq$3 billion years) and the variations within the last 1 billion years would hardly be noticeable in the measurements.

3. The lunar production crater size distribution cannot be directly determined for certain size regions and ages, since either statistically significant figures cannot be determined, or the distributions because of impact superimposition are in the state of equilibrium ("saturation"). Such regions are, for example, D$\leq$300 m and age more than 3.5 billion years or D<1 km and age >4 million years.

4. The lunar crater population can be described with the same size distribution function in the size regions where

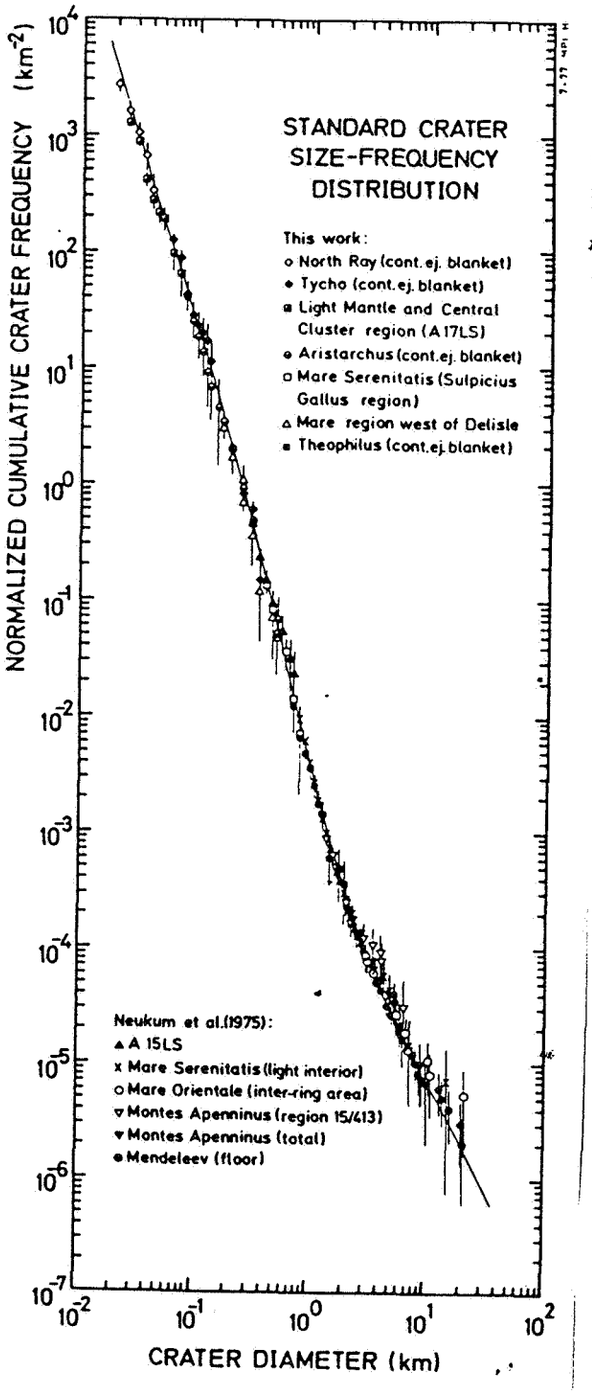

Figure 21. Standardized production distributions of the Moon with approximation by a polynomial of the 7th degree in LogD. (Figure Konig, 1977).

measurements are accessible. This means that to compare crater frequencies for the purpose of determining the age, one reference function can be used with regard to the same diameter, even if the distribution law may be different in the nonaccessible region. /66

5. The distribution function does not follow a simple power law, but a structure in the region 20 m<D<20 km is so complex that logN(D) can only be approximated well by a polynomial of the degree >7 in logD (compare Neukum et al., 1975; König, 1977) which is given in Figure 21 (as a polynomial of the 7th degree).

The region D≥5 km, which is statistically occupied somewhat weakly, was very recently analyzed more precisely by the author. In particular, there is no description of the distribution for populations in the region D>20 km. These populations may be measured in very old regions of the Moon highland. Moreover, it is possible to obtained quantitatively over the entire front side of the Moon the distribution of Copernicus-Eratosthenic craters (post-mare distributions) with D>20 km (Wilhelms, 1979). Thus the distribution in the region D>20 km may be measured over a large age span (about 4.4 to 1 billion years; see following Chapter IV.1.2.).

The connection of the frequency for D<20 km with a frequency of D>20 km to determine the distribution over the entire accessible diameter range of less than 100 km and more than 100 km can be carried

out in several ways:

1. Direct connection of the frequencies for D<20 km and D>20 km in regions in which data for both diameter regions are available and which through their equal age fixes per se the distribution of small craters with regard to large craters. Examples of this are populations on Imbrium ejecta and Oriental ejecta (compare Figure 22). But in such cases it is not possible /68
to cover the entire diameter range of interest.

2. Determination of frequencies of small craters (D<20 km) and large craters (D>20 km) in different regions, whose age is known. The connection of the frequencies to determine the distribution in the entire diameter range takes place by standardization of the corresponding frequency on the time interval of the impact rate F(t), which naturally must be known. In particular for ages $t<3 \cdot 10^9$ years, all measurements indicate (following Chapter) an impact rate which is constant on the average. The crater population regions of this age are therefore easily compared with each other, since the frequencies are linear in t ($F(t) \sim t$).

Analyses of the crater population of the described type have been carried out individually. An example for the procedure indicated in ¶2 is shown in Figure 23. All frequencies fall after standardization on $F(t) \sim t$ on a smooth curve (constant impact rate, see next Chapter). The curve is the lunar standard distribution described here and indicated further below. Accordingly it is found that the distribution obtained here is a good approximation for the lunar production distribution for the last 3 billion year in the studied diameter range. The consistency of the representation shows that a function of constant impact rate is very probably correct.

A synthesis of the data of Neukum et al. (1975), Neukum and König (1976), König (1977), and the latest data for $D \geq 20$ km allows the determination of the size distribution in the diameter range $10\ m \leq D \leq 300$ km (Neukum, 1983). A polynomial of the 11th degree in logD approximating the standardized logarithmic cumulative frequencies gives the complex variation of the distribution with /70
sufficient precision. This polynomial has the form

$$\log N = a_0 + a_1 \log D + a_2 (\log D)^2 + \ldots + a_{11} (\log D)^{11}.$$

Its coefficients are:

$a_1 = -3.6269$ $\quad$ $a_7 = 0.0379$

$a_2 = 0.4366$ $\quad$ $a_8 = 0.0106$

$a_3 = 0.7935$ $\quad$ $a_9 = -0.0022$

$a_4 = 0.0865$ $\quad$ $a_{10} = -5.180 \cdot 10^{-4}$

$a_5 = -0.2649$ $\quad$ $a_{11} = 3.970 \cdot 10^{-5}$

$a_6 = -0.0664$

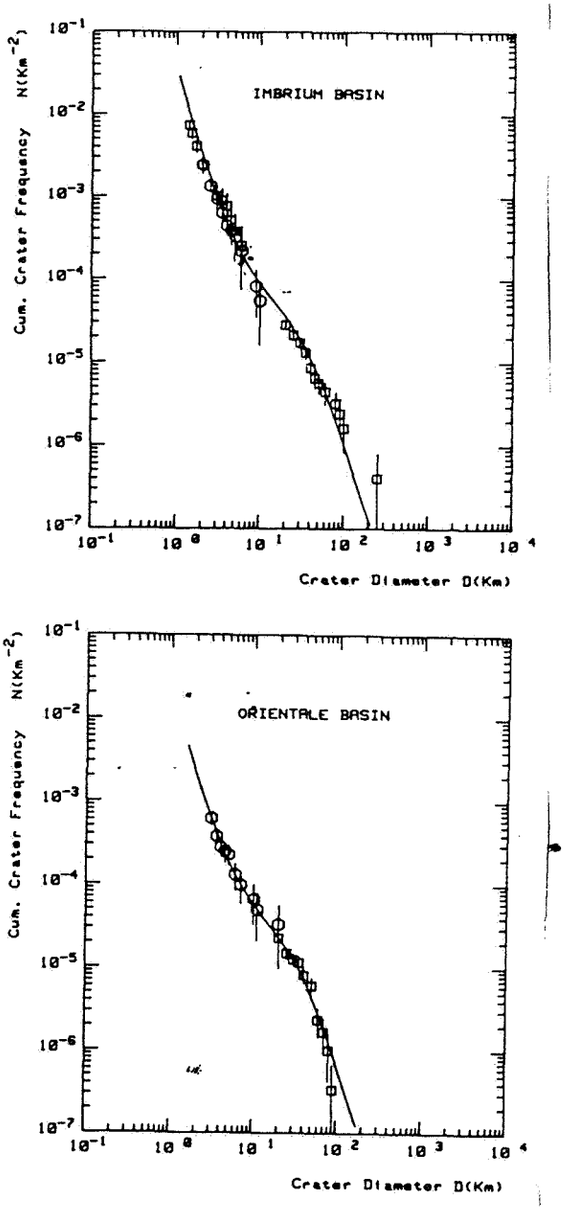

Figure 22. Frequencies of small craters (D<20 km) and large craters (D>20 km) of surface of the same age of Imbrium and Oriental ejecta. Because of the same age the frequency distribution is fixed mutually in both regions. The continuous line curve is the lunar standard distribution derived here, whose variation has been determined by other measurements possible for smaller and larger craters. (Data of Neukum et al., 1975a and Wilhelms, 1979).

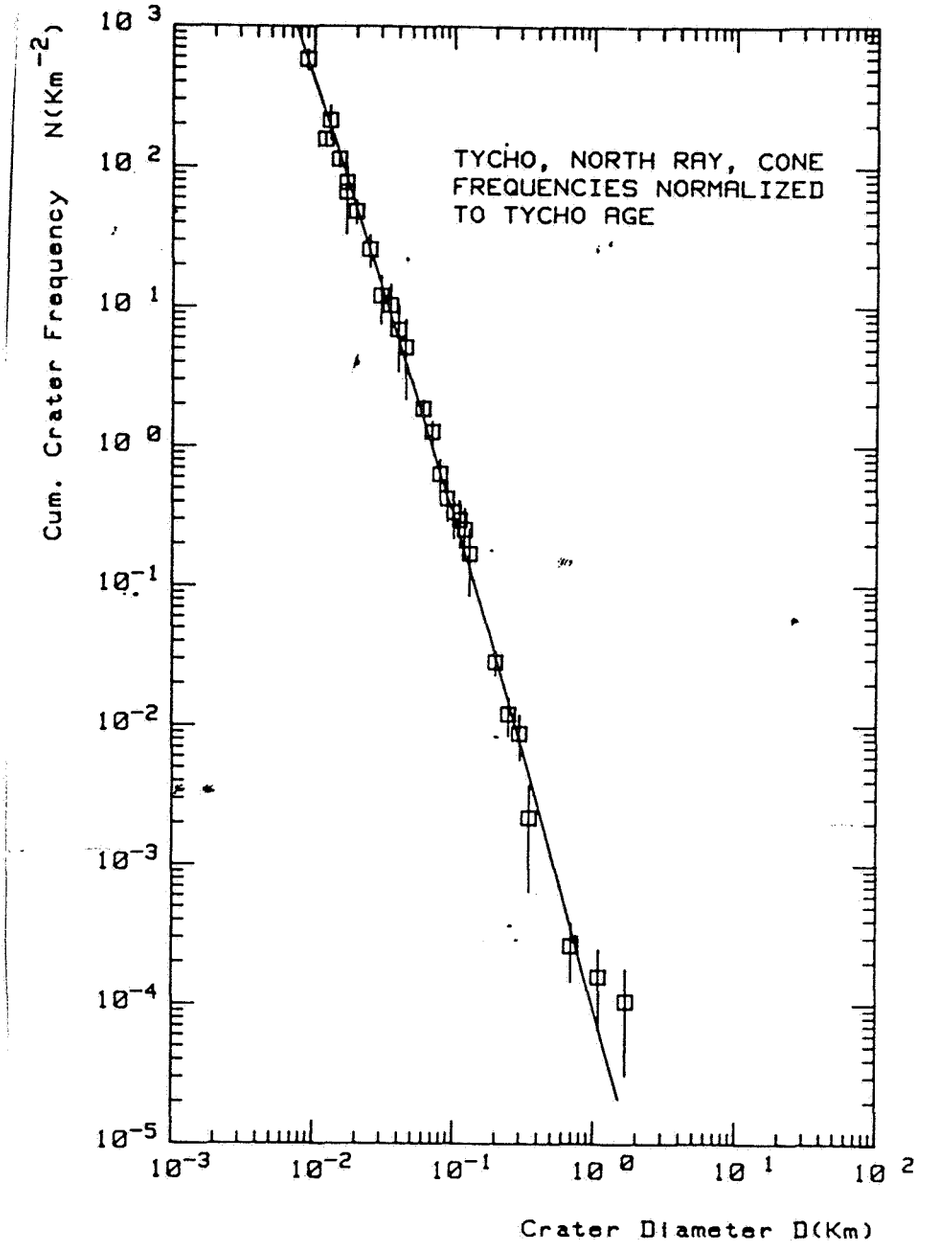

Figure 23. Standardization of crater frequencies of different younger lunar regions assuming constant impact rate (F(t)~t) to the frequency of the measured superimposed craters on the crater Tycho. The frequencies fall on the lunar standard distribution.

This formula gives the cumulative frequency N per km^2, when the diameter D is given in km. The coefficients are valid in the region 10 m$\leq$D$\leq$300 km, but not beyond. On the average, the quality of the approximation in the region 10 m$\leq$D$\leq$300 km is better than 50% (standard deviation). The distribution function is consistent with the earlier obtained expressions (Neukum et al., 1975a; König, 1977) and the corresponding ranges of validity within 50%.

To obtain a general mathematical expression for the cumulative distribution function for a special region, we must further add an additive term to the polynomial formula, which takes into account the age t_o of the region. $\log N = a_o + a_1 \log D + \ldots + a_{11} (\log D)^{11} + \log F(t_o)$, where $F(t_o)$ is the time integral of the impact rate, to which the region was exposed over the period of its existence. For the numerical approximation we took arbitrarily $a_o + \log F(t_o) = 2.5340$ ($N(D=1\ km) = 2.92 \cdot 10^{-3}$).

The standard distribution now makes it possible to compare with each other crater frequencies of populations in different diameter ranges and to determine relative ages of geological units on which the crater frequencies are measured. In this case, it is proper to refer to the same reference diameter, here D=1 km or D=10 km. The distribution function is represented in Figure 24 in comparison with distribution laws from older literature (Shoemaker et al., 1970; Baldwin, 1971; Hartmann and Wood, 1971), in which functions with constant distribution index α were used in the form $N \sim D^{\alpha}$. Such formulas are only valid in a very limited amateur range, and their application can lead to considerable errors, as is illustrated in the Figure. /71

The distribution function is a very complex function with values of the distribution index between -1 and -4. This is particularly apparent from the representation of the relative frequency in Figure 25. We see clearly the deviation from the distribution postulated in the older literature cited with $\alpha=-2$ in the region D>5 km. In the region D<1 km, α is on the averge at -3, that is, the frequency increases sharply towards more craters. These characteristics will be discussed hereafter.

IV.1.2. Size Distribution on the Oldest Surfaces of the Moon

The distribution of craters in the region D$\geq$20 km on the oldest part of the Moon crust has been for years the object of scientific controversies. A number of authors (compare Hartmann and Wood, 1971; Shoemaker, 1970; Hartmann, 1972) considered these populations as in "saturation", that is, an equilibrium with destructive processes, predominantly those of direct impact superimposition (compare Chapter III.4.1.). This seemed to be indicated also by the distribution $N \sim D^{-2}$, which was measured approximately and which should be adjusted for such a state under certain assumptions. Another group of authors however

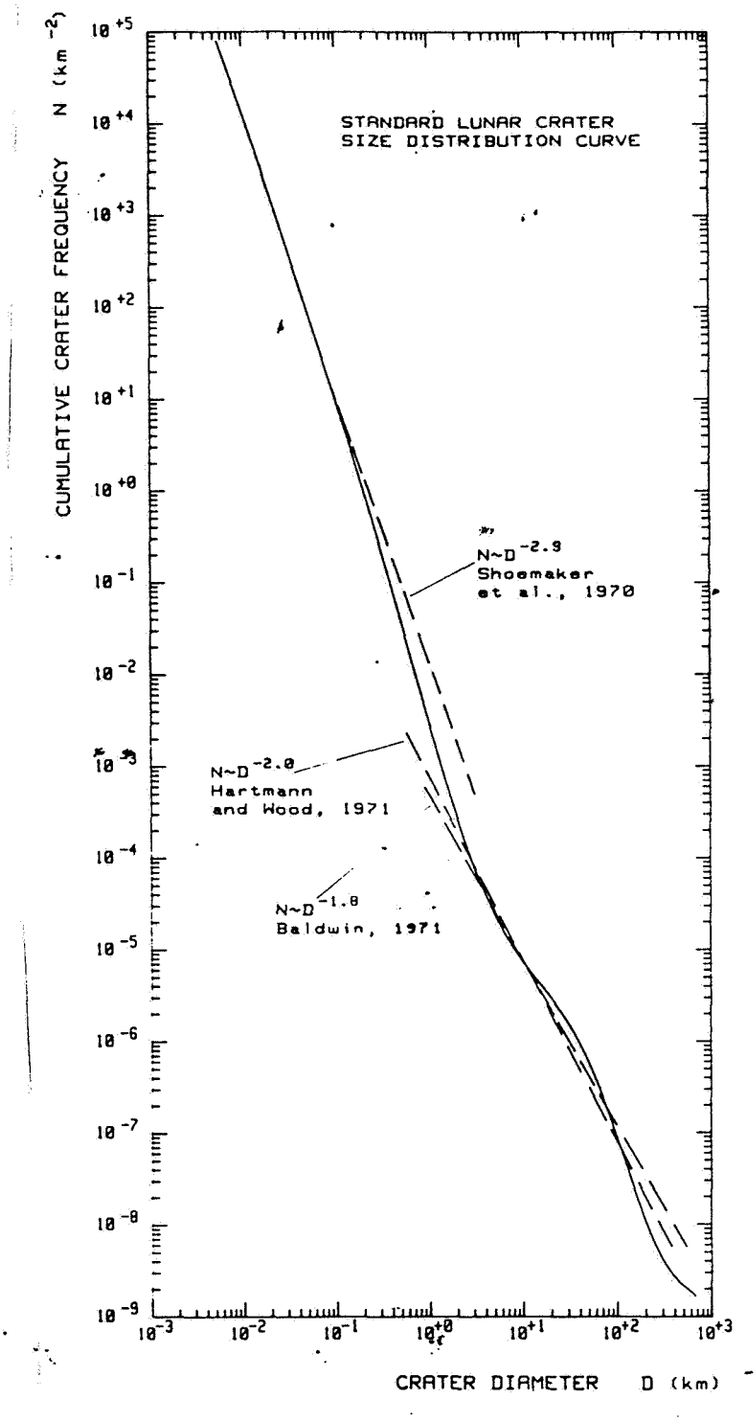

Figure 24. Comparison of the crater size distribution function deduced with descriptions from the literature. They are suited to be standardized and plotted in the region of their indicated validity.

acknowledged deviations from the D^{-2} distribution, and established in investigations that at least the larger craters (D>30--50 km) did not lie so closely together that significant numbers of craters of this size should have been eliminated by impact superimpositions (Neukum, 1971; Neukum and Wise, 1976; Baldwin, 1971; Woronow, 1977; Strom, 1977). An explanation of these problems is now possible. The measurements show clearly that the distribution in the oldest regions of the Moon for D>20 km does not follow a D^{-2} equilibrium distribution. We can only be dealing (at least basically) with a production distribution. This statement is confirmed by the results of analysis of the younger highland and mare populations. In Figure 26, average frequencies of pre-nectarian, nectarian and eratosthenian-copernican populations were plotted as compared with the highland frequency. Here the distributions are identical within the limits of errors, that is, the distributions were stable over the entire period covered. In particular, an equilibrium distribution $N=K \cdot D^{-2}$ should show a basically constant coefficient K (compare Chapter III.4.1.). Thus the distribution shows clearly the different ages of the studied regions and populations, which is the characteristic of populations in the production state. /73

Strom (1977) argued that the distributions of the post-mare craters differ from those of the pre-mare craters. These agruments cannot be followed here. A detailed analysis of the distributions over the representation as relative frequency shows that within statistical areas all distributions are identical, even post-mare distributions (i.e. eratosthenian-copernican distributions). The distribution found by Strom was analyzed by the author and may be the product of poor statistics (Neukum, 1983). It is apparent from Figure 26 that the distribution for D<50 km of the older regions as compared with each other and the standard distribution appear to be somewhat flatter than those of the younger regions. This is interpreted as the effect of the partial elimination of the smaller craters still occurring as an effect of the increasingly dense crater population, that is, the older populations are with regard to the smaller crater (20 km<D<50 km) not exactly in production, but far removed from distribution equilibrium. /76

IV.1.3. The Population of Subkilometer Craters: Primary or Secondary Craters?

In this section we will discuss in detail the question as to whether the lunar crater population in the region D<1 km consists basically of primary or secondary craters.

Many authors (compare Shoemaker, 1965; Brinkmann, 1966; Soderblom et al., 1974) have interpreted the sharp increase of frequencies around D=1 km as the contribution of secondary craters. Shoemaker designated the secondary crater as "background secondaries", since no primary sources can be identified.

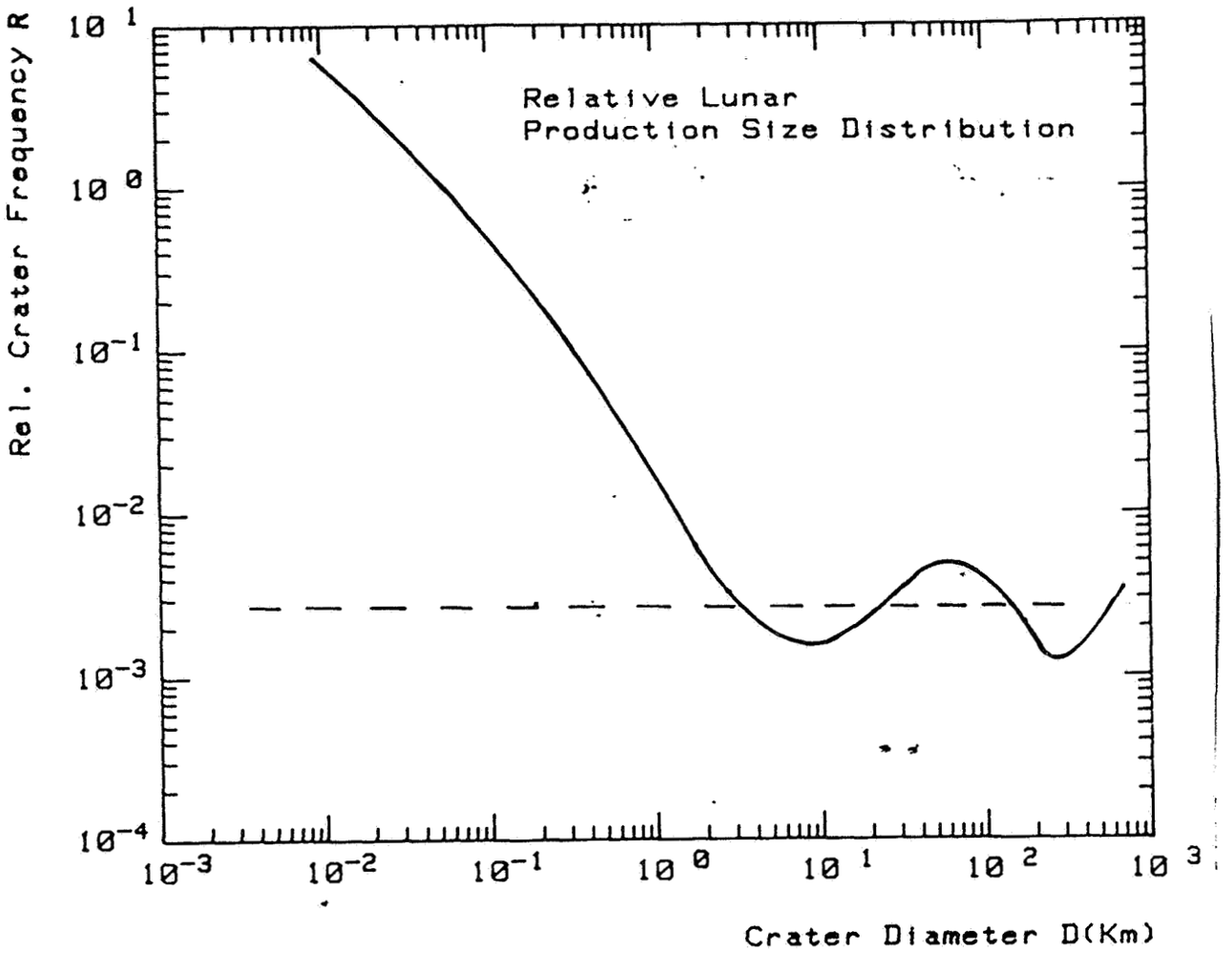

Figure 25. Lunar standard crater size distribution (continuous curve) in relative representation. The horizontal dashed lines are equal counts and correspond to relative distribution $N \sim D^{-2}$ or a differential distribution $n \sim D^{-3}$.

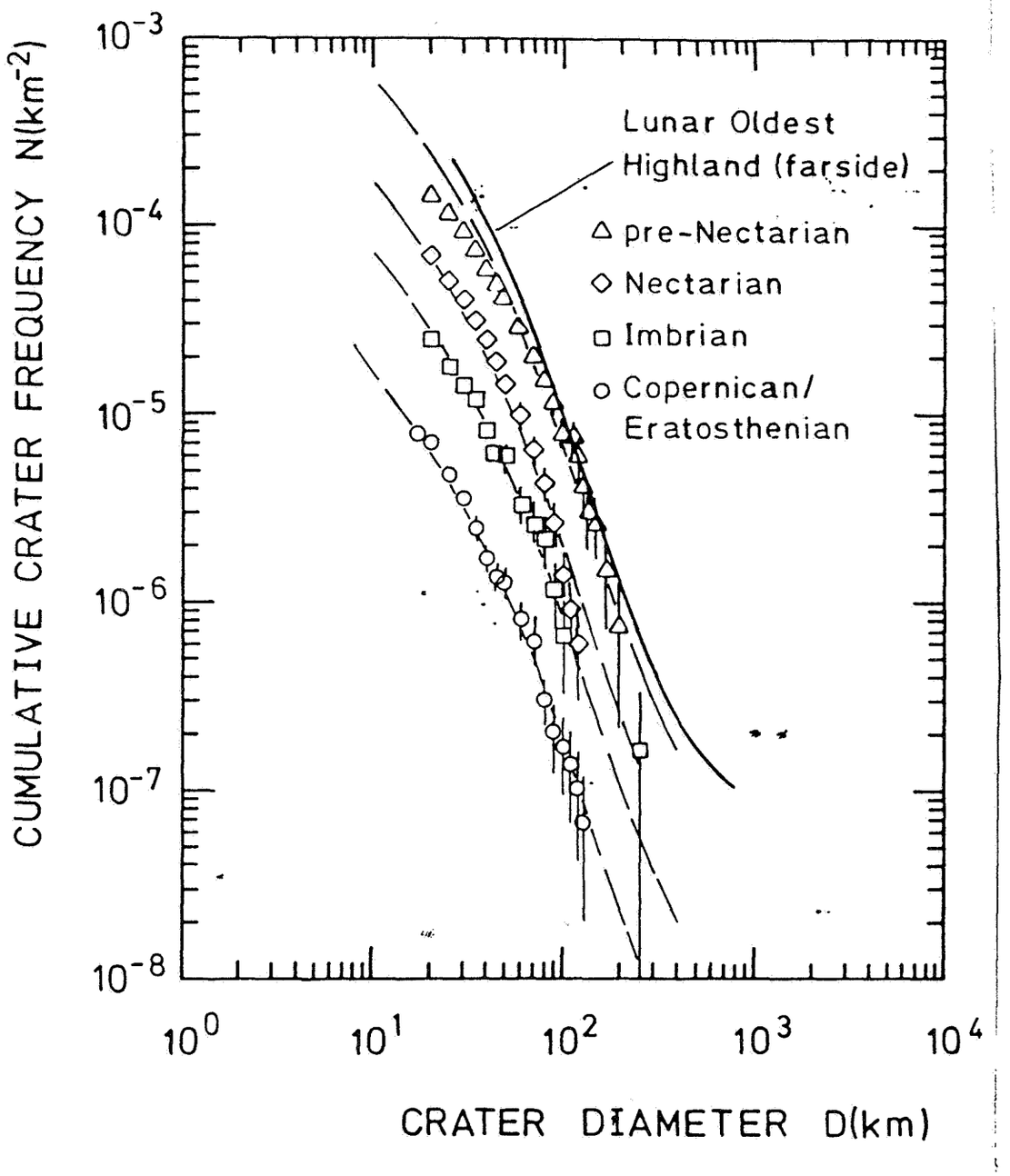

Figure 26. Size distribution of lunar craters with D≥20 km. The distributions follow basically standard distribution (continuous curves). This proves the stability of the distribution over more than 4 billion years.

Here the idea is that large craters ($D \gtrsim 10$ km) produce an ejection, which flies over ballistically long distances around the Moon and when striking it produces craters statistically distributed over the Moon's surface in the region $D \lesssim 1$ km, which behave like primary impact through this mechanism of distribution over the Moon.

Soderblom et al. (1974) use arguments to explain also the distributions on Mars for $D < 1$ km, which show a sharp increase like the distributions of the Moon, similar to a secondary crater population (compare also Chapter V.1.). The arguments will be illustrated here.

Assuming a simple exponential function $N \sim D^{\alpha}$ for the primary distribution, Soderblom et al. derived a relationship between D_c, the diameter for which the frequencies of primary craters and seocndary craters are equal, and D_{max}, the diameter of the largest primary crater which contributes to the secondary crater population:

$$D_c = D_{max}\left[\frac{\alpha}{(\beta-\alpha)\,k^{\beta}}\right]^{1/(\alpha-\beta)} \qquad /77$$

where $\beta = -3.5$ is the distribution index of the secondary crater distribution

$$N_{sec} = (D_{sec}/KD)^{\beta}$$

N_{sec} is the cumulative frequency of the secondary crater, which is produced by a primary crater with diameter D and D_{sec} represents the secondary crater diameter; k=const. The value for $\beta = -3.5$ stems from observed distribution of lunar secondary craters in scattered fields of primary craters and from studies of experimental nuclear craters (Shoemaker, 1965).

Soderblom et al. (1974) concluded from their investigations, that $D_c \approx 1$ km is a value which is compatible with the contributions of primary craters of the size $D \approx 50$ km (these are the largest craters in the range of their measurement radius) and their conclusions are that the diameter distribution of the Mars crater increasing sharply for $D \lesssim 1$ km arises through the contribution of secondary craters.

This interpretation overlooks the fact that D_{max} is a function of the age, and an accidental consistency for a test region and an age do not provide any generally valid finding.

A correct treatment of the problem for the case of the Moon gives for a simple power size distribution law of the form $N \sim D^{\alpha}$, taking into account the dependence of time of the frequency $N \sim D^{\alpha} \cdot F(t)$ (compare Chapter III.2.) for $N(D_{max}) = 1$ (the largest

crater with diameter D_{max}, which contributes to the secondary crater population)

$$D_{max} \sim F(t)^{-1/\alpha} . \qquad /78$$

For two regions of the Moon of different age, t_1 and t_2, we obtain from $D_c \sim D_{max}$:

$$D_c(t_2)/D_c(t_1) = F(t_2)^{-1/\alpha}/F(t_1)^{-1/\alpha} .$$

If we start from a distribution of primary craters with $\alpha \approx -2$, as observed in the region $D \gtrsim 10$ km, and $t_1 = 3.2 \cdot 10^9$ years, $t_2 = 3.9 \cdot 10^9$ years, we obtain

$$D_c(t_2) \; / \; D_c(t_1) \approx \sqrt{10} .$$

One should therefore establish, as shown in Figure 27, a suitable slipping of the value of D_c with the aid of the populations. But this is not observed. This situation is an argument difficult to contradict against a secondary crater distribution in the region $D \lesssim 1$ km, and speaks clearly in favor of the interpretation that we are dealing with a primary crater distribution in the entire region studied.

A supporting argument for the interpretation as primary crater distribution is provided by comparison of the younger ($t \leq 100$ million years) crater population for the Moon in the region $D > 10$ m and the measurements on Moon soil in the region $D < 1$ cm. Naturally standardization must be carried out on the time integral $F(t)$, while on the basis of the observations it is assumed (see Chapter IV.2.) that the impact rate was constant during the studied time, that is $F(t) \sim t$. In Figure 28 these data are compared with each other. The data for the region $D < 1$ cm come from microcrater measurements on Moon rocks (Neukum, 1971; Hörz et al., 1971; Fechtig et al., 1975) and are consistent with the in situ measurements of interplanetary dust by detectors on spacecraft (Grün, 1981). Only the sharp distribution observed in the region $D > 10$ m is compatable with the measurement in the region $D < 1$ cm. An extrapolation within approximately $N \sim D^{-2}$ of large craters ($D \gtrsim 1$ km) would lead to a discrepency of several orders of magnitude. /81

IV.2. Empirical Relationship Between the Crater Frequencies and Radiometric Ages

By comparison of superimposed crater frequencies of geological units of the Moon relative ages (= crater retention ages) may be determined. This takes place conveniently by measurement of the crater frequencies in suitable diameter ranges which can be covered, an approximation of the lunar standard distribution to

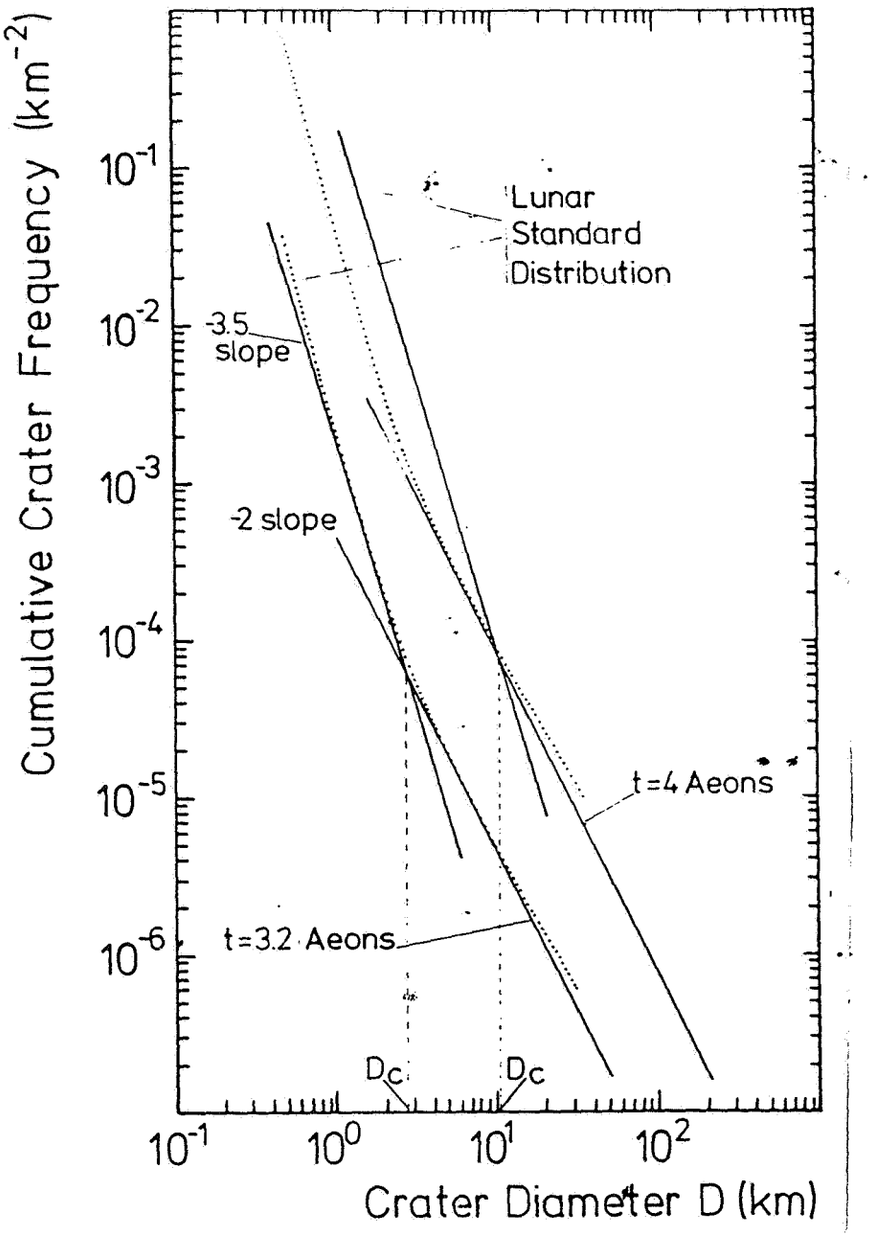

Figure 27. Theoretical dependence of contribution of secondary craters to the primary population, here $N \sim D^{-2}$. The value of D_c should be shifted as a function of time, which is not observed in the lunar crater populations (Standard distribution, dotted line curves). (1 eon = $1 \cdot 10^9$ years).

/80

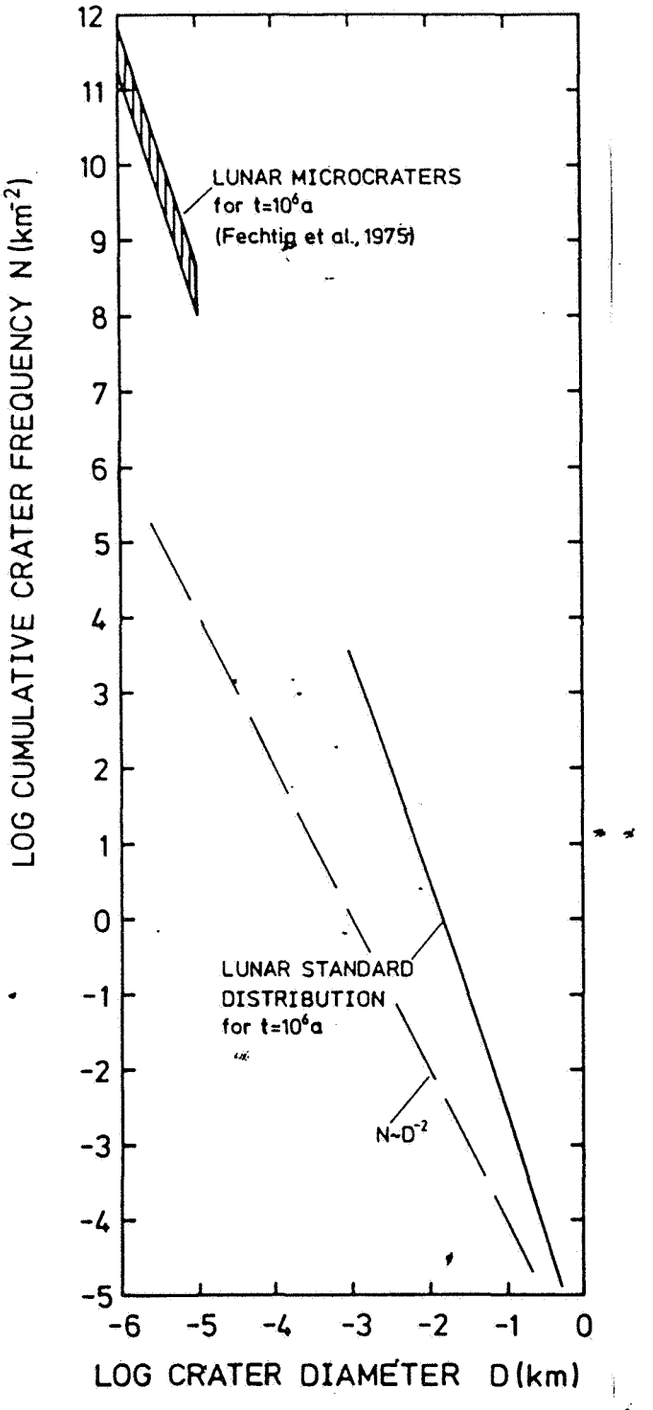

Figure 28. Age standardized ($t=10^6$ years) cumulative distribution in the range D<1 cm (lunar microcrater) and D>10 m. The continuous curve is the lunar crater production distribution (standard distribution) for an age of 10^6 years.

the measurement data with reference to the frequencies of the same diameter. The reference diameter D=1 km proved to be convenient for mare regions and highland regions, which are not much older than the Imbrium basin, since crater frequencies around D=1 km can often be measured directly and thus extrapolations over a too large diameter range can be avoided.

Through the Apollo Moon landings with soil sampling and radiometric dating of the Moon rocks, it is now possible for us to correlate the radiometric age of the rocks of the landing areas with the crater frequencies determined from image data. This correlation allows empirical determination of the lunar impact chronology, that is, the determination of the crater frequency accumulated over a certain period of exposure (= age) on the Moon as a function of the age. By determining these functional dependences, we achieve two scientific goals:

--Absolute determination of age for any regions of the Moon from crater frequency measurements.

--Determination of lunar impact rate as a function of time.

IV.2.1. Cratering Chronology of the Moon /82

The problem of the correlation of crater frequencies of the Apollo landing sites with the corresponding radiometric aga data was discussed by different authors (Shoemaker et al., 1970a, b; Neukum, 1971; Baldwin, 1972; Hartmann, 1972; Soderblom and Boyce, 1972; Soderblom et al., 1974; Neukum et al., 1975b; Neukum, 1977). A comparison of the cratering chronologies of the different orders was carried out by Neukum and Wise (1976) and Neukum (1981). Figure 29 gives a comparison of the different results. The interpretation of the different authors agrees within a factor 2--3.

In recent years the radiometric age data of the Moon rocks were reinterpreted. Moreover, a large number of more exact measurements were carried out on crater frequencies. Furthermore our knowledge of the lunar crater production distribution (compare Chaper IV.1) improved considerably primarily in the region of large craters. This development makes a new analysis of the lunar cratering chronology necessary, which is carried out below.

Figure 30 gives a survey of the front side of the Moon with the landing sites of the American Apollo missions and the Soviet Luna missions. A detailed description of the landing sites and type of samples collected may be found, for example, in the publication by Taylor (1975). Here some characteristics of crater populations and rock ages of the landing sites used to determine the cratering chronology and the relevant structures will be given (compare also Basaltic Volcanism Study Project, 1981). The crater frequency measurements used to determine the

cratering chronology are shown in Figure 31. Compilations of radiometric image data are shown in Figure 32 (mare rock ages) and Figure 33 (highland rock ages). /85

/83

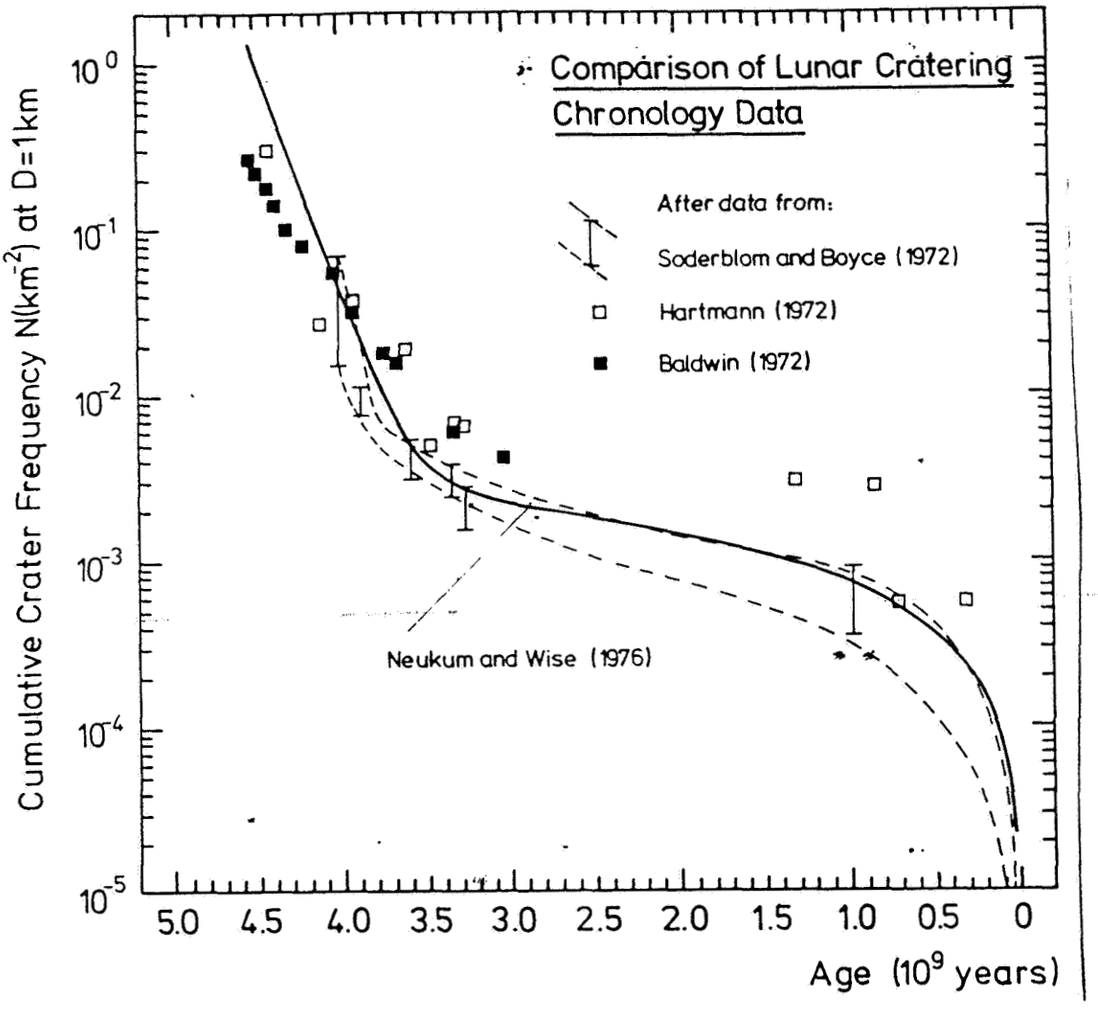

Figure 29. Comparison of lunar cratering chronology data (Figure: Neukum, 1981).

/84

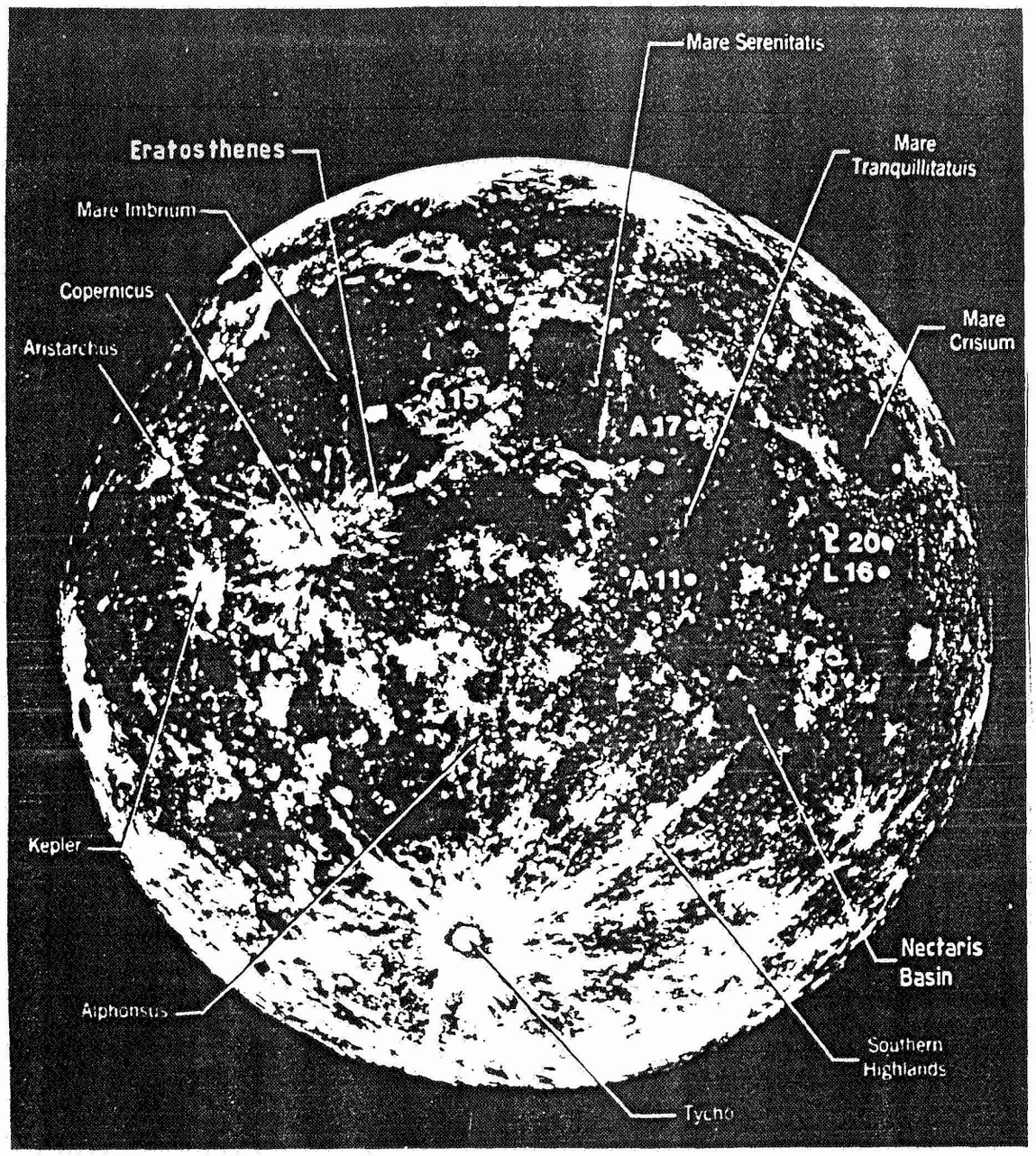

Figure 30. Front side of the Moon with location of the Apollo and Luna landing sites and prominent structures.

1. Mare Data

The age data compiled in Figure 31 of lunar mare basalt confirm the situation discussed in detail by Neukum and Horn (1976), that the Apollo landing sites, like the other mare regions of the Moon) were affected partly over several hundred million years by consecutive lava overflows. In particular, the Apollo 11 landing site show two distinct age groups ("High-K" and "Low-K" basalts). The other landing sites show less marked age spread, but the indefiniteness in the age of the "geological unit" is typically ±100 million years. (The error in the radiometric age determinations is typically less than 50 million years). All ages except the one for the Luna 16 landing site have been covered sufficiently by measurement points.

The crater frequency distributions, and the Apollo 11 landing in particular (Figure 31; compare also Figure 26), show partly certain irregularities, corresponding to several lava flows. The Apollo 12 distribution shows irregularity typical of a two-stage lava flat history; but a direct correlation of the two populations with the age data is not apparent, so that only an average frequency can be correlated here with the average age.

In Figure 31 the crater frequency is shown, which was measured on the Tycho crater (compare Figure 30) (Neukum and König, 1976; König, 1977). The age of this crater cannot be determined directly because of the want of rock samples. But ejection material from Tycho seems to have deposited at the Apollo 17 landing site (Howard, 1973; Muehlberger et al., 1973; Lucchitta, 1975; Wolfe et al., 1975; Arvidson et al., 1976).

Thus, secondary craters have been produced resulting in the /88
fresh exposure of rock from lower layers. The exposure ages show an accumulation at 109 million years (Guinness and Arvidson, 1977), the most probable age of the Tycho crater and its secondary craters and the Apollo 17 landing site. Similarly, the conclusion was drawn that the Apollo 12 rock samples collected were ejection material from the crater Copernicus (Shoemaker et al., 1970b) which indicates an age of 850 million years for Copernicus (Silver, 1971; Eberhardt et al., 1973; Alexander et al., 1973). The crater frequency data (Figure 31) were measured on Copernicus itself (Neukum and König, 1976; König, 1977).

2. Highland Data

The lunar highland rocks consist usually of brecchia highly metamorphized by meteorite impact (compare Stöffler et al., 1979). A part of the inclusion underwent in this connection heating of several hundred degrees Celsius, a small portion (several weight-percent of ejection material, compare Stöffler, 1981) was totally melted. Therefore it may be expected that the

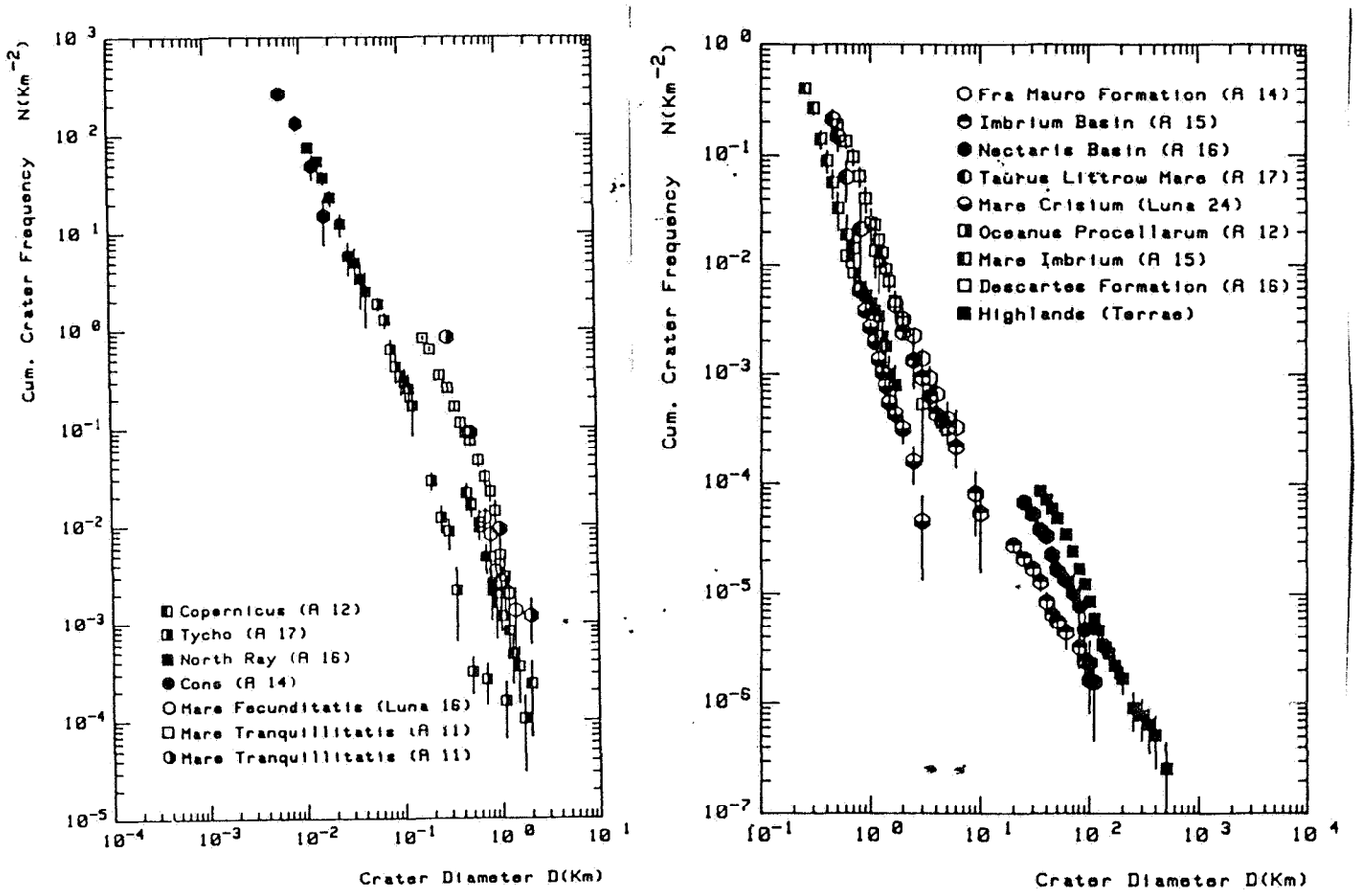

Figure 31. Frequency distribution of crater populations of the Apollo and Luna landing sites and others to determine the crater chronologies of relevant structures (Data Shoemaker et al., 1970; Greeley and Gault, 1970; Neukum et al., 1975a; Neukum and König, 1976; König, 1977; Wilhelms, 1979; Moore et al., 1980; Neukum and Wilhelms, 1982).

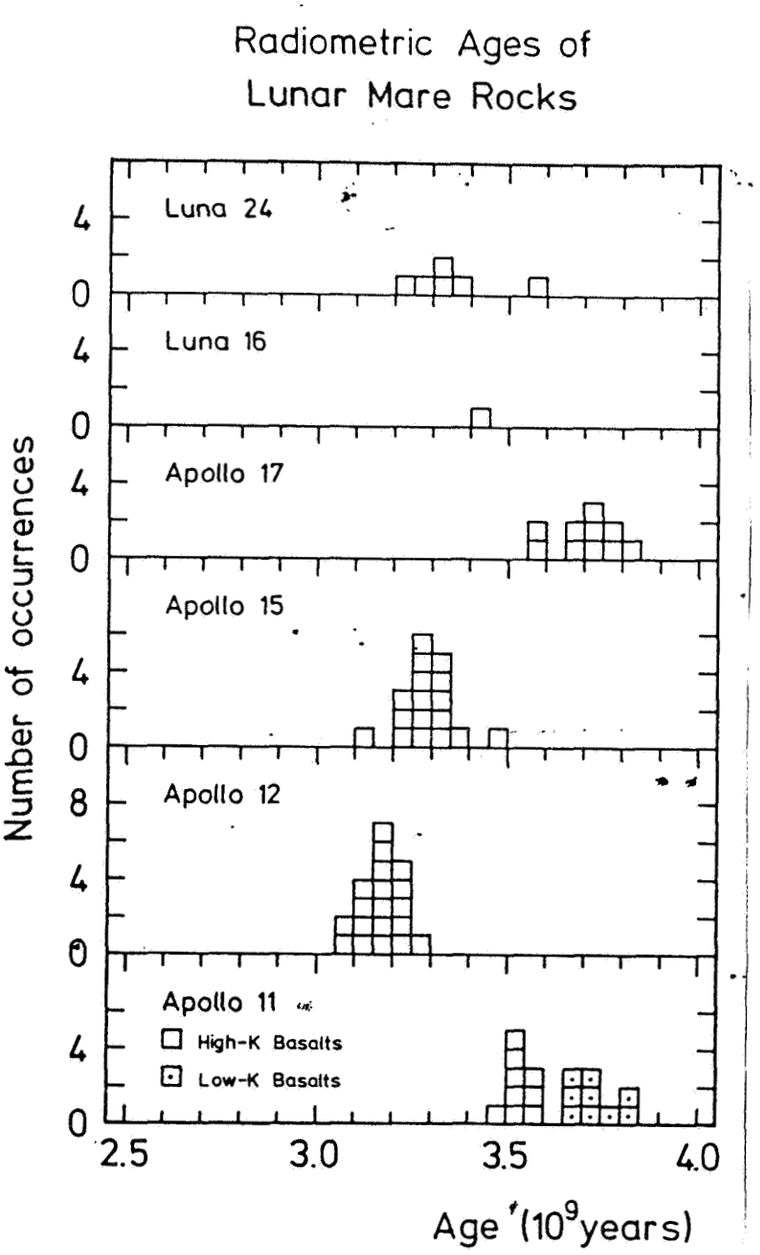

Figure 32. Histograms of radiometric ages of lunar mare rocks (compilation of data from Basaltic Volcanism Study Project, 1981).

radiometric age data do not show a sharp clear metamorphosis age but a more or less broad distribution, as may be seen in Figure 33. The interpretation of these data however, is very diverse (compare Basaltic Volcanism Study Project, 1981; Turner, 1977; Tera and Wasserburg, 1974; Maurer et al., 1978; Schaeffer et al., 1976; Kirsten and Horn, 1974; Jessberger et al., 1977). On one hand the large impacts, which produce basins like Imbrium and Nectaris, have certainly caused considerable redistribution by ejection of material over large regions of the Moon. In the vicinity of the basins it is more probable to find material which shows impact metamorphosis caused by impact processes. On the other hand, at the time of production of the large basins and even after deposit of their ejection material, smaller craters have had a locally limited strong effect of redistribution and metamorphization of material. Moreover, ejection material from large craters, in particular large basins, can be mixed strongly in the deposit with local material (Oberbeck et al., 1977). The quantization of the complicated processes and their corresponding effect on the rocks is very difficult. /90

The interpretation favored in the relevant literature for highland dating is that the effect of large impacts on local events may well have dominated and the age distribution in Figure 33 reflects the recession of the radiometric data by the formation of large lunar ring basins. Tera et al. (1974) drew from the occurrence of age accumulation at a value of about 4 billion years, the conclusions that at that time the impact rate was extremely high, higher than after or before, and called this bombardment "terminal lunar cataclysm". Later analyses of many authors (above mentioned references) showed that very different age groups can be identified in the data. The interpretations of the age distribution and the assignment to different basins are, however, still very controversial, while basically two positions must be differentiated (compare Basaltic Volcanism Study Project, 1981):

a) Formation of all large basins of the front side of the Moon within less than 100 million years within the period of 3.8 to 3.9 million years ago (defenders of the idea of "terminal lunar cataclysm").

b) Continuous decrease of the impact rate of formation of large basins between about 4.4 and 3.8 billion years.

Hereafter arguments will be given in favor of the impact rate (including large basins) undergoing a sharp (but continuous decrease between about 4.4 and 3.8 billion years, and that the occurrence of a "terminal lunar cataclysm" is suggested neither by the radiometric age data nor by the geological observations.

The interpretation of the age data in this study states that /91
the peak of the distribution of Figure 33 reflects approximately the time of turning back the radiometric clock through a large

/89

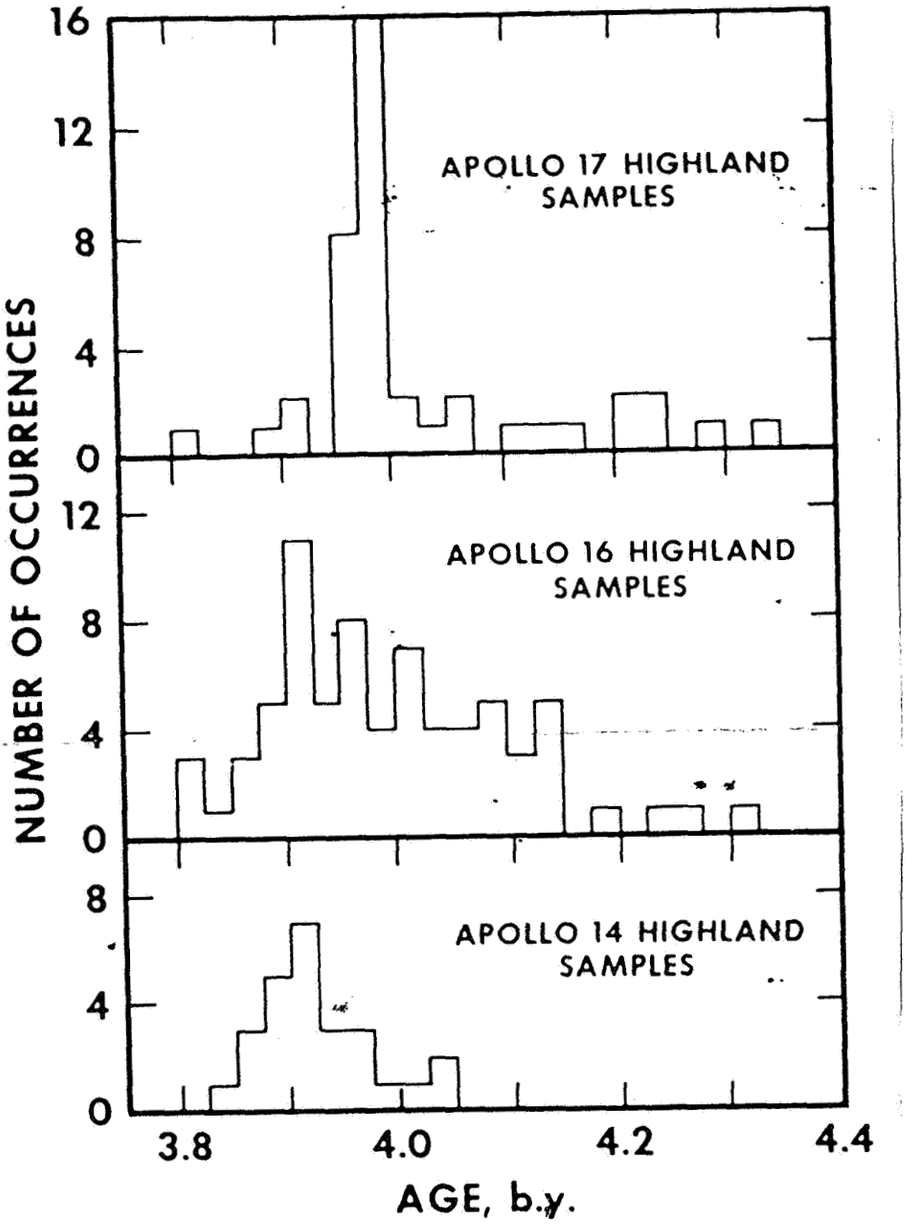

Figure 33. Histograms of radiometric ages of lunar highland rocks (Figure: Basaltic Volcanism Study Project, 1981).

impact event. This controdicts an interpretation which is given by many authors (compare Jessberger, 1981; Basaltic Volcanism Study Project, 1981), in which the youngest ages of some totally melted inclusions of the rock give the time of the event. Here this interpretation was not followed, since local impacts after the large event connected with the basin have probably contributed to the impact metamorphosis and the reduction of the radiometric aid. We interpret the latest melting processes as at least partly local effects.

In the interpretation of the age of the highland rocks it should be taken into consideration that the Imbrium event has affected a considerable portion of the front side of the Moon and that Imbrium ejection material was deposited in large amounts also in the Apollo landing areas, 14, 15, 16 and 17. Figure 34 shows the distribution of Imbrium and nectarian materials or basins of the front side of the Moon. The material in the landing areas consists mainly of Imbrium ejecta, in the Apollo 16 landing area (compare Figure 35), however, a very large contribution of nectaris ejection may also be expected.

A detailed discussion of the problems of the thickness of the basin ejecta at the Apollo landing sites was carried out by McGetchin et al. (1973) (Figure 36). In spite of the criticism of the results (for example, Pike, 1974), the estimate by McGetchin et al. may well be qualitatively correct and shows clearly that in the Apollo 14, 15 and 17 landing sites, great thicknesses of Imbrium ejection material should occur as the upper layer, apart from a possible thin layer of oriental ejection. Moreover, in the Apollo 16 landing site, nectaris ejection material occurs in very large thickness (several hundred meters), but at greater depth. Of course, east of the landing area we have the hilly Descartes formation and the Kant Plateau (Figure 35) /94 which are interpreted mainly as nectaris ejection material. The probability of collecting nectaris ejection at the Apollo 16 landing site is thus relatively high.

In the more exact study of the Apollo-16 rocks, two age accumulations are found (Maurer et al., 1978). These age data are shown in Figure 37. We interpret the peak at $4.1 \cdot 10^9$ years as the age of the nectaris ejecta at the Apollo-16 landing area. A similar interpretation was put forward by Wetherill (1981).

Imbrium ejection material should occur also in great thickness at the Apollo-17 landing site (edge of the Serenitatis Basin) (Figure 36). Under it probably lie layers of serenitas ejection itself and ejecta of the Crisium Basin. The stratigraphic sequence, as given by Figure 36, is however, not sure (Neukum and Wilhelm, 1982). The age data (Figure 33) show a well defined peak at 4 billion years, which could be assigned both to the Imbrium event and the Serenitatis or Crisium event. Unfortunately the analysis of the crater population on the Serenitas edge also shows that there is crater size distribution highly

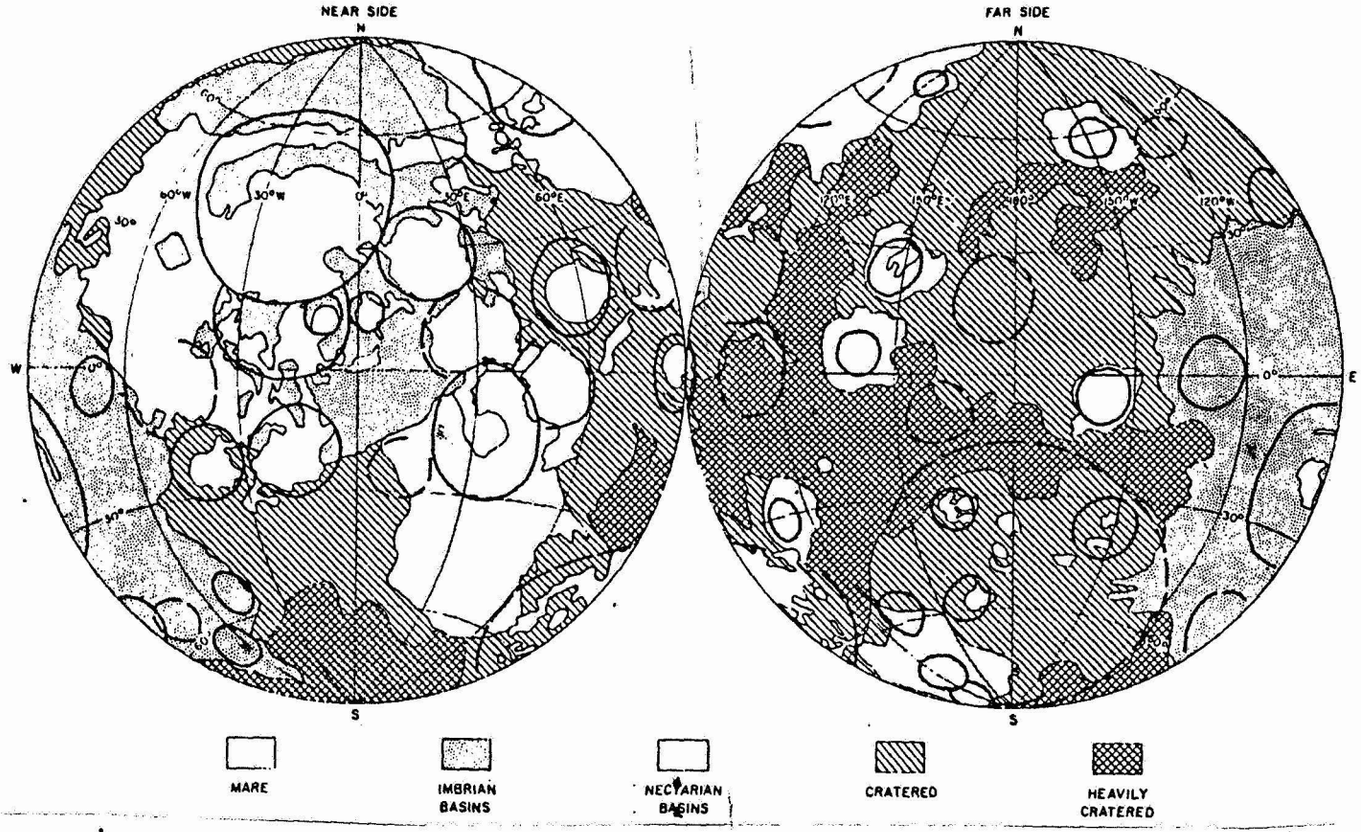

Figure 34. Map of the distribution of large basins (D>200 km) of the Moon and the Imbrium and nectarian materials (Figure: Taylor, 1982).

/93

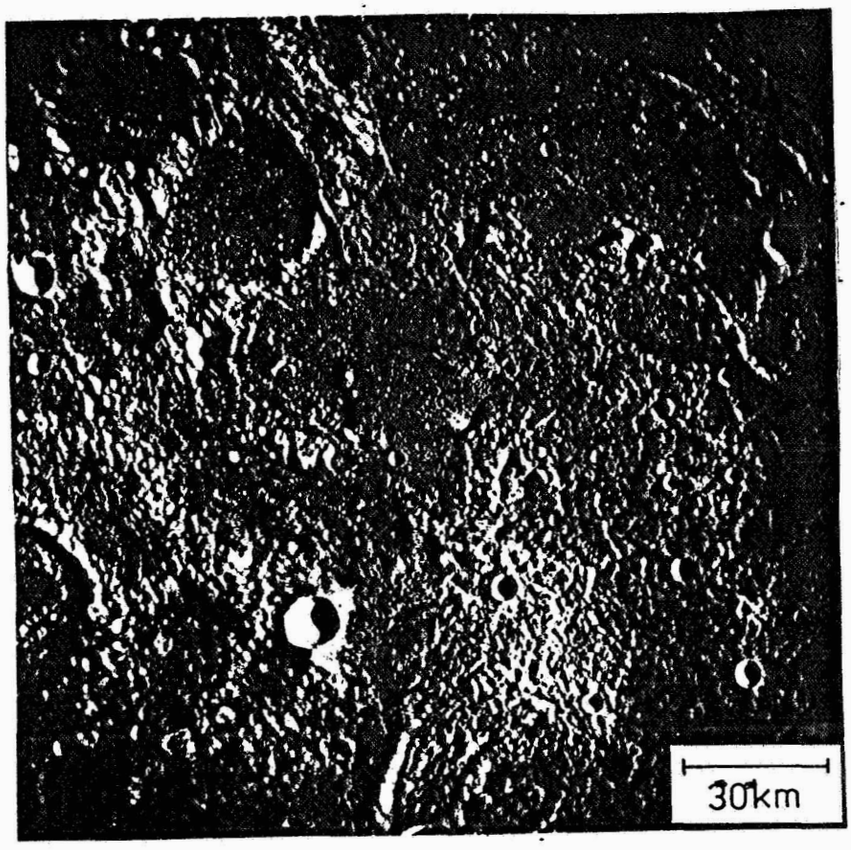

Figure 35. Apollo 16 landing area (cross) with the light plains of the Cayley formation in the west (probable Imbrium ejecta) and the hilly Descartes formation (possibly nectaris ejecta) in the east. The influencing of the region by Imbrium ejecta may be recognized from the furrowed surface with lineations from northwest to southeast (especially top left).

disturbed by the alternating superimposition with ejection material: the smaller craters (D<10 km) show Imbrium crater frequencies, that is, are accumulated after superimposition with Imbrium ejection (Neukum, 1977a). The larger craters are very strongly eroded, partly filled up, and really difficult to determine quantitatively, so that pre-Imbrium crater frequencies cannot be indicated with certainty. The question of correlation of the Serenitatis age data with crater frequencies must therefore be left open.

In the assignment of highland rock ages to crater frequencies, the procedure is such that both age and crater frequency of the landing areas themselves are involved. In some cases however, the genetic assignment must be taken into account, such as, for example, in the case of the crater frequencies which were measured on nectaris material lying far away (for example, on the basin edge). The assigned age is then the value which was obtained from the Apollo rock ages taking into account the genetic relationships (such as, for example, the age of the Nectaris Basin from Apollo-16 data). /96

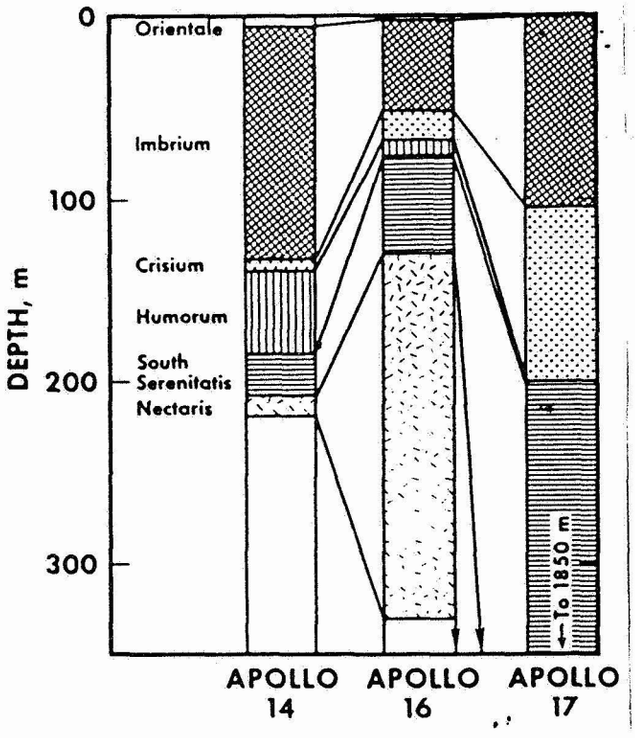

Figure 36. Average thickness of the ejection materials of lunar basins at the Apollo-14, 16 and 17 landing sites (Figure: McGetchin et al., 1973).

The crater frequency data for the craters North Ray (Apollo-16 landing site) and Cone (Apollo-14 landing site) were determined on their ejecta cover (König, 1977; Moore et al., 1980). Assigned ages are the exposure ages of the ejection material with values of 50 and 24 million years (Drozd et al., 1974).

A comparison of the lunar crater frequencies and assigned ages for mare and highland regions is given in Table 2. In addition, the production frequency of terrestrial phanerozoic craters (North America and Northern Europe) converted for lunar impact conditions (see Chapter IX) and assigned age of the cratons are given (data Grieve and Dence, 1979; reinterpreted). The crater frequencies are listed in values of cumulative frequencies for D=1 km and D=10 km, which were obtained through the lunar standard distribution from the data of Figure 31.

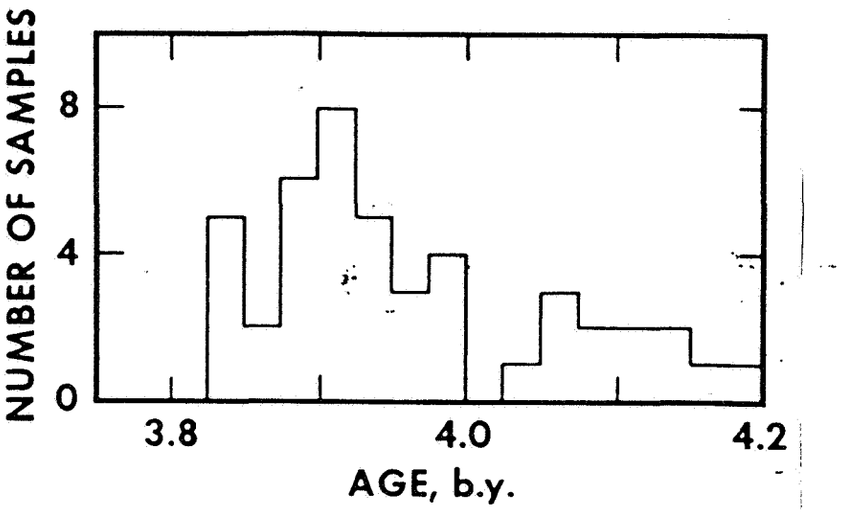

/95

Figure 37. Histogram of highly precise $^{39}Ar/^{40}Ar$ ages of Apollo-16 rock samples (Figure: Basaltic Vocanism Study Project, 1981; original data of Maurer et al., 1978).

/96

The lunar impact chronology is obtained from the correlation of the crater frequencies with the radiometric ages, as shown in Figure 38. The correlation is basically identical with those of Neukum (1977) and Neukum and Wise (1976).

The mathematical expression of the impact chronology curve is:

$$N(1) = 5.44 \cdot 10^{-14}(\exp(6.93 \cdot t)-1) + 8.38 \cdot 10^{-4} t.$$

N(1) is the cumulative crater frequency per km^2 at D=1 km; t is the age in units of 10^9 years.

/98

Through this relationship it is possible to determine absolute ages for any surfaces of the whole of the Moon by measurements of the crater frequency on image data. The time resolution is good for the range $4.5 \cdot 10^9$ years > t>$3.5 \cdot 10^9$ years. For a typical error in N of less than ±30% this means a time resolution of better than 30 million years, not counting errors in the impact chronology determination.

In the range t<3.10^9 years, the error in the time resolution is linear in N. For ages $3 \cdot 10^9$ years > t>$1 \cdot 10^9$ years, the curve is not covered by measurement points, but interpolated between the average values around t=$3.2 \cdot 10^9$ years and t<$1 \cdot 10^9$ years.

In Figure 38 the dependence on t is only given for D=1 km and D=10 km. The general dependence with regard to the crater diameter is defined by the lunar production crater frequency

TABLE 2. CRATER FREQUENCY OF LUNAR STRUCTURES AND TERRESTRIAL PHANEROZOIC CRATERS AND ASSIGNED ABSOLUTE AGE

/97

Lunar or terrestrial structure	N(D=1)(km^{-2})	N(D=10)(km^{-2})	Age (10^9a)
Highland (Terrae)	$(3.6 \pm 1.1)\ 10^{-1}$	$9.2\ 10^{-4}$	4.35 ± 0.10
Nectaris Basin (A 16)	$(1.2 \pm 0.4)\ 10^{-1}$	$3.1\ 10^{-4}$	4.10 ± 0.10
Serentitatis Basin (A 17)	-	-	3.98 ± 0.05
Descartes Formation (A 16)	$(3.4 \pm 0.7)\ 10^{-2}$	$8.7\ 10^{-5}$	3.90 ± 0.10
Imbrium Basin (A 15)	$(3.5 \pm 0.5)\ 10^{-2}$	$8.9\ 10^{-5}$	3.91 ± 0.10
Fra Mauro Formation (A 14)	$(3.7 \pm 0.7)\ 10^{-2}$	$9.4\ 10^{-4}$	3.91 ± 0.10
Taurus Littrow Mare (A 17)	$(1.0 \pm 0.3)\ 10^{-2}$	$2.6\ 10^{-5}$	3.70 ± 0.10
Mare Tranquillitatis (A 11)	$(9.0 \pm 1.8)\ 10^{-3}$	$2.3\ 10^{-5}$	3.72 ± 0.10
Mare Tranquillitatis (A 11)	$(6.4 \pm 2.0)\ 10^{-3}$	$1.6\ 10^{-5}$	3.53 ± 0.05
Mare Imbrium (A 15)	$(3.2 \pm 1.1)\ 10^{-3}$	$8.2\ 10^{-6}$	3.28 ± 0.10
Oceanus Procellarum (A 12)	$(3.6 \pm 1.1)\ 10^{-3}$	$9.2\ 10^{-6}$	3.18 ± 0.10
Mare Fecunditatis (Luna 16)	$(3.3 \pm 1.0)\ 10^{-3}$	$8.4\ 10^{-6}$	3.40 ± 0.04
Mare Crisium (Luna 24)	$(3.0 \pm 0.6)\ 10^{-3}$	$7.6\ 10^{-6}$	3.30 ± 0.10
Copernicus (A 12)	$(1.3 \pm 0.3)\ 10^{-3}$	$3.3\ 10^{-6}$	0.85 ± 0.2
Tycho (A 17)	$(9.0 \pm 1.8)\ 10^{-5}$	$2.3\ 10^{-7}$	0.109 ± 0.004
North Ray (A 16)	$(4.4 \pm 1.1)\ 10^{-5}$	$1.1\ 10^{-7}$	0.0500 ± 0.0014
Cone (A 14)	$(2.1 \pm 0.5)\ 10^{-5}$	$5.3\ 10^{-8}$	0.0260 ± 0.0008
Phanerozoic craters (North America+Europe, lunar equivalent)	$(3.6 \pm 1.1)\ 10^{-4}$	$9.2\ 10^{-6}$	0.375 ± 0.075

distribution, that is, the lunar standard distribution. Through this function equivalent frequencies can be indicated for any diameter.

IV.2.2. Dependence on Time of The Impact Rate

The cumulative impact rate ϕ is given by deducing in time the impact chronology relationship $\partial N/\partial t=\phi$. The result for D=1 km is:

$$\phi(1) = 3.77 \cdot 10^{-13} \exp(6.93 \cdot t) + 8.38 \cdot 10^{-4} \ (km^{-2}\ 10^{-9}\ years^{-1}).$$

where t is to be indicated in units of 10^9 years. This function is shown in Figure 39 in units ($km^{-2}10^{-8}$ $years^{-1}$). Between 4.5 and 3.5 $\cdot$ 10^9 years an exponential decrease of the impact rate is obtained ("Smooth Decay") with a time constant $\tau=1/\lambda=1.44 \cdot 10^8$ years for a half life $T_{1/2}=1.0 \cdot 10^8$ years. For $t<3 \cdot 10^9$ years we obtain a constant value of the cumulative impact rate of $\phi=8.38 \cdot 10^{-5}$ ($km^{-2}10^{-8}$ $years^{-1}$). The constancy of the rate during this period is confirmed very well by the measurement points for $t<1 \cdot 10^9$ years. In earlier publications (Hartmann, 1972; Neukum et al., 1975b; Neukum and Konig, 1976; Shoemaker et al., 1979) the data for $t<1 \cdot 10^9$ years seem to indicate a higher impact rate than on the average for the last 3 $\cdot$ 10^9 years. The new, more certain data show that the earlier interpretations are not supported. In particular, the terrestrial data (phanerozoic craters) were earlier systematically too high to be adjusted entirely within the figure to the impact rate constant over the last 3 $\cdot$ 10^9 years. The terrestrial frequencies derived from the very carefully conducted investigations by Grieve and Dence (1979) are very consistent, however, with the lunar data, after conversion to lunar impact conditions. Only the Copernicus point (like before) is too high. The value for the crater frequency was ascertained several times. But it is quite possible that the interpretation of the Copernicus age from measurements of the Apollo-12 samples is wrong. /101

For t=0 (today) from Shoemaker et al. (1979) a value for the impact rate of the Apollo-Amor asteroids (compare Meeus and Combes, 1974) converted to D=1 km and D=10 km is given. This value is too high by a factor 3 as compared with the relationship obtained from the lunar measurements. The determination of the Apollo-Amor impact rate is <u>a priori</u> exposed to great uncertainties because of the imprecise knowledge of their frequencies and difficult diameter determination (conversion from albedo values). Kresak (1980) gives, for example, impact rates which lie below the values of Shoemaker et al. (1979) by a factor 3, but are very consistent without data. Another problem is the conversion of asteroid diameter into crater diameters ("Scaling law") (compare Chapter IX). The deviation of the Shoemaker diameter could by explained already by systematic error of this type on the order of a factor 2 in the diameter ratio (compare

/99

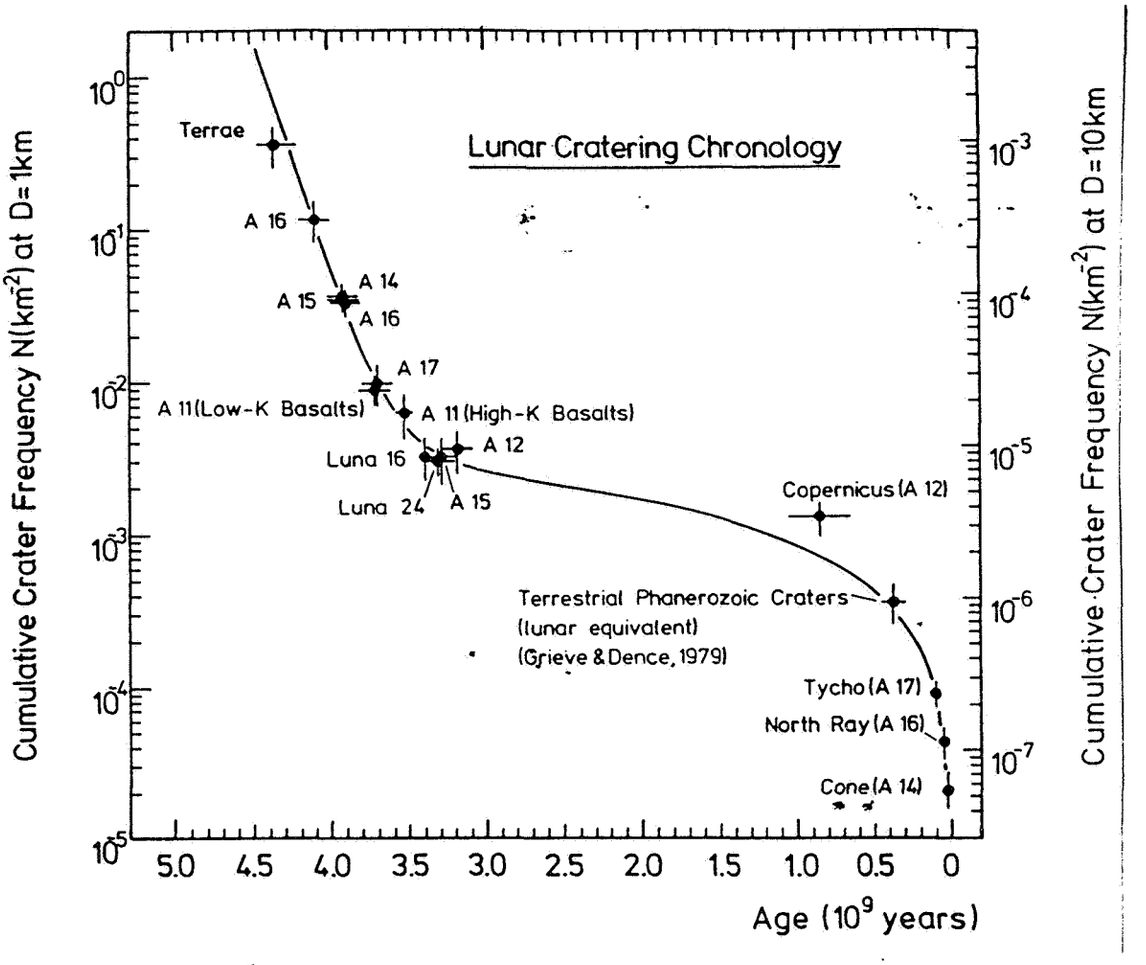

Figure 38. Lunar Impact Chronology.

Figure 63).

/101 It is very informative to consider on one hand, how many craters of a certain size could have been expected during the last 100 million years on the Moon or on the Earth. The lunar /102 chronology and the lunar crater size production distribution may be converted to terrestrial impact conditions according to the relationships discussed in Chapter IX. From this, we may derive a functional dependence of the crater diameter on time, for craters which have been produced on an average (N(D)=1). This functional dependence is shown in Figure 40. Thus, on the average, at least one crater must be expected on the Earth with a diameter of D≥100 km per 100 million years. The effect of the Earth and its climate, primarily when such an impact had taken place in the ocean (evaporation of giant amounts of water) could be very great. It is therefore quite possible that such an impact could have been causally responsible for the catastrophic change in

/100

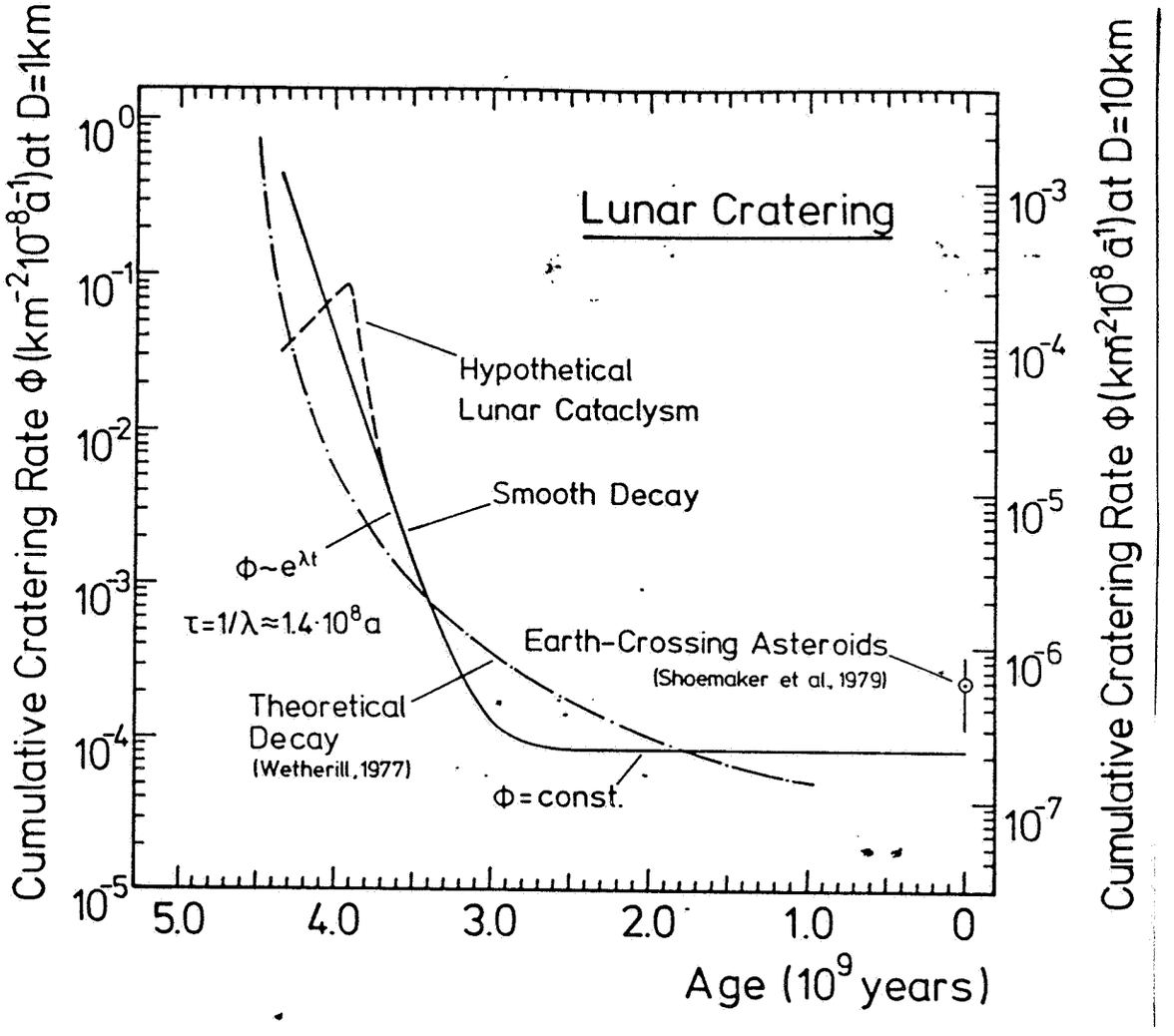

Figure 39. Dependence on time of the lunar impact rate.

climate in the biosphere, with the elimination of the entire species on the Cretacean-Tertiary boundary, as has been speculated upon by different authors (for example,,Alvarez et al., 1980).

The appearance of very large impact structures with diameters of possibly several thousand kilometers (Figure 40) more than $3.8 \cdot 10^9$ years ago may well have influence permenantly the young crust of the Earth, so that it could have become stable only later. This would probably be one of the reasons why unlike the Earth's Moon, no rock age of $>3.8 \cdot 10^9$ years was observed.

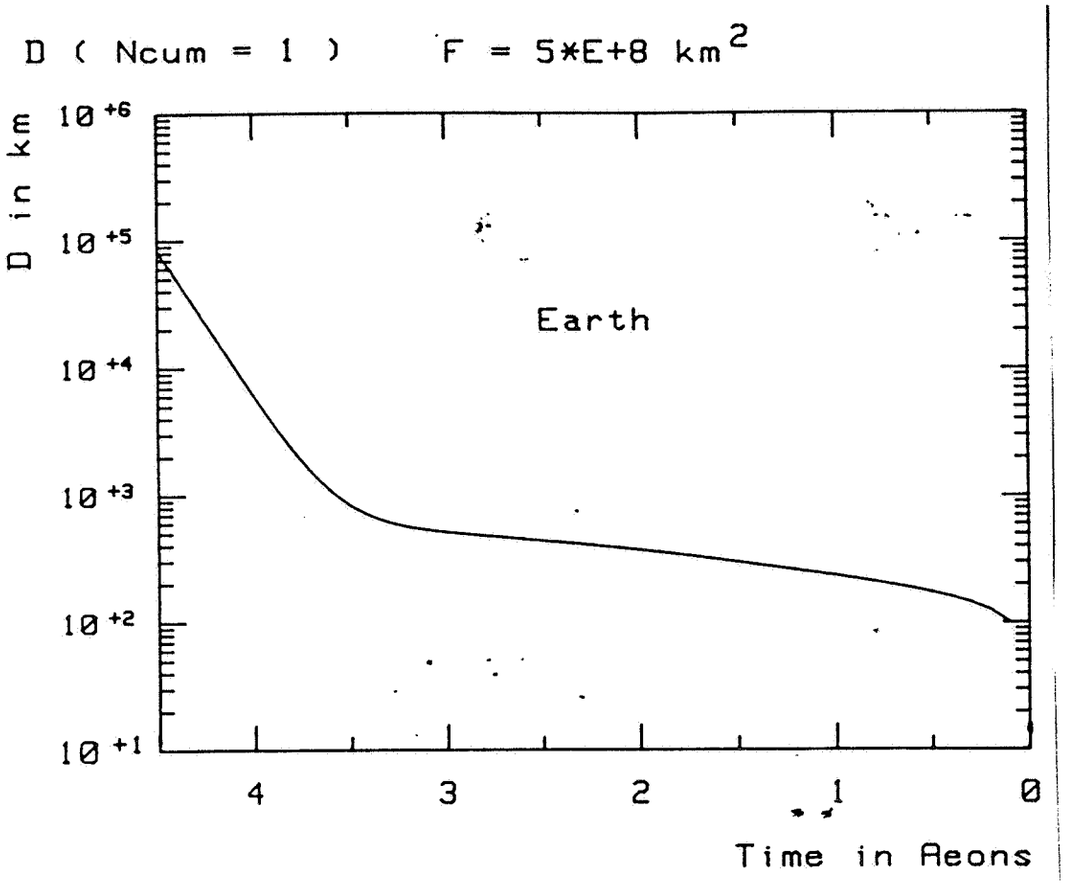

/103

Figure 40. Crater size and function of the age for the entire surface of the Earth for an impact to be expected once in the average time and of the magnitude $\geq D$, $(N(D)=1)$. (1 Eon = 10^9 years).

IV.2.3. Was There a "Terminal Cataclysm" of Meteorite Bombardment 4 Billion Years Ago?

/102

As discussed before, the accumulation of highland rock ages at $4 \cdot 10^9$ years led to arguments by various authors that at that time the impact rate may have been much higher that before or afterwards, that is, a "cataclysm" or "terminal cataclysm" if the lunar meteorite bombardment may have taken place (Tera et al., 1974). There are many dynamic arguments (compare Wetherill 1975; 1976) to the effect that the production of such a fluctuation in the impact rate, which must have also taken place for all terrestrial planets, would only be possible by means of events of very low probability, such as, for example, the destruction of a large body within the Roche limit of the Earth with production of many small bodies of masses around 10^{20}--10^{23} g, which were then

/104

redistributed in the internal Solar System and would produce the large basins. Populations of bodies in moderately eccentric orbit would have developed, however, in such a way as shown in Figure 39 ("Theoretical Decay"). Such a small decrease of the impact rate, although not necessarily as precise as the one shown, and based on certain initial values, is much more likely to be expected theoretically. The theoretical discussion of this topic is however very complex and is at present the object of intensive research (compare Wetherill, 1981).

Hereafter arguments will be put forward which are derived from the direct observations and seem to oppose, or at least are not in favor of the "terminal cataclysm".

In Figure 39 a "hypothetical lunar cataclysm" is indicated (in dashed lines). This is the dependence on time of the impact rate, which would have been obtained, say, if the large basins of the front side of the Moon (Imbrium, Serenitatis, Crisium, Humorum and Nectaris) had been produced within the period of 3.8 to $3.9 \cdot 10^9$ years ago, as is favored by some authors on the basis of their age measurements (for example, Jessberger, 1981). But this would immediately lead to difficulties with the stratigraphic data, since the predominant number of craters and large basins ($D>20$ km) are of pre-nectarian age (Wilhelms, 1979; Neukum and Wilhelms, 1982), that is, the impact data must have been previously higher, not lower. This situation may be seen in detail from the basin frequencies given in Table 3 and applies in very similar proportions to smaller craters (compare Figure 26).

Naturally it is possible that in the oldest crater populations /105
we are looking back only 4 to $4.1 \cdot 10^9$ years and the lunar highland crust could not carry the impacts before that time. However, this is contradicted by the early differentiation of the lunar highland crust around $4.4 \cdot 10^9$ years (compare Basaltic Volcanism Study Project, 1981).

Another argument in favor of a smooth decrease comes from the crater population data themselves. The distributions show the same characteristics over all ages (compare Figure 26). There seems to be one population of objects with constant size distribution, whose impact rate decreased in the approximately exponential manner after the accretion of the Earth-Moon system.

In Figure 41a the cumulative crater size distribution is shown, as measured in the oldest regions of the Moon. One characteristic of the distribution is that for $D>80$ km, the /107
distribution decreases relatively sharply, say according to $N \sim D^{-2.9}$, but for $D>200$ km, there is a dependence according to $N \sim D^{-1.5}$. Figure 41b shows even more clearly this variation in the distribution law by representing the data in relative distribution. Very similar characteristics are found in the oldest populations of the Moon and Mercury (compare Chapter V, VI). The diameter range $D>200$ km is a region of the large ring

basins, whose frequency decreases much less according to the diameter than that of the craters in the region D<200 km. (Here the innermost ring is chosen as the diameter of the basin. If its most prominant ring was chosen as the basin diameter, the distributions would decrease even more smoothly, say according to $N \sim D^{-1}$). Now it could be argued in the sense of the "cataclysm" hypothesis that the large basins were produced by a special population of objects, and these objects may be responsible for the presumably increased appearance of large basins 3.9 to 4 billion years ago. But as we showed before, there is no obvious recognizable break in the size distribution of large craters of basins and as a function of the impac rate of the corresponding size range. Nevertheless, it has not so far been explained why such a striking difference in the appearance of large impact structures on the Moon is observed over a period of a few hundred million years and ages $>3.8 \cdot 10^9$ years. The appearance of large basins on very old surfaces of the Moon and Mars and Mercury (and their nonexistence in regions of ages which are only a few hundred million years less) defines a relatively sharp time horizon ("marker horizon", Wetherill, 1981).

TABLE 3. LUNAR BASIN FREQUENCIES FOR D>265 KM. (Neukum and Wilhelms, 1982)

	Number
Imbrium Basin	3
Nectarian Basin	11
Pre-Nectarian Basin	30*)

*)12 basins are included, whose existence is not fully certain (very old, eroded structures).

We may show that the combination of the fast decrease of the impact rate along with a special characteristic of the size distribution of the ring basin causes this effect of "marker horizon". In Figure 42 for the Earth's Moon the crater size to be expected on the average one (for N(D)=1) is plotted as a function of the age. In case a) the distribution characteristics shown in Figure 41 for small craters, $N \sim D^{-2.9}$, are used in the entire diameter range D>100 km. In case b) the actually observed distribution approximated by the lunar standard distribution is used with the smooth size distribution of the large basins. Thue it is found (for the same dependence on time of the impact rate) that the particular distribution characteristics of the large craters and basins leads to the striking difference /109

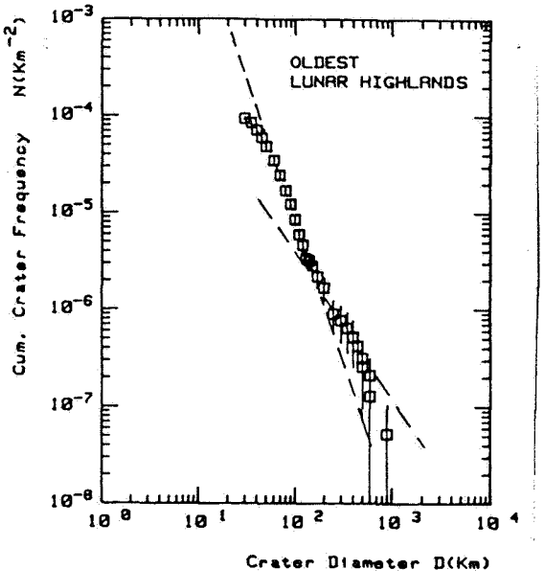

Figure 41a. Cumulative size distribution of crater populations of the oldest parts in the lunar highland. For comparison distributions $N \sim D^{-2.9}$ and $N \sim D^{-1.5}$ are plotted.

in the curves of large impact structures over only a hundred to 200 million years of difference in age. This special characteristic of size distribution results therefore in an effect which produces so to say, a "overincrease" of the decrease of the bombardment with a sudden appearance of the ring basin at a time (looking back into the past) and forwhich we have N(D=200 km)=1.

With the above given arguments it cannot be proved necessarily that a smooth decrease of the impact rate must have taken place. The studies of the crater population and the stratigraphic data however indicate a smooth decrease and are against a "terminal cataclysm" of the impact rate. The age data also do not compel us in any way to take an interpretation in favor of a "terminal cataclysm", but are fully compatible with the uncertainties in the interpretation of measurements with a smooth decrease of the impact rate, as was obtained here.

IV.3. Examples of Relative and Absolute Dating of Lunar Structures Through Crater Frequency

The lunar stratigraphic system refers to large impact structures and their materials (compare Shoemaker and Hackman, 1962; Mutch, 1972). It is represented in a modern form (Wilhelms, 1983) in Figure 43 combined with absolute age data of stratigraphic units through direct radiometric dating of Moon rock and through the determination of crater retention ages and application of Moon impact chronology. The relative and absolute assignment of age /111
to lunar structures through crater frequency measurements is possible in general with this now completely defined system with regard to relative and absolute crater retention age.

The determination of the relative age of very large lunar craters was carried out by Neukum and Konig (1976). Wilhelms (1979) and Neukum (1977b) measured crater frequencies on large basins for the stratigraphic assignment of the these structures. The application of lunar standard distribution and impact chronology gives the relative and absolute ages listed in Table 4.

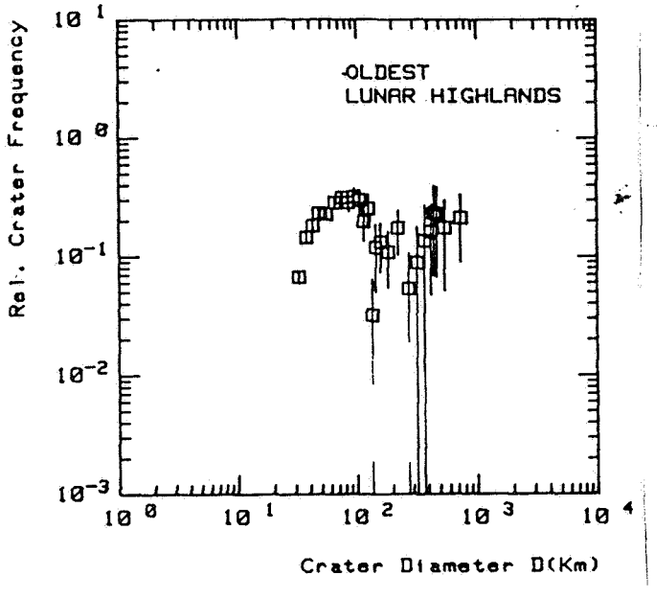

Figure 41b. Relative size distribution of the crater populations of the oldest portions of the lunar highlands. In the region D<60 km the population is no longer entirely in the production state (part of the craters were eliminated by superimposition of other impacts), and this shows approximately the same decreasing distribution characteristics as the production size distribution. (Compare Figure 25).

From the radiometric age data of the Mare Basalt, the conclusion may be drawn that the filling of the lunar maria with basaltic lava took place at the time of about 3.1 to 3.8 · 10^9 years ago. Crater data showed that in all probability however, the volcanic activity of the Moon lasted longer and began already earlier, particularly in the highland (compare Neukum, 1977b; Ryder and Spudis, 1980; Basaltic Volcanism Study Project, 1981).

Boyce et al., (1974) drew from their data the conclusion that the youngest lava flows in the Mare Imbrium (compare Figure 12) are much younger than 3 · 10^9 years, with the most probable age around 2.5 · 10^9 years. Crater frequency data of Neukum and König (1976) and the use the lunar impact chronology presented here give an age between 2.8 and 3 · 10^9 years. Younger regions have not been found so far. The basaltic volcanism of the Moon ended accordingly later, about 2.5 billion years ago. After this period of endogenous activity, the face of the Moon was altered only by the formation of several large radiation craters, such as, for example, Copernicus, Kepler, Aristarchus and Tycho.

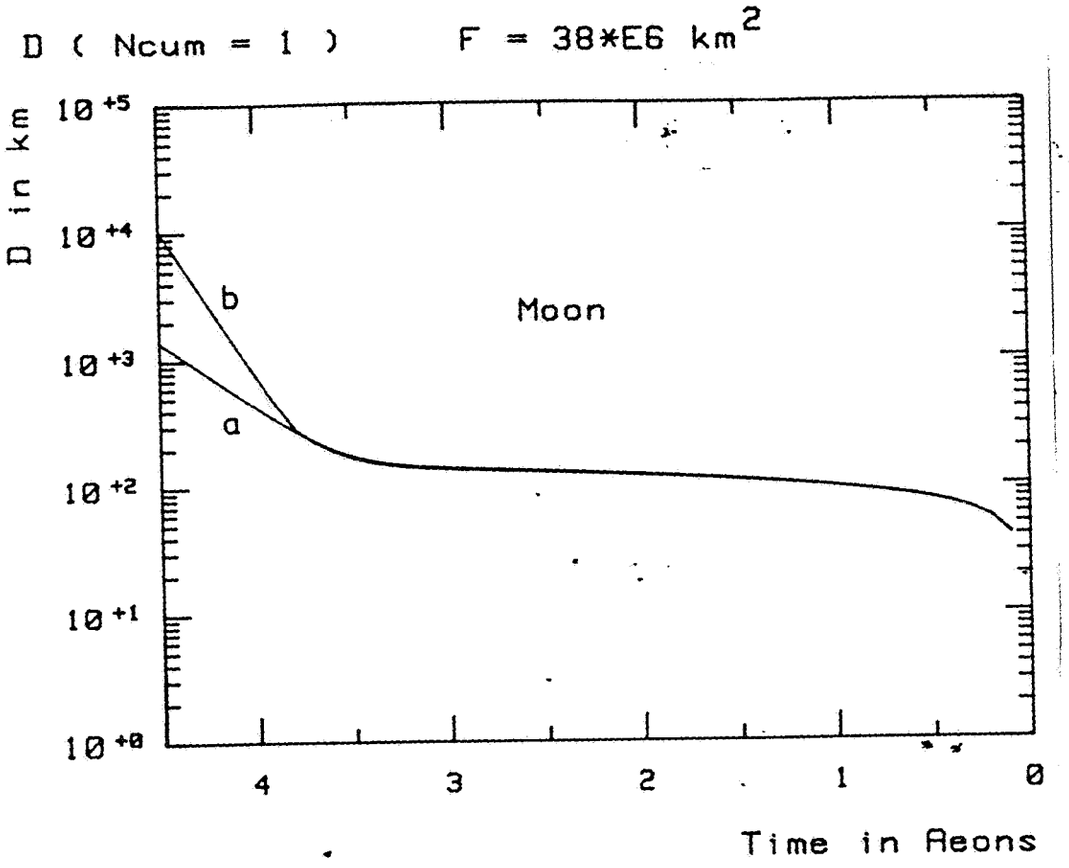

Figure 42. Crater size as a function of the age for the total surface of the Earth's Moon for an impact to be expected on the average once in time of size $\geq D$, (N(D)=1) for different distribution functions: a) $N \sim D^{-2 \cdot 9}$, b) lunar standard distribution. (1 eon = 10^9 years).

Stratigraphic Age	Reference Structure	Radiometric Age (10^9a)	Relative Crater Retention Age N(1) (km^{-2})	Absolute Crater-Retention Age (10^9a)
Copernican				
———	Crater Copernicus	0.85	$1.3\ 10^{-3}$	1.5
Eratosthenian				
———	Crater Eratosthenes		$3.0\ 10^{-3}$	3.2
Imbrium				
———	Imbrium Basin	3.9	$3.5\ 10^{-2}$	3.9
Nectarian				
———	Nectaris Basin	4.1	$1.2\ 10^{-1}$	4.1
Pre-nectarian				
———	Oldest Highland	4.4	$3.6\ 10^{-1}$	4.3

Figure 43. - Lunar stratigraphic system with relative and absolute ages.

TABLE 4. EXAMPLES OF RELATIVE AND ABSOLUTE CRATER RETENTION IN AGE OF LUNAR GEOLOGICAL STRUCTURES

/112

Geological Structure	Relative Crater Retention Age		Absolute Crater Retention Age (10^9 a)
	$N(D=1km)/km^2$	$N(D=10km)/km^2$	
Highland (Terrae)	$3.32\ 10^{-1}$	$8.42\ 10^{-4}$	4.25
Ring Basin			
Apollo	$1.38\ 10^{-1}$	$3.50\ 10^{-4}$	4.12
Birkhoff	$2.46\ 10^{-1}$	$6.24\ 10^{-4}$	4.20
Crisium	$5.70\ 10^{-2}$	$1.45\ 10^{-4}$	3.99
Hertzsprung	$5.68\ 10^{-2}$	$1.44\ 10^{-4}$	3.99
Humboldtianum	$8.13\ 10^{-2}$	$2.06\ 10^{-4}$	4.04
Humorum	$5.95\ 10^{-2}$	$1.51\ 10^{-4}$	3.99
Imbrium	$3.71\ 10^{-2}$	$9.41\ 10^{-5}$	3.92
Keeler-Heaviside	$3.82\ 10^{-1}$	$9.69\ 10^{-4}$	4.27
Korolev	$8.12\ 10^{-2}$	$2.06\ 10^{-4}$	4.04
Lorentz	$2.63\ 10^{-1}$	$6.67\ 10^{-4}$	4.21
Milne	$1.96\ 10^{-1}$	$4.97\ 10^{-4}$	4.17
Mendeleev	$8.37\ 10^{-2}$	$2.12\ 10^{-4}$	4.04
Mendel-Rydberg	$9.76\ 10^{-2}$	$2.48\ 10^{-4}$	4.07
Moscoviense	$7.29\ 10^{-2}$	$1.85\ 10^{-4}$	4.02
Nectaris	$1.00\ 10^{-1}$	$2.54\ 10^{-4}$	4.07
Schroedinger	$2.60\ 10^{-2}$	$6.59\ 10^{-5}$	3.86
Smythii	$2.93\ 10^{-1}$	$7.43\ 10^{-4}$	4.23
Orientale	$2.24\ 10^{-2}$	$5.68\ 10^{-5}$	3.84
Freundlich-Sharonov	$1.57\ 10^{-1}$	$3.98\ 10^{-4}$	4.14
Crater			
Langrenus	$5.10\ 10^{-3}$	$1.29\ 10^{-5}$	3.51
Theophilus	$4.75\ 10^{-3}$	$1.20\ 10^{-5}$	3.50
Aristoteles	$5.07\ 10^{-3}$	$1.29\ 10^{-5}$	3.51
Aristarchus	$1.52\ 10^{-4}$	$3.86\ 10^{-7}$	0.18
Kepler	$8.62\ 10^{-4}$	$2.19\ 10^{-6}$	1.03
Delisle	$1.50\ 10^{-3}$	$3.80\ 10^{-6}$	1.78
Eratosthenes	$3.00\ 10^{-3}$	$7.61\ 10^{-6}$	3.20
Diophantus	$1.50\ 10^{-3}$	$3.80\ 10^{-6}$	1.78
Lambert	$4.80\ 10^{-3}$	$1.22\ 10^{-5}$	3.50

V. PRODUCTION CRATER DISTRIBUTION AND IMPACT CHRONOLOGY OF THE PLANET MARS

The crater populations of Mars, just like the Earth's Moon, /113
allow the study of the geological development of the planet through the analysis of crater frequencies. The relative dating takes place through direct comparison of crater frequencies, though it is not measured in the same diameter range, through the crater size production distribution. The production distribution, as we now know, and against earlier assumptions, is not the same as that of the Earth's Moon. The characteristics of the distribution will be discussed in the next Chapter.

Then models of the impact chronology of Mars will be presented and the possibilities of determining the absolute of the geological units and structures of Mars through crater frequencies is illustrated.

V.1. Analysis of the Production Crater Size Distribution of Mars

Just as in the case of the Earth's Moon there is nothing unanimous in the literature about crater size distribution. An exact knowledge of the distribution is here, however, more important, since Mars was geologically much more active than the Earth's Moon, and these activities have interacted intensely with the crater population. By studying the corresponding effects on the distribution, it is possible to obtain partly very detailed information on the genesis of the geological structures and their development (Neukum and Wise, 1976; Neukum and Hiller, 1981).

The production crater size distribution (standard distribution) of Mars was determined in the region 1 km<D<20 km by Neukum and Wise. Detailed analyses were conducted by Neukum et al. (1978) and Neukum and Hiller (1981). The resulting distri- /114
bution is shown in Figure 44. The distribution shows qualitatively a similar characteristic as the lunar distribution with clear increase for $D \lesssim 1$ km. In the literature many reference distributions may be found of the type of simple power distribution $N \sim D^{\alpha}$ (Figure 44), which are justified by a limited diameter range, but unfortunately are often applied outside their range of validity and thus lead to discrepancies in the interpretation of the measurement data.

Neukum and Wise (1976) compared with each other the production crater size distribution of the Moon and Mars, and drew the conclusion that a large number of effects, which are shown in a simplified manner in Figure 45, may cause the differences in the size distribution of the craters on Mars against those of the Moon. If we assume the same meteorite population as producing the craters for the Moon and Mars, then in the case of single power

distribution of the type $N \sim m^{\gamma}$ (γ=const), then on both planets the same diameter distribution would be produced of the type $N \sim D^{\alpha}$ (α=const), even for different impact velocities, properties of the target etc. For distributions with size dependence γ or α, however characteristic differences would arise in the distribution if we go from one planet to the other (Figure 45). Age differences, that is, differences in the time of exposure of target surfaces, result in similar proportions of the crater frequency for each crater size (Δ log N=const in the right hand half of Figure 45). The same applies to differences in the capture cross section or in the impact rate of the body (for the same velocities). These effects do not influence the shape of distribution in the log-log diagram. In other words, the distributions can, in this case, be shifted vertically (in logN direction) and be brought to cover each half completely.

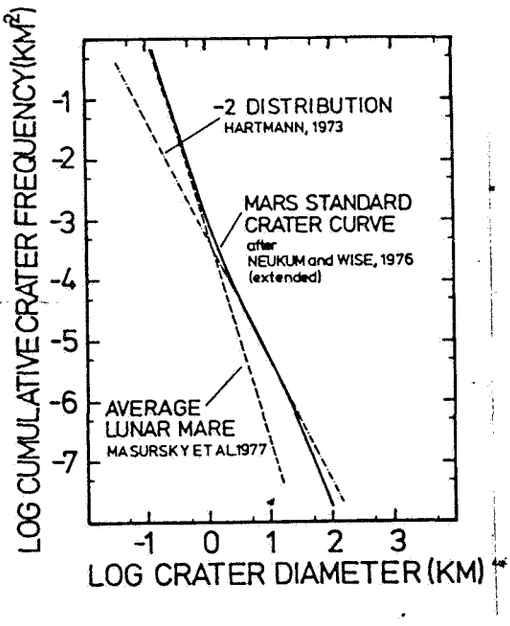

Figure 44. Comparison of difference reference distributions to describe the production crater size distribution of the crater population of Mars. (Figure: Neukum and Hiller, 1981).

Totally different conditions /116 predominate in cases when different average impact velocities arise, or if different target properties (for example, different chemical composition of the rocks, water content, etc.) lead to the production of craters of different size for the same meteorite mass. In this case the distributions (Figure 45, left half) in the log N direction do not cover each other, but appear to be different with regard to flatness or steepness. But they can be made to cover each other by shifting in the LogD direction as compared with the different rate of sizes (if these effects are not different for different crater sizes). Neukum and Wise (1976) explain the differences found by them between the lunar distribution and that of the Moon by a plausible difference in the corresponding average impact velocity, but have not excluded the possibility that target effects may also be involved. Actually in particular the water contents of the Mars soil seems to have had an effect, as was stated by Boyce and Roddy (1978), Boyce (1979), Mouginis-Mark (1979) and Croft et al. (1979). The water content of the Mars soil seems to have also played a greater role in the formation of different crater morphology and is considered mainly responsible for the formation of the ejecta cover surrounding the craters, totally different from

/115

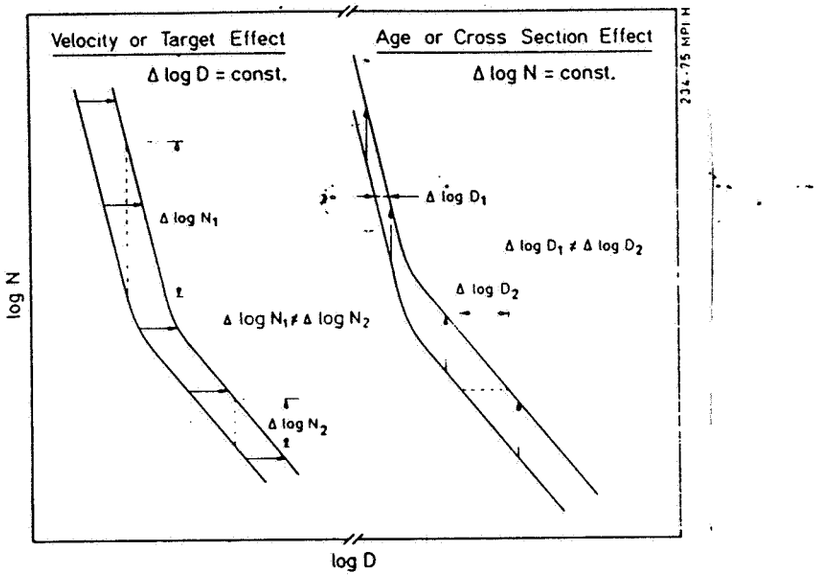

Figure 45. Simplified representation of the effect of different impact conditions on the crater size distribution, whose distribution law deviates from a simple power law.

that of the Moon (Figure 46). /116

A later analysis of target dependence carried out by the author (Neukum, 1983) shows that unfortunately no uniform production crater size distribution exists for Mars, that actually different water content (or different effects of the composition of the Mars soil) have produced different distributions over different geological units of Mars. These effects obviously affect predominantly the region D>5 km (compare Carr, 1981). The resulting average production crater size distribution (standard distribution) of Mars is shown in Figure 47. The fluctuation width of the distribution for the previously studied regions of /119
Mars leads to an uncertainty of about a factor 2 in the cumulative crater frequency N in the indicated diameter range. The average standard distribution of Mars is compared in Figure 48 with the lunar standard distribution. It is found that the differences in the dependence of the distribution on the size are such that in the comparison of crater frequencies of Mars with those of the Moon, the diameter range must be taken into account without fail. Otherwise considerable errors would arise (factor $\lesssim 5$); unfortunately this fact has not been taken into account enough so far in the literature.

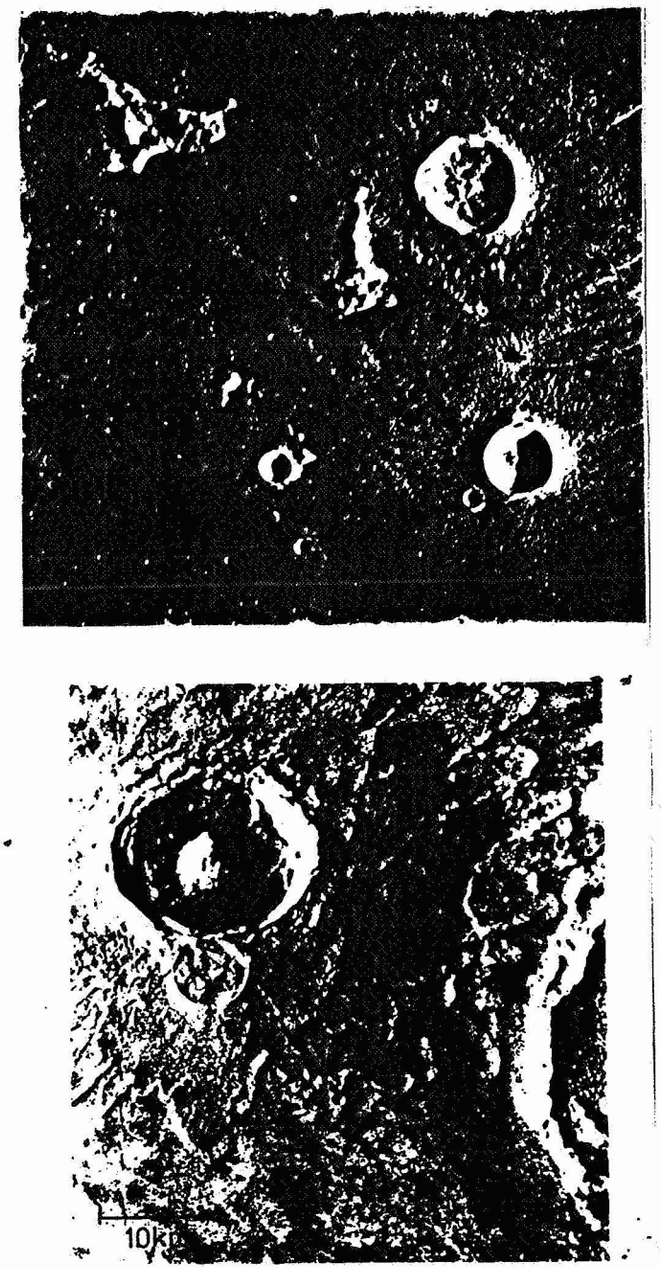

Figure 46. Comparison of typical morphologies of craters of the Earth's Moon (top) and Mars (bottom).

/118

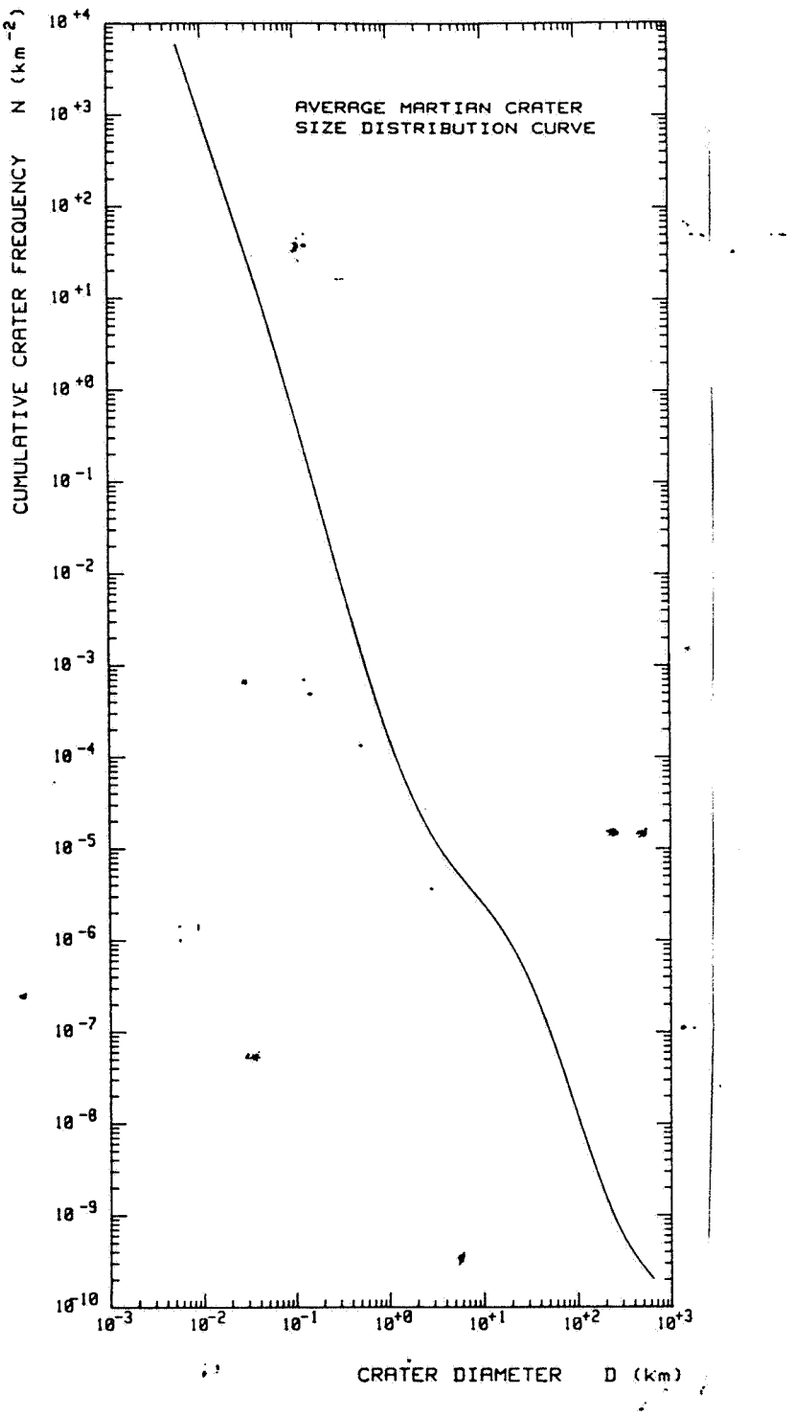

Figure 47. The production size distribution (standard distribution) of Mars.

The mathematical expression of the average standard distribution of Mars in Figure 47 is a polynomial in logD of the form

$$\log N = a_0 + a_1 \log D + a_2 (\log D)^2 + \ldots . a_{11} (\log D)^{11}$$

with

$a_1 = -2.9076$ $\quad$ $a_7 = 2.6348 \cdot 10^{-2}$

$a_2 = 1.1870$ $\quad$ $a_8 = -3.6585 \cdot 10^{-3}$

$a_3 = 0.3842$ $\quad$ $a_9 = -1.6354 \cdot 10^{-3}$

$a_4 = -0.3955$ $\quad$ $a_{10} = 7.3875 \cdot 10^{-5}$

$a_5 = -0.1652$ $\quad$ $a_{11} = 2.8421 \cdot 10^{-5}$

$a_6 = 5.8655 \cdot 10^{-2}$

a_0 is variable and contains the dependece of the distribution on age.

The polynomial is valid in the range 100 m<D<300 km, but not beyond it. Polynomials of lower degree approximate the complicated size distribution only inadequately. The expression given here is consistent within 50% in N with the results of Neukum and Wise (1976) and Neukum and Hiller (1981).

V.2. Impact Chronology of Mars /121

The oldest crater populations of Mars and the Earth's Moon provide information on the bombardment directly after the accretion phase and make it possible for us to learn something about the nature of the meteorite population and the variation in time of the earlier bombardments by comparing the frequencies of large craters and basins.

In Figure 49 the distributions of the oldest crater and basin populations of the highlands of the Moon and Mars are compared with each other. The crater frequencies of the populations are similar to each other, but those of Mars are lower by a factor of 2 to 3. An analysis conducted in Chapter IX of the fine structure of the Mars distribution shows that the characteristic variations for the Moon in the distribution index may also be found in the highland crater populations of Mars, but not exactly at the same diameter. The diameter distribution of the highland crater populations of the Moon and Mars are similar. The differences in crater size distribution (Figure 48) may be explained by differences in the impact conditions (such

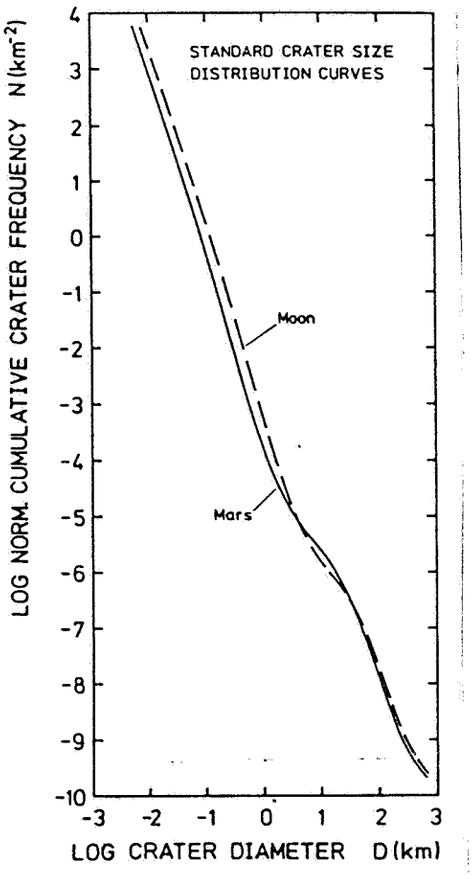

Figure 48. Comparison of the average standard distribution of Mars with the lunar standard distribution.

as, for example, impact velocity, properties of the target, surface gravitation) (compare also Chapter IX). The same population of crater producing objects may occur.

These relationships were identified by Neukum and Wise (1976) and Neukum and Hiller (1981) and can be defined more exactly by the result discussed here on the crater size distributions of the population of Mars and the Moon. An analysis of the crater frequencies of the Chryse Plain of Mars (vicinity of the landing site of Viking-1) indicates that the impact rate must have decreased even further for values of $N(D=1\ km) \approx 1.5 \cdot 10^{-3}$ (km^{-2}) (Neukum, 1983).

For the Moon we know (Chapter IV) that for values $N(d=1\ km) < 2 \cdot 10^{-3}$ (km^{-2}) the impact rate is constant. This situation fits into the picture obtained from the highland data, that the impact rate of Mars for D=1 km was smaller by about a factor of 2 to 3 than for the Earth's Moon. /122

Soderblom (1977) drew the conclusion, on the basis of stratigraphic and crater frequency analyses, that in the diameter range 4 km<D<10 km, the impact rate for Mars during the period after the formation of large basins should be higher by a factor 1.5 than for the Earth's Moon. Hartmann (1977, 1978) and Hartmann et al. (Basaltic Volcanism Study Project, 1981) came to the conclusion, from the study of the impact rate of the present asteroid population, that in the same diameter range, the rate for Mars in more recent times is higher by a factor 2 than for the Earth's Moon.

The youngest basins of Mars show crater frequencies which at D=10 km are higher by a factor 1.5 than those of the youngest basins of the Earth's Moon (Neukum, 1983; compare Table 6). If our conclusion, that the youngest large basins of the Moon and Mars were produced more or less at the same time ("marker horizon", compare Chapter IV.2) is correct, then the impact rate of Mars for D=10 km was higher by a factor 1.5 than that of the Moon; for D=1 km, it was according to the functional dependence over

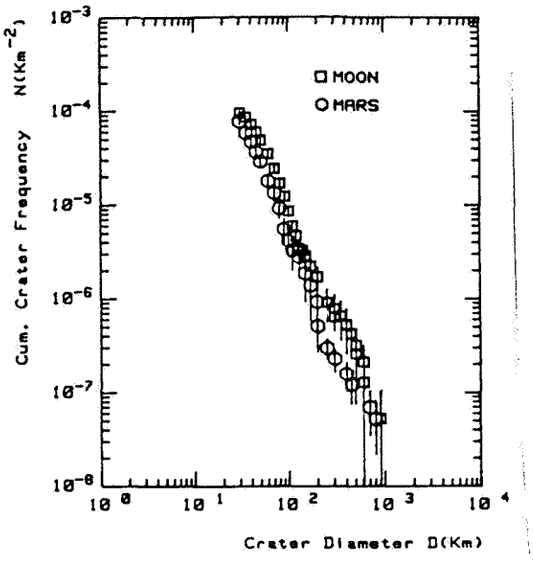

Figure 49. Comparison of the oldest crater and basin populations of the Moon and Mars highlands.

the standard distribution (Figure 48) lower by a factor of 3 than that of the Moon; for D=4 km, it was approximately equal to that of the Moon.

These conclusions confirm the picture obtained by Neukum and Hiller (1981) on the dependence on time of the impact rate, which is shown in Figure 50. According to these investigations, the impact rate for the entire time study for Mars was smaller for D=1 km by a factor 3 than for the Moon, which leads to an impact chronology ("cratering chronology") similar to that of Figure 50 (model I) or the fluctuation of the rate in more recent times ($t<3 \cdot 10^9$ years) occured at a value higher by a factor 2, as shown in Figure 50 (model II). These model cratering chronologies are represented for the range 4 km<D<10 km (N(D=4 km)-N(D=10 km) in Figure 51. Very satisfactory consistency is found with the interpretations of other authors. The values estimated by Shoemaker (1977) from the present asteroid data should be considered as very unsuited and probably somewhat too high, just like the lunar data caused by systematic errors (compare Figure 4), but are very compatible in the indicated range of errors with the cratering chronology models obtained here. /124

The analysis recently carried out by Hartmann et al. (Basaltic Volcanism Study Project, 1981) for D≥4 km gives values which are closer to our data than previously (see Figure 51). Hartmann has thus come much closer to our data in recent years (compare Neukum and Hiller, 1981) but his values are still systematically higher. The problem in the comparison of different models resides in the fact that different reference functions are for production crater size distributions of Mars, which makes a detailed comparison difficult. Moreover, differences occur in the lunar initial data.

V.3. Chronology of the Geological Development of the Planet Mars

A brief summary will be given here about our knowledge of the chronology of the geological development of the planet Mars, as obtained primarily from our analyses of crater populations. More detailed discussions may be found, for example, in the

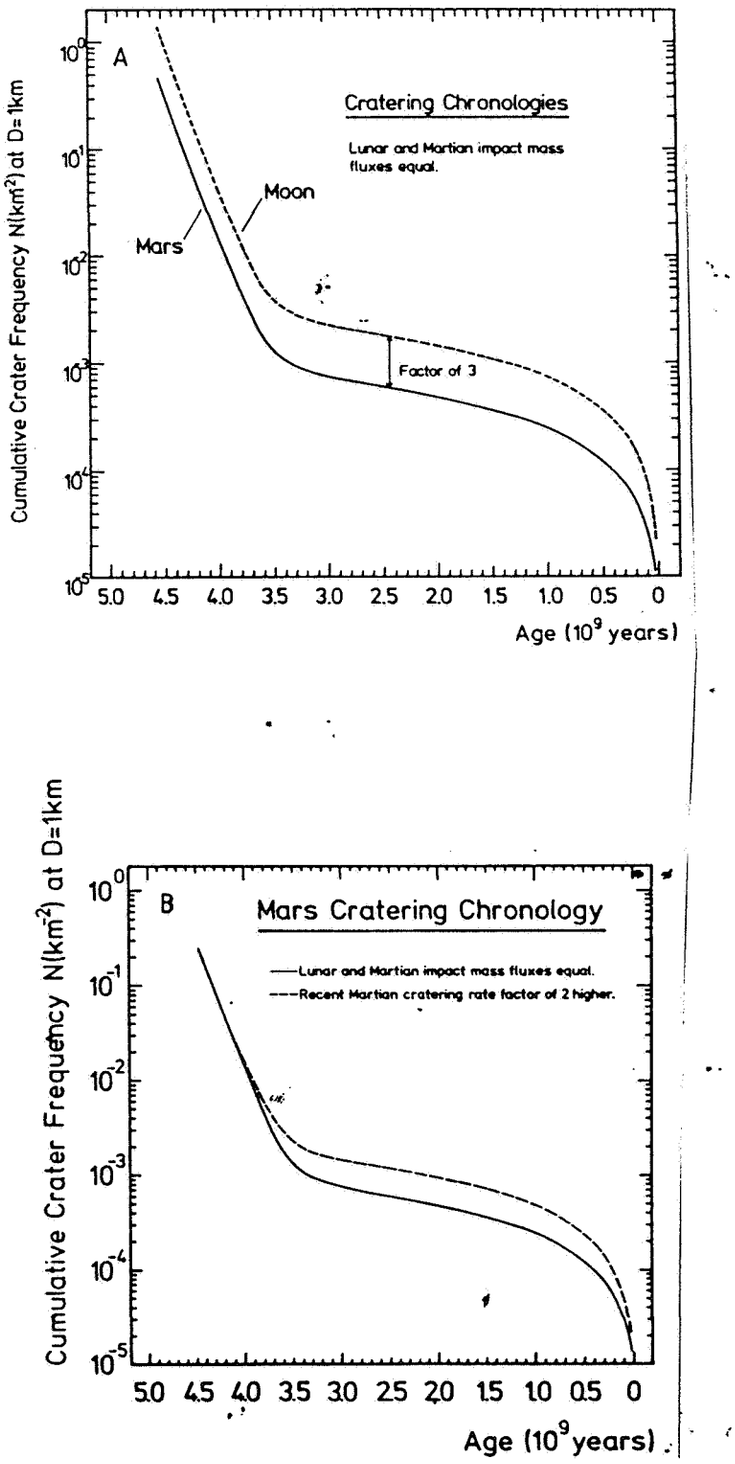

Figure 50. Model cratering chronology of Mars as compared with the cratering chronology of the Moon.

A: Model I

B: Model II (dashed line) as compared with model I.

(Figure: Neukum and Hiller, 1981).

publication of Neukum and Hiller (1981), Basaltic Volcanism Study Project (1981) and Carr (1982).

When in the years after 1971, the Mariner-9 photographs of the Mars surface were interpreted, because of the different photogeological interpretations, the scientific community /126
arrived at the opinion that the superficial structures of Mars must be partly very young (for example, Hartmann, 1973b; Mutch et al., 1976). This opinion was criticized in detail by others for the first time on the basis of our analyses of the crater population of Mars on the basis of Mariner-9 photographic material (Neukum and Wise, 1976). Meanwhile, after high resolution photographic material has become available from the Viking missions, our findings have been confirmed to a great extent (for example, Carr, 1982).

Our detailed analyses on the basis of Viking photographic material (Neukum and Hiller, 1981) confirm our earlier investigations, but give for the youngest structures of Mars, in particular, the Tharsis volcanoes (compare Figures 4 and 6a) a differentiated picture: the vast geological activities of Mars such as extrusion of highland lavas and formation of the northern deep plains (Planitiae) by volcanic processes, the erosion over large areas by (probable) melting of permafrost and fluvial processes and the buildup of volcanoes in the highland and the volcanic complex of the Elysium region in the northern deep plain, all these activities occurred at a time when the cratering rate was still decreasing, that is, the structures show crater frequencies with values of $N(d=1\ km) > 1 \cdot 10^{-3}\ km^{-2}$. On the basis of the cratering chronology model derived by us, this means an age of at least about 1.5 billion years. Only the fastest region, the large youngest volcano complex with the thick shield volcanoes, in particular, Olympus Mons, shows clearly geological activity even in recent times, up to possibly about 100 million years ago. All measurements, however, show clearly that the buildup of these shield volcanoes also began very early with relative crater retention ages of $N(1) \leq 8 \cdot 10^{-4} km^{-2}$ of absolute ages of about 1.5 billion years or more. Accordingly these structures show volcanic activity over extraordinary large periods (more than 1 billion years).

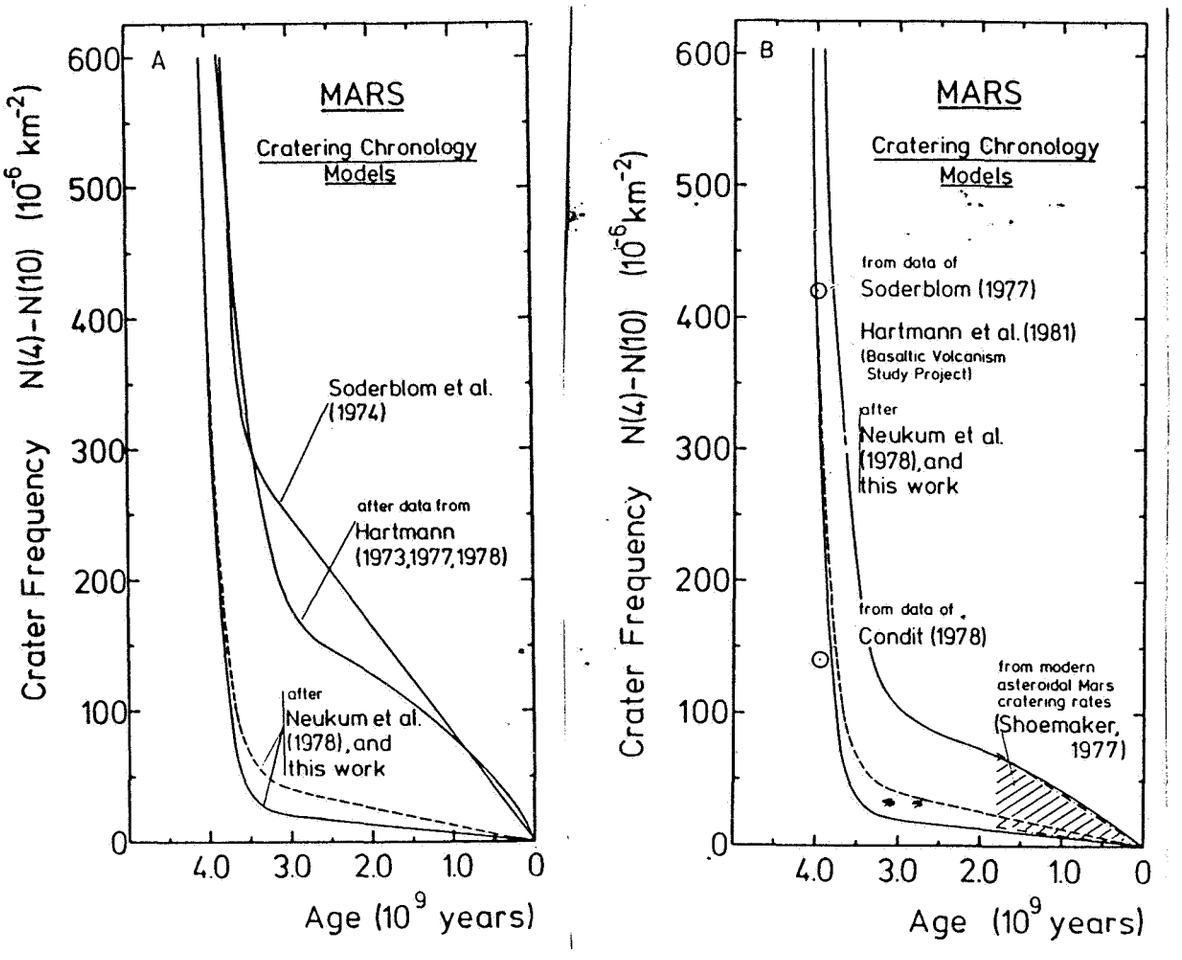

Figure 51. A comparison of the different crater chronologies proposed in the literature for the planet Mars. The crater frequencies are plotted here linearly against age, which renders particularly clearly the abrupt bend in the frequencies at t≅3.5 million years. The crater frequencies which are indicated here for the range 4 km<D<10 km (N(4)-N(10)), may be converted through the standard distribution of Mars (Figure 47) into values for other diameters. An approximation of the cratering chronology model by different authors is found over the last few years. A: Comparison with older data. B: Comparison with younger data. (Figure: Neukum and Hiller, 1981; modified).

Figure 52 gives a summary of our modern ideas of the geological development of the planet Mars. The uncertainty in the models amounts still to a factor 2 to 3, as is apparent approximately in the two models. The capacity of determination of age through crater frequencies resides, however, in the fact that a clear relative determination of age is possible for large portions of the planet by obtaining the sequence of events, and moreover, at least a rough absolute dating of the surface structures of Mars. /127

The method gives, in spite of the uncertainties in the models, very good possibilities of absolute determination of age with errors of 200 million years for an age of more than $3 \cdot 10^9$ years (values of $N(1)>2 \cdot 10^{-3}$ km^{-2}). For ages $<3 \cdot 10^9$ years, the absolute determination of the age through crater frequencies is precise so far only with a factor 2 to 3 in N with regard to the chronology model. The better the impact rate for this period (for example, from astronomic data of the impact rate of the present asteroids) can be determined, that is, the more the bending point between exponentially decreasing impact rate and constant impact rate, the more accurate the method. Recent years have shown that the data are becoming increasingly better and it may be possible to reduce the uncertainties to less than factor 2. Studies in this direction are very important for planetology, since it is known that we cannot expect mass samples by "sample return" missions for the next 15 to 20 years.

Later investigations on a special type of differentiated meteorites, the so-called SNC meteorites, showed that these may come possibly from Mars (compare, for example, Basaltic Volcanism Study Project, 1981). These meteorites have crystallization ages of about 1.5 billion years, which would fit in well with our picture of cratering chronology, model II. But at the present time, the interpretation of the sample as ejection material of large impacts on the planet Mars is still speculative (although dynamically possible, perhaps (Nyquist, 1982)) and in particular no compelling evidence was found up to now on the geochemical aspect, even though the later isotope measurements indicate compatibility with a Martian origin (Burghele et al., 1983). /128

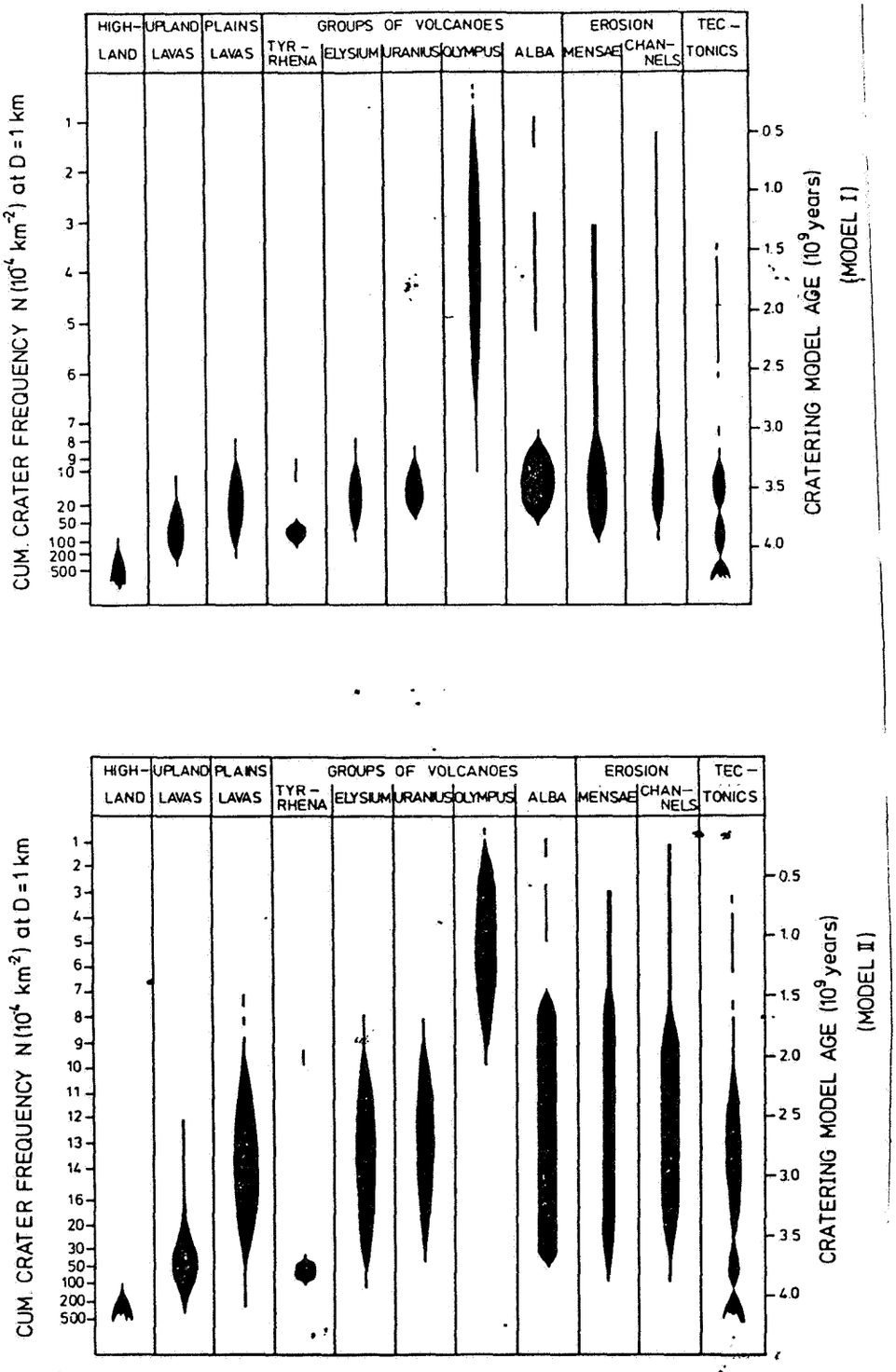

Figure 52. Representation of the geological activity of the planet Mars with relative crater retention ages and absolute crater retention ages (cratering model age) on the basis of the different cratering chronology models. (Figure: Neukum and Hiller, 1981).

VI. CHARACTERISTICS OF THE CRATER POPULATION ON THE PLANET MERCURY

The surface of Mercury is remarakably similar to that of the Moon's highland. A detailed description of the superficial structures may be found in a publication of Strom (1979). The characteristics of the oldest crater populations of Mars will be discussed within the framework of this study, and a comparison will be carried out with the corresponding population of the Moon and Mars. /130

Measurements of the crater with D>20 km and the large basins (D>200 km) in the regions most densely covered with craters on Mercury give accumulated crater frequency distribution in Figure 53a (Neukum, 1982). This distribution is compared in detail in its representation as relative frequency with that of the Earth's Moon (Figure 53b). A very similar characteristic of the distributions of both planets occurs with similar variations of the distribution index, particularly with a bend at D≈100 km (Mercury) and D≈60 km (Moon). We will designate hereafter these diameters as inflection diameters D_{inf}. (The average lunar production distribution collected for the elimination of small craters (standard distribution) is used here; the actual lunar measurement data (compare Chapter IV.2.) give an inflection diameter at D=80 km, which, however, arises through erosion effects (elimination of small craters by superimposition).

The great similarity of the distributions of the Earth's Moon and Mercury suggests a corresponding similarity of the basic mass-velocity distribution of the crater producing meteorites. (Compare Chapter IX). Actually the distributions coincide with the limits of the measurement errors, if D(Mercury)=1.6 D(Moon) is assumed for the same crater producing meteorite mass. (Here a possible deviation of the measured Mercury distribution from the production distribution for the smaller craters, as it is observed in the case of populations of the Moon highlands, was not taken into consideration). This consistency can be explained to a great extent by plausible differences in the impact velocities (compare Chapter IX). The standard distribution resulting thus from the standard distributions for the Moon is for the oldest crater populations of Mercury: /132

$$\log N = a_0 + a_1 \log D + a_2 (\log D)^2 + \ldots\ldots + a_{11} (\log D)^{11}$$

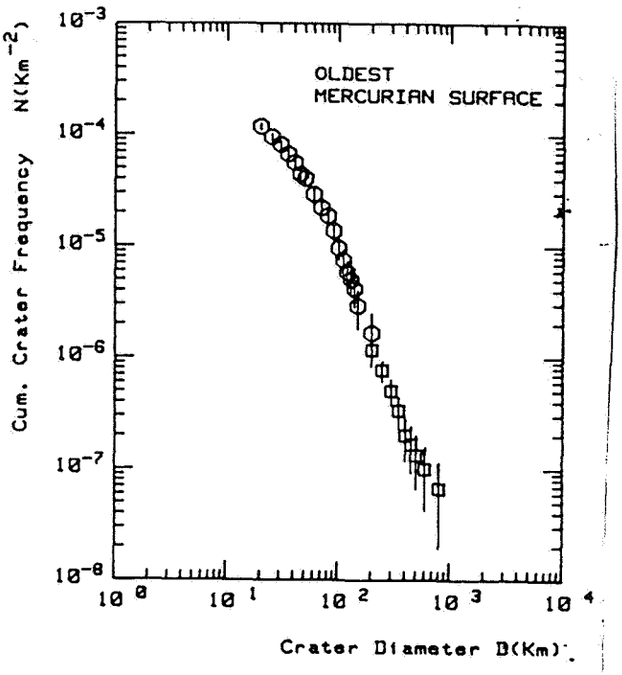

Figure 53a. Cumulative crater frequency of the oldest crater populations of Mercury.

with

$a_1 = -3.7110$ $a_7 = 1.7797 \cdot 10^{-2}$

$a_2 = -0.0072$ $a_8 = 1.3702 \cdot 10^{-2}$

$a_3 = 0.6259$ $a_9 = -1.1013 \cdot 10^{-3}$

$a_4 = 0.3054$ $a_{10} = -6.0711 \cdot 10^{-4}$

$a_5 = -0.1559$ $a_{11} = 3.97 \cdot 10^{-5}$

$a_6 = -0.1068$

The coefficient a_0 contains the dependence on a of the crater frequency and is thus variable.

The production distribution in the region D<20 km may be determined only inadequately because of insufficient photographic material. Our measurements (Neukum, 1975, 1983) suggest that it is similar to that of the Earth's Moon. This would fit in with the above described picture, that we are dealing with very similar mass distribution of the Moon and Mercury crater producing meteorite populations, and that very probably the standard distribution indicated above for Mercury for craters with D>20 km applies also for smaller craters up to sizes of D≅1 km.

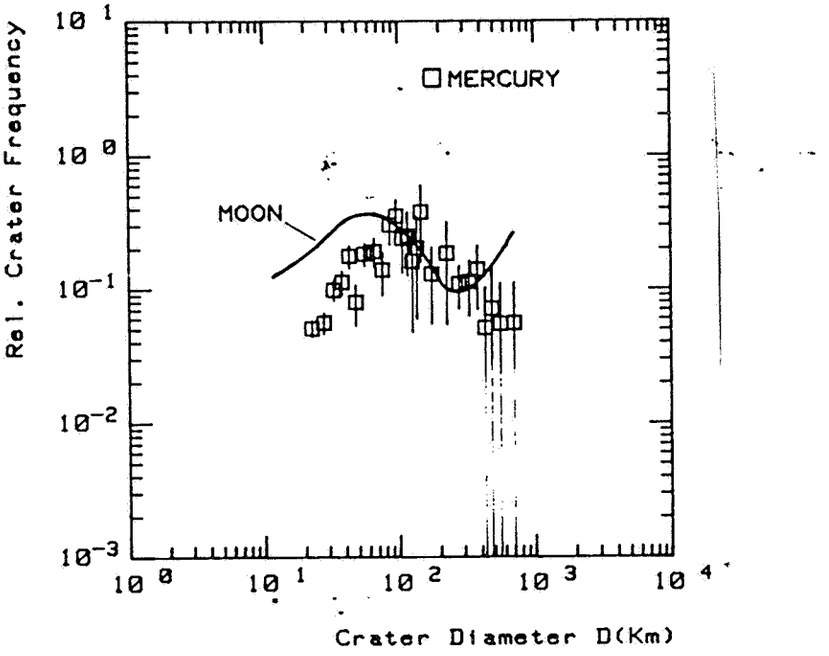

Figure 53b. Relative crater frequency of the oldest crater populations of Mercury as compared with lunar relative standard distribution (oldest population).

VII. EMPIRICAL DEDUCTION OF THE CRATERING CHRONOLOGY OF MERCURY

Since we have no radiometric age data, we can only attempt /133
to develop a model of the cratering chronology of Mercury by determining the impact rate at certain times and assuming the same dependence on time of the impact rates as in the Earth-Moon system.

Hartmann et al. (Basaltic Volcanism Study Project, 1981) came to the conclusion, on the basis of consideration of impact probabilities of the present asteroid and comet populations of Mercury, that the ratio of the crater production rates of Mercury to the Moon is about 2:1 for craters with $D \geq 4$ km. We will use the fact of the "marker horizon" and assume that the youngest basins of the Moon, Mars and Mercury occurred at approximately the same time about 3.9 billion years ago. The youngest Mercury basin, which we know (about 60% of the Mercury surface is not known, since it is not covered by photographic data) gives for D=4 km and D=10 km values of $N(4)=6.2 \cdot 10^{-4}km^{-2}$ and $n(10)=7.1 \cdot 10^{-5}km^{-2}$ (Figure 54).. The youngest Moon basins Schrödinger and Orientale, give approximately $N(4)=3.4 \cdot 10^{-4}km^{-2}$ and $N(10)=6.0 \cdot 10^{-5}km^{-2}$ (compare Chapter IV.3).

A slightly higher crater production rate in this diameter range is found for Mercury than the Moon. This is qualitatively consistent with the conclusions of Hartmann et al. (Basaltic Volcanism Study Project, 1981) for the recent bombardment and supports the assumption of the same time dependence of lunar and Mercury impact rates. The Mercury cratering chronology model derives from the Moons cratering chronology of Chapter IV through the comparison for the values of the basins "marker horizon" and taking into account the production crater size distribution of Mercury (standard distribution) as shown in /135
Figure 55. This chronology is sure only to a factor of 2 to 3 in N, but it allows thus a good absolute determination of the age with errors of 100 to 200 million years for structures older than 3.5 billion years ($N(1)>1 \cdot 10^{-2}km^{-2}$).

Table 5 contains relative and absolute crater retention ages resulting from our measurements. It was found that the oldest crust of Mercury is somewhat younger that the oldest crust of the Moon. Basaltic volcanism with filling of the Caloris Basin took place immediately after the formation of the basin about 3.9 billion years ago, quite similarly as in the case of the younger basins of the Earth.

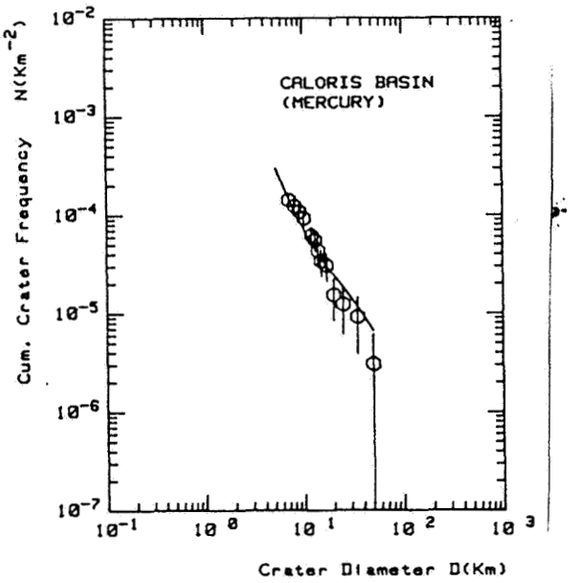

Figure 54. Crater frequency of the Caloris Basin of Mercury. The continuous curve is the standard distribution of Mercury craters.

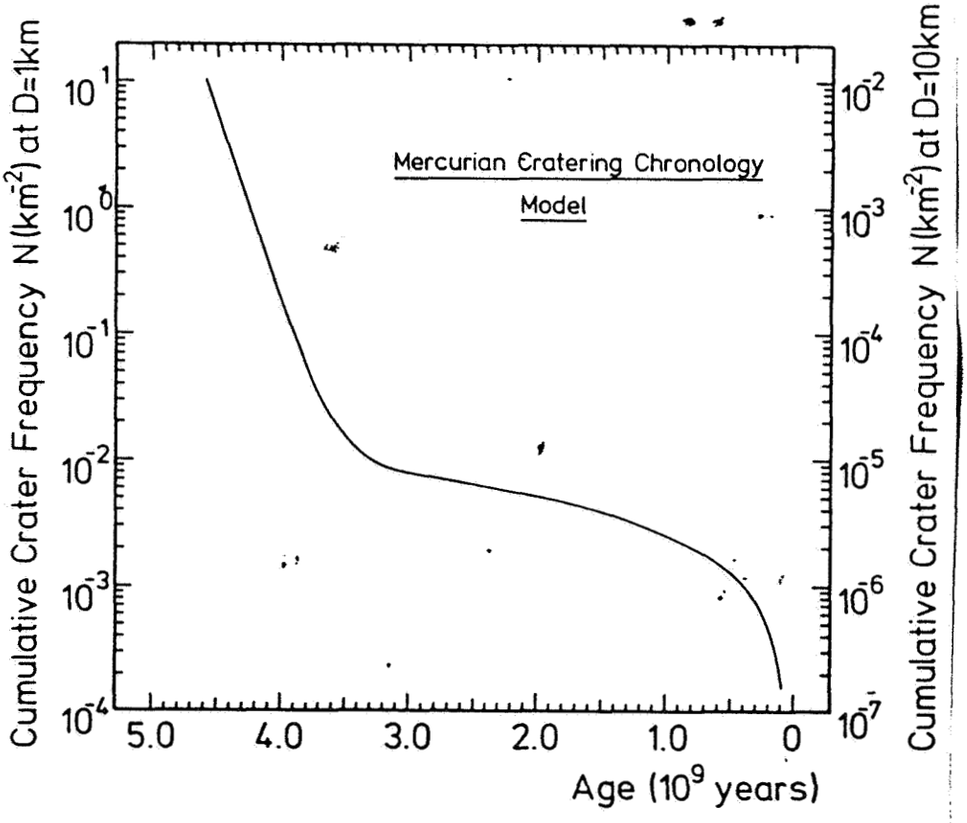

Figure 55. Cratering chronology model for the planet Mercury.

TABLE 5: RELATIVE AND ABSOLUTE CRATER RETENTION AGE OF MERCURY'S GEOLOGICAL STRUCTURE (Data Neukum, 1983)

/136

Geological Structure	Relative Crater Retention Age		Absolute crater-Retention Age
	$N(D=1km)/km^2$	$N(D=10km)/km^2$	(10^9 a)
Highland	$6.27\ 10^{-1}$	$5.99\ 10^{-4}$	4.18
Beethoven Basin	$1.60\ 10^{-1}$	$1.53\ 10^{-4}$	3.98
Chekhov Basin	$4.23\ 10^{-1}$	$4.04\ 10^{-4}$	4.12
Caloris Basin	$7.17\ 10^{-2}$	$6.85\ 10^{-5}$	3.85
Caloris-Mare (Interior)	$7.17\ 10^{-2}$	$6.85\ 10^{-5}$	3.85
Dostoevski Basin	$5.74\ 10^{-1}$	$5.49\ 10^{-4}$	4.17
Haydn Basin	$3.82\ 10^{-1}$	$3.65\ 10^{-4}$	4.11
Pushkin Basin	$3.61\ 10^{-1}$	$3.45\ 10^{-4}$	4.10
Raphael Basin	$3.86\ 10^{-1}$	$3.69\ 10^{-4}$	4.11
Tolstoi Basin	$2.78\ 10^{-1}$	$2.66\ 10^{-4}$	4.06

VIII. CHARACTERISTICS OF THE OLDEST CRATER POPULATIONS OF THE MOONS OF JUPITER AND SATURN

The photographic data transmitted by Voyager-1 and 2 /137
(compare Smith et al., 1979, 1981, 1982) allow us to conduct only a rough comparative study of the crater populations of the moons of Jupiter and Saturn in the size range $D \gtrsim 4$--10 km (see Table 1) because of limited spatial resolution. The crater populations studied by different authors (Smith et al., 1979, 1981, 1982; Strom et al., 1981; Neukum, 1981; Strom and Woronow, 1982) show a size distribution deviating from those of the internal Solar System. Strom and Woronow (1982) differentiate in their analyses (Figure 56) different populations, which they believe they see partly only in the internal Solar System and partly only in the external Solar System. They draw therefore the conclusion that there are different populations of crater producing objects in different parts of the Solar System. In this study their conclusions are not shared in all cases, and in the following Chapter we will discuss in greater detail the relationships between the populations in the internal Solar System and the satellites of Jupiter and Saturn. First of all, however, it is proper to provide some detailed considerations of the crater populations in the oldest regions of the Jupiter moons, Ganymede and Callisto and some satellites of Saturn. Here only measurement data which seem to be certain to some extent are used. (Many of the data published and interpreted in the literature up until now were obtained from nonrectified photographic material).

The Jupiter moons Ganymede and Callisto show very good crater populations, which probably arose mainly in the first couple of hundred million years after accretion of the moons and solidification of their crusts (compare Smith et al., 1979). The crust of Callisto shows little endogenous activity, so that the crater population was hardly disturbed. Ganymende's surface /139
was renewed several times by tectonic processes with new formation of crust material, but large portions of the old crust have remained (Figure 57).

In Figure 58 crater frequencies of the oldest populations of Ganymede and Callisto are shown in comparison with the oldest lunar highland populations. Similarities of the distribution are identifiable, but the frequencies of Ganymede and Callisto are clearly below those of the Moon's highland and decrease somewhat more sharply. An analysis of the distribution characteristics of the form of relative frequencies (Figure 59) shows that striking similarities occur: the distribution for Ganymede shows a variation similar to the lunar distribution of the distribution index for the characteristic bending of the relative frequency at 40 km crater diameter (as compared with the crater diameter at 60 km for the Moon). The distribution of Callisto seems to have a similar characteristic, but this cannot be stated with

/138

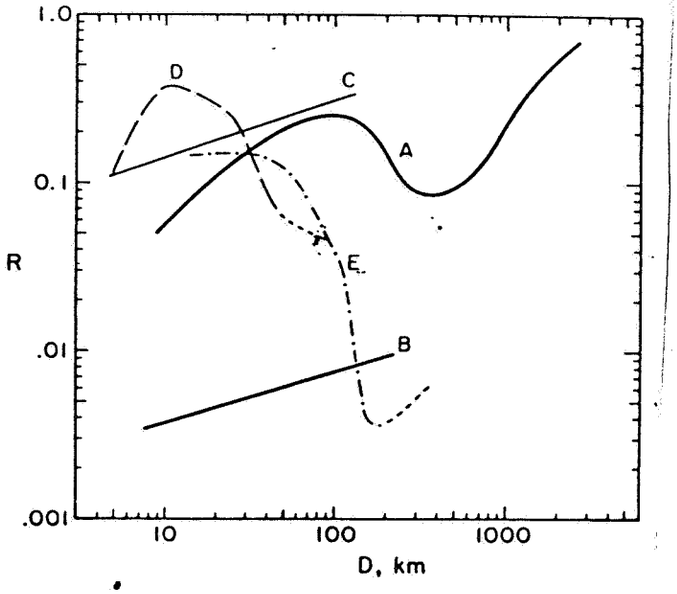

Figure 56. Relative crater frequencies of crater populations which were obtained on different planets and moons of the Solar System by Strom and Woronow (1982). The populations occur according to these measurements: A: Mercury, Moon and Mars; B: Moon and Mars; C: Tethys, Dione and Rhea; D: Mimas, Enceladus, Tethys, Dione; E: Ganymede and Callisto. Our measurements confirm the findings for A and D, but not exactly for E (although similar). The findings for B (younger Eratosthenian-Copernican populations) are not supported, but their variation is obtained according to measurements similarly to A in the plotted size range.

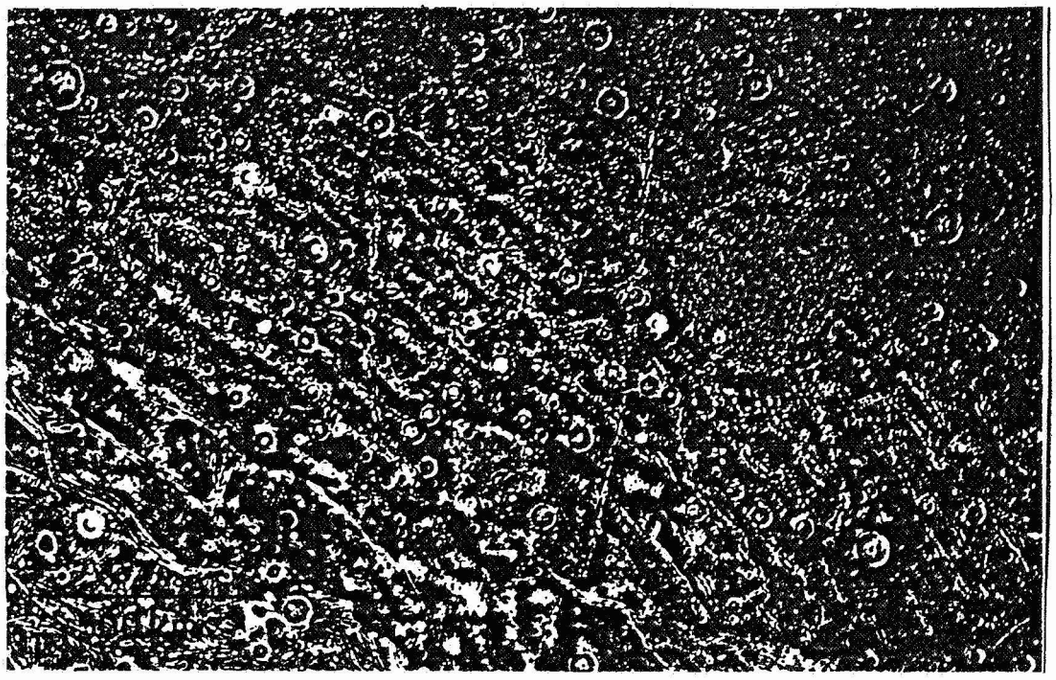

Figure 57. Region of old (darker) crust of Ganymede (Galileo Regio) with the oldest population of craters which have partly lost their shape by flowing of ice, but are still identifiable, large, round, brighter structures).

certainty for smaller craters because of the limited spatial resolution of the photographic material. A shifting of the lunar distribution in the ratio D(Moon)/D(Ganymede)=1.5 reproduced the distribution for Ganymende. For Callisto such a satisfactory consistency cannot be found, but the measurements are of poorer quality because of insufficient photographic data.

The distribution curve obtained with the transformation D(Moon)/D(Ganymede)=1.5 is shown in Figure 60 using the data of Galileo Regio and the youngest basins of Ganymede (Gilgamesh). This youngest basin was defined similarly to the considerations for the internal Solar System at around the "marker horizon" for the decrease of the early bombardment. Similar crater frequencies are obtained: $N(10)=2.9 \cdot 10^{-5}km^{-2}$ for the Gilgamesh basin of Ganymede as compared with $N(10)=5.7 \cdot 10^{-5}km^{-2}$ for the Oriental Basin of the Earth's Moon. The ratio of the frequency between Galileo Region as the oldest crust and Gilgamesh as the youngest basin resembles very much the similar lunar ratio (compare Table 6). An attempt could be made to obtain from it cratering chronology similar to that of the Moon with similar half lives. Shoemaker and Wolfe (1982) establish a cratering chronology similar

/141

to that of the Moon on the basis of short and long period comets and certain classes of asteroids in heliocentric orbits as crater producing bodies. But we consider these discussions to be still speculative, since in reality nothing is known about the nature of the crater producing bodies and their impact rates. It is quite possible that the crater producing objects are found in the planetocentric orbits around Jupiter, as was discussed by Strom and Woronow (1982) and Neukum (1982) (compare Chapter IX).

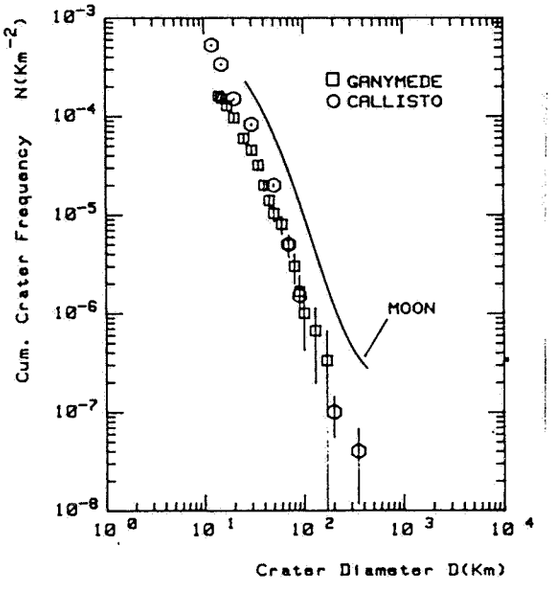

Figure 58. Cumulative distributions of the oldest crater populations of Ganymede and Callisto as compared with the distribution of the lunar highlands. (Data Neukum, 1981 and Strom et al., 1981).

The crater populations of the moons of Saturn are being studied in greater detail at present. The quality of the data is, in our opinion, not yet good enough to make sure statements, like those of Strom and Woronow (1982) in Figure 56. The distribution found by these authors (D, Figure 56) which shows a similar characteristic to the one found by us for the Jupiter moons Ganymede and Callisto, seems however to be confirmed, as is apparent in Figure 61. The inflection diameter of the distribution is from 10 to 20 km (as compared with the lunar curve at D=60 km).

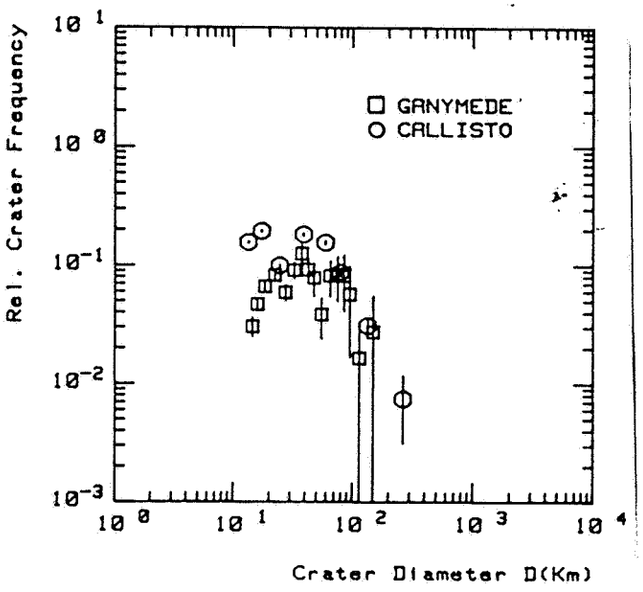

Figure 59. Relative crater. frequencies of the oldest populations of Ganymede and Callisto (from Figure 58).

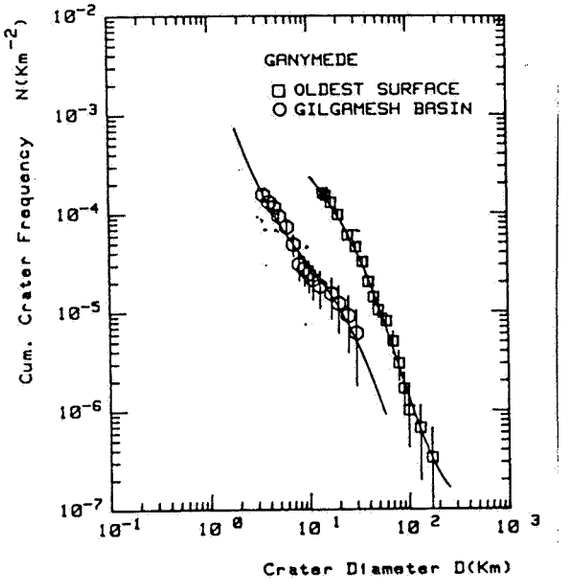

Figure 60. Crater frequencies of structures on Ganymede (oldest crust, Galileo Regio and youngest basin, Gilgamesh). The corresponding continuous curves are the lunar standard distribution transformed with D(Moon)=1.5 D(Ganymede).

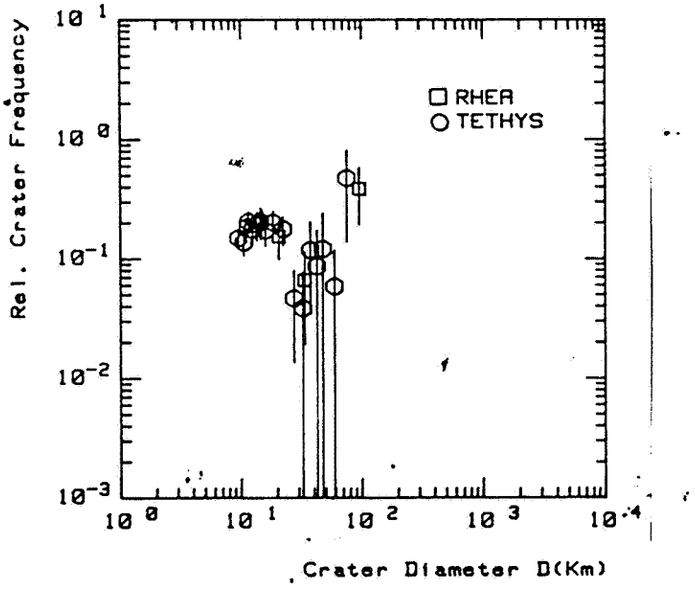

Figure 61. Relative distributions of the oldest crater populations of the Saturn moons Rhea and Tethys. (Data of Plescia and Boyce, 1982).

IX. COMPARISON OF THE EARLY METEORITE BOMBARDMENTS OF THE TERRESTRIAL PLANETS AND THE MOONS OF JUPITER AND SATURN

IX.1. Comparison of the Distribution Characteristics /143

As was stated several times in the previous Chapters, strong similarities exist between the crater population from the time before the end of the early, heavy bombardments with the production of the large basins of the Moon, Mercury and Mars. Their size distributions show a characteristic variability of the distribution index as is represented once again in the example of the relative distribution of the populations of the highland regions (Figure 62).

From the form of the relative distribution it may be seen (compare Chapter III.3.4.), that the cumulative distribution index α varies in the range D=50--100 km from $\alpha \approx -1$ through $\alpha = -2$ to $\alpha \approx -3$. The diameter at which the distribution reaches its peak ($\alpha = -2$) and bends, will hereafter be designated as inflection diameter D_{inf} (Figure 62). Very similar characteristics of the distribution may be observed in the oldest populations of the Jupiter moons Ganymede and Callisto and some Saturn moons, as discussed in the previous Chapter and shown in Figure 62, as an example of the population of Ganymede. The similarities of the crater size distributions are interpreted by us as similarities of the distribution in the basic meteorite populations (Neukum, 1981). According to this interpretation, meteorites of the same mass and density produce crater diameters of different size as the function of impact velocity, density and strength of the substrata, surface gravitation, etc., (compare following Chapter). The different inflection diameters D_{inf} of the distributions would correspond accordingly to approximately the same mass of the striking objects. By comparing the frequencies at the point of inflection diameter, it should thus be possible to determine the impact /145
rates for masses of equal size. We give below first a comparison of the empirical data, which will be supplemented subsequently by a theoretical discussion of the relationships.

The frequencies measured at the inflection point and other diameters of the older populations are given in Table 6. The measured frequencies for the youngest basins are D=1 km and D=10 km, standardized to the lunar values given for a ratio of frequencies measured each time. The following may be derived from the data:

1. The frequencies of the inflection point for the youngest basins, which determine the "marker horizon" at an age of about 3.9 billion years, are identical within a factor 2 for the Earth's Moon, Mercury, Mars and Ganymede. It follows therefore (assuming the above indicated assumption, that the inflection diameter indicates approximately the same meteorite mass) that the flow

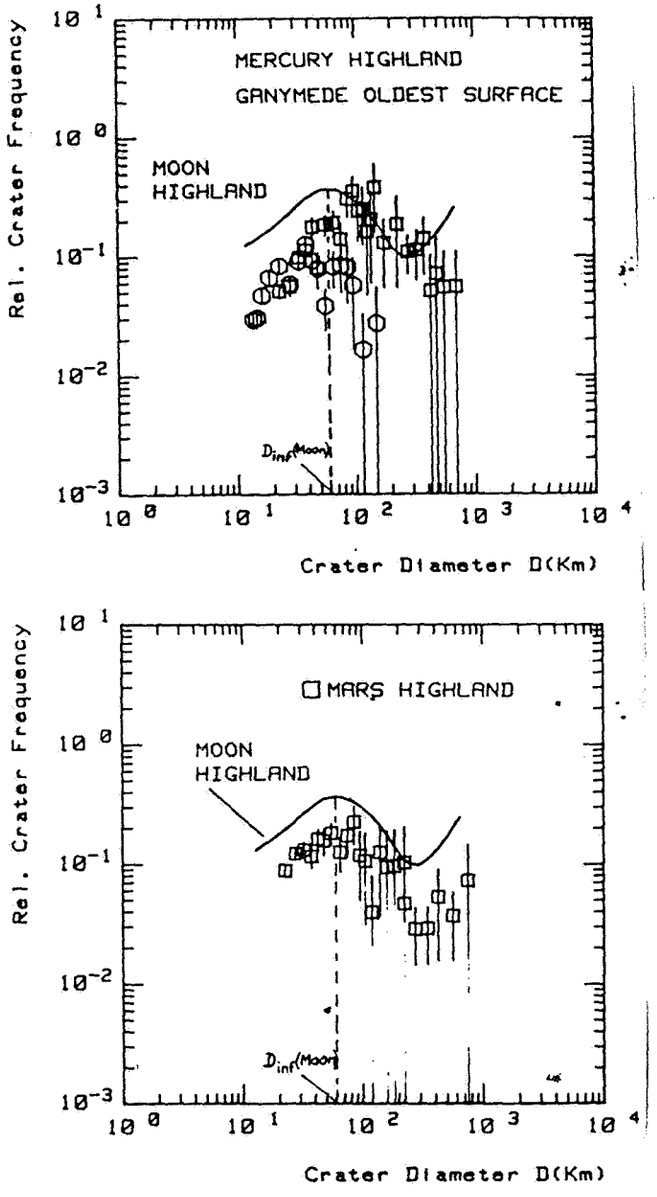

Figure 62. A comparison of the crater populations of the oldest regions of the Earth's Moon, Mars, Mercury and the Jupiter moon, Ganymede, in the form of their relative frequency distributions. The distributions show very similar characteristics with inflection of the variation in the diameter range 40 km<D<100 km (D_{inf}(Moon)=60 km).

of meteorites in this region was the same within the factor 2.

2. The ratio of the frequencies of the oldest highland populations to the corresponding populations of the youngest basins (for any diameter, since the corresponding standard distributions are used) amounts to a factor 7 to 14, that is, in the case of all the studied planets, the ages of the oldest highland regions are identical within about 100 million years (assuming the same decrease of the impact rate).

The situation regarding the great similarity of the bombardment discussed previously individually for the terrestrial planets is clearly verified by these numbers. There is a remarkable similarity in the impact rates of the terrestrial planets. The differences in the inflection crater sizes and in the production distributions of the terrestrial planets may be explained by differences in the impact velocities and in the properties of the target material. But it is not clear whether the impact conditions allow a shift of the inflection diameter to smaller values. This appears to be true possibly only for crater producing bodies in planetocentric orbits (Neukum, 1982). These relationships will be discussed below. /146

TABLE 6. OBSERVED CRATER FREQUENCIES OF THE OLDEST CRATERS OF THE YOUNGEST BASINS AND THE RATIO OF THESE FREQUENCIES /146

Planet	Inflection Daimeter D_{inf} (km)	Relative Crater Frequency am Inflection Diameter (Moon = 1) for	
		Oldest Crater population (High land)	Youngest Basins
Mercury	1oo	0.9	0.5
Moon	60	1.0	1.0
Mars	50	0.6	1.3
Ganymede	40	0.3	0.8
Callisto	~30	0.6	
Rhea	~15	0.6	

	Cumulative crater frequency of the youngest basin with regard to Earth's Moon		Ratio of the crater frequencies between oldest highland and youngest basins for each individual planet.
	D=1km	D=10km	
Mercury	3.1	1.2	7
Moon	1.0	1.0	14
Mars	0.3	1.5	10
Ganymede	0.2	0.5	8

IX.2. Relationship Between Crater Size and Projectile Energy (Scaling Laws)

Between the crater diameter D and the impact energy E there are complicated relationships, which so far it has been impossible to grasp fully either experimentally or theoretically. The uncertainty of the results often exceeds one order of magnitude (compare Figure 63). The most important concrete relationships (scaling laws) between E and D (where D varies e.g. between 1 and 10^8 cm) are described below briefly.

In a totally inelastic collision between two bodies of mass m (projectile) and M (target) with the impact velocity V_i, the kinetic energy

$$E = m \cdot M \cdot V_i^2 / 2(m+M) \qquad (1)$$

is converted into other energy forms (Kittel et al., 1973).

If m<<M, as is basically the case in collisions in the Solar System (for example, meteorite-Earth), equation (1) may be written as

$$E \simeq m \cdot V_i^2 / 2 \qquad (2)$$

that is, practically the entire kinetic energy of the impact is converted.

For craters in silicate target material (rock) according to Gault et al. (1975) and Croft (1977), the kinetic energy of the collision may be divided into five parts (CGS units): /148

1) The part is converted directly into heat, where

$$E_h = k_1 \cdot f(V_i) \qquad (3);$$

k_1=const and $f(V_i)$ is a function of the impact velocity V_i. For $V_i \gtrsim 15$ km/s in the rock, $E_h \approx E/3$.

2) The crushing energy is:

$$E_c = k_2 \cdot D^{3-\alpha\delta} \qquad (4);$$

D designates the crater diameter, $k_2 \approx 10^9$ and $3-\alpha\delta \approx 2.7$.

3) Deformation energy

$$E_d = k_3 \cdot D^3, \quad (k_3 \approx 10^7), \qquad (5);$$

4) Ejection energy

$$E_e = g \cdot k_4 \cdot D^4 \qquad (6),$$

where $10^{-1} \lesssim k_4 \lesssim 10^4$ and $g=GM/R^2$ is the surface gravitation (G is the gravitation constant, M is the mass of the target, R is the target radius).

5) Seismic energy

$$E_S = k_5 \cdot E, \quad (k_5 \approx 10^{-4} - 10^{-5}) \qquad (7).$$

In general E_S is negligible as compared with the other forms of energy.

The energy conservation law for the collision is now /149

$$E = k_1 \cdot f \cdot (V_i) + k_2 \cdot D^{3-\alpha\delta} + k_3 \cdot D^3 + k_4 \cdot g \cdot D^4 + k_5 \cdot E \qquad (8).$$

The terms which contain the kinetic energy $E=m \cdot V_i^2/2$ of the projectiles are grouped on the left hand side, so that

$$F(E) = k_2 \cdot D^{3-\alpha\delta} + k_3 \cdot D^3 + k_4 \cdot g \cdot D^4 \qquad (9),$$

where

$$F(E) = E - k_1 \cdot f \cdot (V_i) - k_5 \cdot E \qquad (10).$$

We have $k_2 >> k_3 >> k_4$, so that for craters smaller than 10 m, equation (9) becomes approximately

$$D \sim (F(E))^{1/(3-\alpha\delta)}, \quad (D \lesssim 10 \text{ m}) \qquad (11)$$

For larger craters ($\gtrsim$1 km) the term in D^4 predominates, so that

$$D \sim g^{-1/4} (F(E))^{1/4}, \quad (D \gtrsim 1\text{km}) \qquad (12).$$

The middle term in equation (9) may predominate for diameters between 10 m and 1 km. In this case we have

$$D \sim (F(E))^{1/3}, \quad (10 \text{ m} \lesssim D \lesssim 1 \text{ km}) \qquad (13).$$

Equations (11) to (13) indicate different scaling possibilities of D as a function of the kinetic impact energy, with exponents between 1/3 and 1/4.

According to Melosh (1980) one of the more realistic crater scaling laws is that of Gault (1974). It is based on impact experimental craters of nuclear bomb explosions. Written in CGS units, it is

$$D = 2.96 \cdot 10^{-2} \rho_p^{1/6} \cdot \rho_t^{-1/2} (\sin\theta)^{1/3} (g_M/g)^{3/16}; \quad (14) \qquad /150$$

ρ_p and ρ_t indicate the density of the projectile and the target, respectively and θ is the angle between the impact velocity and the target surface ($\theta=45°$); g_M/g is the ratio between the surface

gravitation of the Moon and the corresponding target planet.

The factor (g_M/g) is not contained originally in the Gault formula. The exponent 3/16 was formed as the average between 1/4 and 1/8, because according to Chabai (1977) it is not possible in the present stage of the research to differentiate between the two exponents; these exponents may be derived from dimension considerations (compare Holsapple and Schmidt, 1982). The experimental value 1/6 found by Gault and Wedekind (1977) is close to 3/16. Even the crater which was left behind by the Moon Probe Ranger-VIII on the Moon indicates a scaling exponent of the gravitation between 1/4 and 3/16 (Baldwin, 1968).

Other scaling laws, which give the crater diameter D as a function of the impact energy E are those of Dence et al. (1977)

$$D = 1.90 \cdot 10^{-3} E^{0.333} \cdot (g_E/g)^{3/16} \text{ for } D < 2.4\ 10^5 \text{ cm and} \qquad (15).$$
$$D = 1.71 \cdot 10^{-2} E^{0.294} \cdot (g_E/g)^{3/16} \text{ for } D > 2.4\ 10^5 \text{ cm}$$

(g_E/g) is here the ratio between the surface gravitation of the Earth and that of the target. Unfortunately Dence et al. (1977) indicate no dependence on density, so that equation (15) is valid mainly for the surface rocks of bodies similar to the Earth.

The formula of Shoemaker (1979) is, except for a deviation of 5%, the same as that of Dence et al. (1977):

$$D = 1.63 \cdot 10^{-2} E^{0.294} (g_E/g)^{3/16} \text{ for } D \gtrsim 3 \cdot 10^5 \text{ cm} \qquad (16). \qquad \underline{/151}$$

Croft (1977) choses the logarithmic form to represent the (E,D) dependence.

$$D = 2.53\ (E/\rho_t \cdot g)^{0.25}, \quad (D < 10 \text{ km for the Moon.}) \qquad (17)$$

$$\log D = (\log(2E/3\rho_t \cdot g) - 19.08 + 21.47\ R^{-0.58} - 1.88\ R^{-0.62})/$$
$$/(3.51 - 21.80\ R^{-0.62}) + 5, \quad (D > 10 \text{ km for the Moon}), \qquad (18)$$

All values are given in CGS units, except for the target planet radius R, which must be given in km. The curvature effect of the planet surface, which is represented by the R terms, is in most cases negligible, so that equation (18) is converted into

$$D \simeq 0.327\ (E/\rho_t \cdot g)^{0.285} \qquad (19).$$

The three crater scaling laws (equations (14), (15), (17), (18)) are shown graphically in Figure 63 for the Moon with a target velocity V_i=10 km/s and $\rho_p=\rho_t$=3 gcm^{-3} for the terrestrial planets

(continuous lines), and $\rho_p=\rho_t=1$ gcm^{-3} for the ice covered satellites of the large planets (interrupted lines).

Numerical calculations by O'Keefe and Ahrens (1982) suggest that the collision of an ice ball of density 1 gcm^{-3} with an anorthositic target ($\rho_t=2.94$ gcm^{-3}) takes place in a similar manner as the collision between rocks. Unfortunately, so far there are only a few experiments on formation between craters and ice, mostly for low energies (<10^{12} erg) and low velocities (<6 km/s). The target bodies were partly cooled to temperatures up to 80K, to simulate the environmental conditions of the ice satellites of Jupiter and Saturn. An analysis of the experiments by Pohl (1982) gives us most important results: 1) the craters in ice are similar to the craters in sand and solid rock. 2) The dependence of the dimensions (for example, diameter D) on the energy of the projectile is likewise similar ($D\sim E^{1/3.4}$). /152
3) The diameter in ice is for the same energy (<10 ergs) on the projectile 3 to 4 times greater than in solid silicate rock.

The interrupted lines in Figure 63 for $\rho_p=\rho_t=1$ gcm^{-3} may therefore be at least qualitatively correct. Unfortunately the uncertainties are very great; the difference between the different (E,D) scaling laws is almost one order of magnitude.

It seems that the relationship of Croft (1977) tends to overestimate the crater diameter. According to the Croft dependence law, even bodies of 10^{20} g or about 10^{-6} Moon masses should be sufficient to form the largest Moon basins observed (for example, Mare Imbrium); it seems improbable that the maximum distance between the Moon mass and the largest observed Moon meteorites is so large. Wetherill (1981) gives 10^{21}--10^{22} g for the Imbrium meteorites, while Safronov (1969) derives from the slopes of the planetary rotation axes mass values for the largest meteorites occurring of 10^{-2}--10^{-4} of the mass of the target planet.

The dependence of (D/d) as a function of the projectile diameter d ($m=\pi \cdot \rho_p \cdot d^3/6$) according to equation (16) is shown in Figure 64. The impact velocities used in the calculation $V_i=14.1$ km/s for the Moon and $V_i=17.8$ km/s for the Earth corresponds to average impact velocities of bodies which are in orbits similar to those of the Apollo and Amor asteroids, with eccentricities e=0.6 (Chapter IX.3). This relationship between the crater diameter D and projectile diameter d represents the basis of the conversion of asteroid diameters observed in the telescope into crater diameters (compare Chapters IV and V).

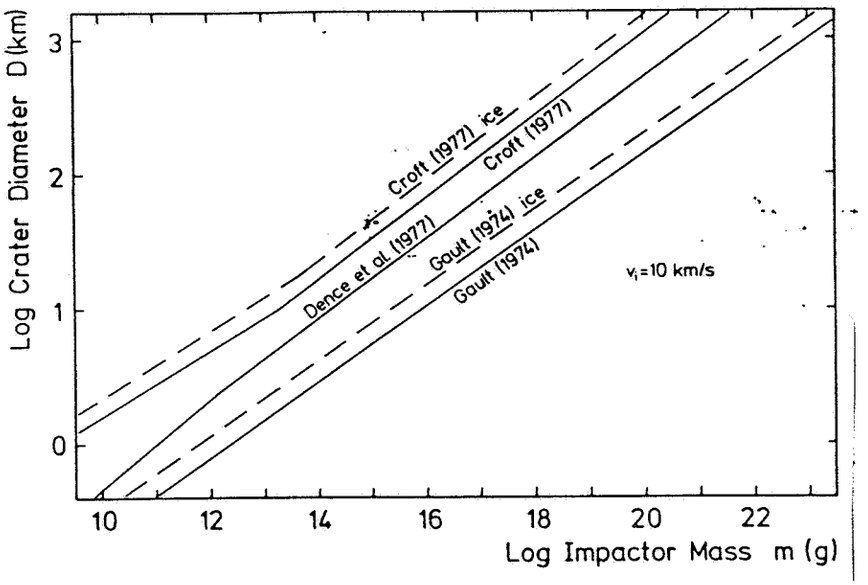

Figure 63. Crater diameter D as a function of the projectile mass m for the scaling laws from equations (14), (15), (17), (18) for the density 3 g/cm^3 (continuous lines) and density 1 g/cm^3 (dashed line).

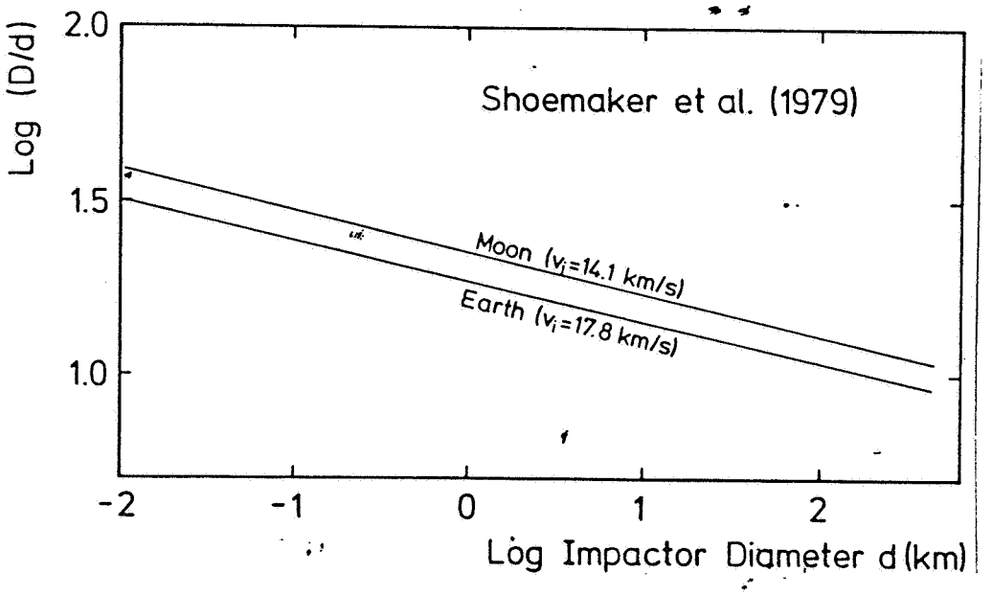

Figure 64. Ratio (D/d) of crater diameter to projectile diameter as a function of the projectile diameter d for heliocentric projectile orbits of the eccentricity e=0.6 (V_i= impact velocity).

IX.3. Characteristic Velocities of the the Crater Producing Meteorite Populations and Their Average Lifetime

We discuss below the observations made on crater populations and the general relationship of the theoretically possible mass and velocity distributions and survival times of meteorite populations with certain plausible orbit characteristics. In this connection, we will discuss individually the question as to whether the oldest crater populations of the terrestrial planets and the satellites of Jupiter and Saturn were produced by meteorites in heliocentric or planetocentric orbits. /154

By means of the scaling laws (equations (14), (15), (17), (18)) conclusions can be drawn regarding the mass and velocity distribution of the meteorite populations which caused the observed craters. Because the Croft law (equations (17), (18)) gives most probably much too large crater diameters D, and the formula of Dence et al. (1977) does not contain explicitly the density of target and projectile (equation (15)), there remains for the application to the terrestrial planets (density of surface rocks 3 gcm^{-3}) and Jupiter and Saturn satellites (density of surface materials 1--2 gcm^{-3}) only the Gault law (equation (14)). Naturally the results would not confirm much from each other even if other scaling laws were used, because the exponents of the energy E are similar (0.28 to 0.294) and relative crater frequencies and crater diameters are calculated.

Besides the gravitation sphere (see further on, equation (22)) of the planets and satellites, the larger meteorites decribe Kepler ellipses. The eccentricities are generally assumed to be equal to 0.6. This value corresponds approximately to that of the object similar to the Apollo asteroids and to the observed meteor and meteorite orbits (compare Öpik, 1966). It lies between the value of the eccentricity of the Mars asteroids ($e \approx 0.38$) and that of the long period comets ($e \approx 1$) and should also be relevant for the last stages of the accretion of planets. /155

The relative velocity U between the meteorite and a fictitious particle in the circular orbit around the parent body is very important hereafter, because it can be expressed for the simplest case of the spherically symmetrical distribution of U by means of the eccentricity e (Öpik, 1966):

$$e^2 = 5U^2/3V_c^2 + 2U^4/3V_c^4 \qquad (20).$$

For $e \lesssim 0.6$, the effect of the term $2U^4/3V_c^4$ is less than 10%, so that hereafter the simple relationship

$$e = (5/3)^{1/2} U/V_c \qquad (21)$$

is used. $V_c=(GM_{\odot,D}/\ell p,s)^{1/2}$ indicates the Kepler circular orbit

around the parent body. The radius of the gravitation sphere $s_{p_1}s$ of a planet or a satellite of Mars M_p and M_s is equal to

$$s_{p,s} = \ell_{p,s}(M_{p,s}/2M_{\odot,p})^{1/3} \tag{22}$$

ℓp and ℓs is the distance between Sun and planet or planet satellite, repectively, and $M_\odot$ and M_p the mass of the parent body, that is, the mass of the Sun or the mass of the planet, respectively.

Simple relationships for the average impact velocity may be given on the basis of Laplace two-body approximation for the following three cases (compare Shoemaker and Wolfe, 1982).

1. Collision between heliocentric meteorites and planets.

Let U_∞ be the relative velocity between the meteorite on the edge of the gravitation sphere of the planet and the fictitious particle in the Kepler circular obit. Let U_p be the relative velocity of the planet with eccentricity e_p with regard to the same particle. The relative planet-meteorite velocity on the edge of the gravitation sphere is then /156

$$U_h = (U_\infty^2 + U_p^2 - 2U_\infty U_p \cos\theta)^{1/2} \tag{23}$$

where θ is the angle between the vectors $\vec{U}_\theta$ and $\vec{U}_p$. With an averaging, the $\cos\theta$ is eliminated because of spherical symmetry, and equation (23) is converted into

$$U_h^2 = U_\infty^2 + U_p^2 \tag{24}$$

where $U_\infty = (3/5)^{1/2} e V_c \qquad U_p = (3/5)^{1/2} e_p V_c$.

e and e_p represent the eccentricity of heliocentric orbit of meteorite and planet, respectively. With the two-body approximation there follows then for the impact velocity

$$V_i = (2GM_p/R_p + U_\infty^2 + U_p^2)^{1/2} \tag{25}$$

where R_p is the planet radius.

2. Collision between heliocentric meteorites and satellites of a planet.

The velocity of the meteorite at the average distance ℓ_s from the satellite orbit is according to equation (25)

$$V_s = (2GM_p/\ell_s + U_\infty^2 + U_p^2)^{1/2} \tag{26}$$

The relative velocity with regard to the fictitious circular orbit particle is then similar to equation (23), (24)

$$U_c = (G M_p/\ell_s + V_s^2)^{1/2} \tag{27}$$

and the average relative velocity regarding the satellite orbit with eccentricity e_S is

$$U_h = (U_S^2 + U_C^2)^{1/2} \tag{28}$$

where $U_S=(3/5)^{\frac{1}{2}}e_S V_C$. Finally we obtain the average impact velocity similar to equation (25) as:

$$V_i = (2\ G\ M_S/R_S + U_h^2)^{1/2} = (2\ G\ M_S/R_S + 3\ G\ M_P/\ell_S + U_\infty^2 + U_P^2 + U_S^2)^{1/2} \tag{29}$$

3. Collision between planetocentric meteorites and satellites of a planet. /157

The relative velocity between meteorites and satellites on the edge of the gravitation sphere of the satellite is similarly to equation (23):

$$U_h = (U_\infty^2 + U_S^2)^{1/2} \tag{30},$$

where $U_\infty=(5/3)^{\frac{1}{2}}$ and V_C and e now represent the eccentricity of the meteorite orbit with regard to the satellite. The impact velocity sought is then similarly to equation (25), (29)

$$V_i = (2\ G\ M_S/R_S + U_\infty^2 + U_S^2)^{1/2} \tag{31}$$

Table 7 shows the impact velocities obtained for e=0.6, where the distance between the Moon and Earth was assumed to be equal to the two extreme values (Roche limit at 2.88 Earth radii and present distance). It is found that the (heliocentric) impact velocities on Mercury are larger, and on Mars are smaller than that on the Earth. This would mean according to equation (14) for the same meteorite mass, and assumed identical target densities, correspondingly larger or smaller crater diameters, in qualitative agreement with the empirical finding for the differences in inflection diameters of the distributions (Table 6). But for the Jupiter and Saturn satellites the heliocentric impact velocities obtained would lead to shifts to much larger diameters, especially for the ice-covered surfaces of the satellites (compare Figure 63 and equation (14)). The planetocentric velocities are generally smaller by a factor 3--5 than the corresponding relevant heliocentric ones. In the case of the Jupiter and Saturn satellites, they would lead without taking into account the target density dependences, to a shift of the inflection diameter to smaller diameters for the same mass distribution of the meteorite population. But the target density dependence may partly compensate for this effect.

By means of the Gault relationship (equation (14)) and the velocities given in Table 7, the diameter ratios between craters are formed on the different celestial bodies on one hand and Moon craters on the other (Table 8). For the same meteorite /159

TABLE 7. AVERAGE IMPACT VELOCITIES FOR HELIOCENTRIC AND PLANETOCENTRIC METEORITE ORBITS OF THE ECCENTRICITY e=0.6

/158

Object	V_i (km/s)	
	Heliocentric	Planetocentric
Terrestrial Planets		
Mercury	23.6	-
Earth	17.8	-
Moon Roche Limit	16.2	2.37
Moon Present Value	14.1	2.37
Mars	12.4	-
Jupiter Moons		
Amalthea	46.3	12.3
Io	30.8	8.43
Europa	24.7	6.73
Ganymed	20.0	5.76
Callisto	15.7	4.52
Saturn Moons		
1980 S3	27.8	7.34
Mimas	25.2	6.65
Enceladus	22.3	5.86
Tethys	20.1	5.32
Dione	17.9	4.67
Rhea	15.4	3.99
Hyperion	9.86	2.35
Japetus	7.25	1.63

The average radius for Amalthea is 83 km, for 1980 S3 60 km and for Hyperion 148 km, according to Thomas and Veverka (1982), Smith et al (1982).

mass, crater diameters are obtained which generally at maximum are twice as large as those of the craters on the Moon, except for the internal moons of Jupiter and Saturn, where the craters for heliocentric meterorite orbits should be 3 to 4 times larger for the same meteorite mass.

A comparison of the theoretical data with the empirical data is given in Table 9. The empirically obtained inflection diameters (assuming an equal mass) would require for e=0.6 velocities which would not be totally consistent for other theoretical values. In particular we obtain for Mercury (heliocentric) impact velocities which are higher by a factor 2 than the theoretical values. We cannot exclude the possibility that the empirically obtained value of the inflection diameter of D=100 km for Mercury is too high, since the distribution was not corrected by erosion effect of the destruction of small craters by impact superimposition. In the case of the Earth's Moon, this correction resulted in a corresponding variation of the inflection diameter of 80 km to 60 km. A similar correction for Mercury would give satisfactory consistency with the theoretical values.

In the case of Jupiter and Saturn satellites, the empirically obtained inflection diameter for the same mass (with regard to the inflection diameter of the Earth's Moon) gives through the scaling relationship velocities, which are lower than the theoretical planetocentric values, and are partly below those required by the satellite's own gravitation, determined minimum impact velocities. This would mean that the inflection diameters obtained for the satellites of large planets cannot be referred to the same masses as those of the terrestrial planets, that is, /161
the mass distribution laws of the populations of Jupiter and Saturn system would be different from that of the internal planets. Naturally the uncertainty of the dependence of the scaling of the density (equation (14)), in particular for the existing ice targets, is so large that within these uncertainties the values obtained for assuming identical masses for the inflection diameters both of the internal planets and for the values of Jupiter and Saturn satellites, would be compatible; that is, within the uncertainties of scaling, the characteristic shifts of the inflection diameters both in the internal and in the external Solar System would be compatible with the assumption of the same mass distribution of the crater producing meteorites. This applies for the Jupiter and Saturn system naturally only for the case when the meteorites were in planetocentric orbits. For meteorites in heliocentric orbits, very high impact velocities are obtained, which would lead in shift of the inflection diameter (refer to the Moon) to <u>higher</u> values.

Smith et al. (1979, 1981, 1982) and Shoemaker and Wolfe (1982) attempted to explain the bombardment of Jupiter and Saturn satellites by meteorites in heliocentric orbits. Through the

TABLE 8. DIAMETER RATIO RELATIVE TO THE MOON D/D_{Moon} FOR THE IMPACT VELOCITIES FROM TABLE 7

/160

Object	Moon in Roche Limit		Moon/ Present Value	
	Heliocent.	Planetocent.	Heliocent.	Planetocent.
Mercury	1.05	-	1.14	-
Earth	0.75	-	0.81	-
Mars	0.74	-	0.80	-
Amalthea	4.86	2.30	5.23	2.49
Io	2.02	0.98	2.19	1.06
Europa	1.90	0.92	2.05	0.99
Ganymede	1.65	0.83	1.79	0.89
Callisto	1.51	0.74	1.62	0.81
1980 S3	4.45	2.10	4.79	2.28
Mimas	3.39	1.59	3.68	1.74
Enceladus	2.96	1.39	3.20	1.51
Tethys	2.46	1.16	2.66	1.25
Dione	2.22	1.04	2.39	1.13
Rhea	1.95	0.92	2.10	0.99
Hyperion	2.09	0.94	2.27	1.00
Japetus	1.32	0.58	1.43	0.62

high velocity and high capture cross sections, however, at least the internal satellites of Saturn would have been destroyed several times by such a bombardment and once again undergone accretion, as discussed by Smith et al. (1982). An argument against bodies in the heliocentric orbit is, however, that crater densities of different magnitude of the Moon in different places of its surface would have to found, which is against the observations. This will be discussed below.

The internal satellites of Saturn and Jupiter are in synchronous rotation with regard to the parent body (Smith et al. 1979; 1981; 1982). The dissipation function of the tidal friction for Saturn is $Q \approx 7 \cdot 10^4$ (Goldreich and Soter, 1966) and the maximum duration to produce synchronism, is then (Peale, 1977) /162
10^7 years for Mimas, $6 \cdot 10^7$ years for Tethys, $2.7 \cdot 10^8$ for Dione and 10^9 for Rhea, that is, during the entire bombardment, whose traces we see today, the satellites must have been mainly in synchronous rotation.

In case of synchronous rotation, the apex point of the

TABLE 9. OBSERVED AND THEORETICAL INFLECTION DIAMETERS AS COMPARED WITH THE MOON, ASSUMING THAT THE DIFFERENCES IN THE INFLECTION DIAMETERS CORRESPOND TO DIFFERENCES IN THE VELOCITIES (SAME METEORITE MASS). FOR THE OBSERVED INFLECTION DIAMETER D_{inf} (OBSERVED) THE IMPACT VELOCITIES $V_{i,inf}$ DERIVED FROM THE SHIFT WITH REGARD TO THE MOON ARE INDICATED FOR BODIES WITH ECCENTRICITIES e=0.6 AND e=0.1. $V_{i,min}$ CORRESPONDS TO THE MINIMUM IMPACT VELOCITY CAUSED BY THE PLANETARY BODY'S OWN GRAVITATION

Object	D_{inf} (Observed) (km)	$V_{i,inf}$ (km/s)	$V_{i,min}$ (km/s)	D_{inf} (theor) (km)
		Heliocentric e=0.6		Planetocentric e=0.6
Mercury	100	46.3	4.27	68
Moon	60	14.1	2.37	60
Mars	50	13.4	5.03	48
		Planetocentric e=0.6		Planetocentric e=0.1
Ganymede	40	3.44	2.74	36
Callisto	30	1.97	2.42	35
Rhea	15	0.35	0.66	26

/160

movement of the satellite around the planet must remain approximately constant with regard to the satellite surface. Because of the satellites' own movement around the planet, large differences must occur in the impact rate from heliocentric meteorites at the apex and antiapex point. Thus for long periods of eccentricity e≈1, the ratio between the crater frequencies in the apex and antiapex points on Mimas is 18.3, on Tethys 10.5, on Dione 8.2, and on Rhea 6.1 (Smith et al., 1981; Shoemaker and Wolfe, 1981). These great differences in the crater densities must not be considered, but comparable crater densities (Strom and Woronow, 1982). This represents an additional argument in favor of the bombardment of these satellites by planetocentric bodies; the latter have much lower relative velocities with regard to the satellite than a heliocentric projectile (see Table 7), and therefore the difference in the apex-antiapex cratering is not as striking as for heliocentric projectiles. /162

One problem arising in the interpretation of the crater producing meteorites like those in the planetocentric orbit in the Jupiter and Saturn system is that of the lifetime of these bodies, that is, the question as to whether the observed

cratering of the Moon is consistent with the plausible dependence on time of the impact rates. This relationship will be studied hereafter. The Saturn system is most suitable as the model case for the studies, since here there is a fairly great variation in the distances from the central planet and at the same time, crater frequency data.

To obtain the dependence of time of the bombardment, first the collision probability, that is the average lifetime of the meteorite until a collision with the corresponding planet or satellite had arrived, must be determined. /163

According to Wetherill (1967), the average collision probability between two heavenly bodies with approximately the same semi-axes and eccentricities e_1 and e_2 is:

$$p_c = 3\, s_c^2\, U/2\,\pi^2 \sin i \cdot a^3 \cdot (1-e^2)\,(1-e^2)\cot\alpha \qquad (33)$$

where i is the mutual orbit slope ($\sin i \approx i = U/(3^{1/2}V_c)$) and $\cot\alpha = U\, a^{1/2}/3^{1/2}(GM(1-e^2))^{1/2}$. If as in our case, the target mass M is much larger than the projectile mass, we may write for the collision radius the simple relationship:

$$s_c = R(1+2GM/RU^2)^{1/2} \qquad (34)$$

where R is the target radius and U the relative velocity towards infinity. Even for eccentricities of 0.6, the effect of e_1, e_2 in equation (33) is only 20%.

If the eccentricity terms are disregarded, equation (33) with the indicated relationships will be transformed into

$$p_c = 3\, s_c^2\, GM/2\,\pi^2 a^4 U \qquad (35).$$

The average lifetime of a meteorite is then

$$T_c = 1/p_c = 2\,\pi^2 a^4 U/3 s_c^2\, GM \qquad (36).$$

The average lifetime of heliocentric meteorites with regard to the different planets and planetocentric meteorites with regard to the same satellites is given in Table 10. The short lifetimes of the planetocentric meteorites for the satellites is particularly noteworthy. The possibility of ejection through the large planets was disregarded. /165

The surfaces of the Jupiter and Saturn satellites show just like the Moon, the Earth, Mercury and Mars, crater populations which seem to be of very different age (Smith et al. (1981), so that the accumulation of craters must have occurred during geologically long intervals of time (at least a few hundred billion years). Because of the extremely short lifetime (predominantly $\lesssim 10^4$ year) of planetocentric particles, the observed cratering cannot be explained without further assumptions by

TABLE 10. AVERAGE LIFETIME OF HELIOCENTRIC METEORITES WITH REGARD TO THE PLANET AND OF PLANETOCENTRIC METEORITES WITH REGARD TO THE SATELLITES (e=0.6)

Object	Lifetime of Meteorites (years)
Planets	
Mercury	$6.3\ 10^7$
Venus	$6.8\ 10^7$
Earth	$1.6\ 10^8$
Mars	$3.4\ 10^9$
Jupiter	$7.1\ 10^6$
Saturn	$1.3\ 10^8$
Uranus	$1.2\ 10^{10}$
Satellites	
Moon at present	$6.8\ 10^1$
Amalthea	$3.1\ 10^3$
Io	$1.2\ 10^2$
Europa	$7.9\ 10^2$
Ganymed	$1.2\ 10^3$
Callisto	$9.5\ 10^3$
1980 S3	$5.8\ 10^3$
Mimas	$1.1\ 10^3$
Enceladus	$1.6\ 10^3$
Tethys	$7.7\ 10^2$
Dione	$1.6\ 10^3$
Rhea	$2.8\ 10^3$
Hyperion	$2.8\ 10^6$
Japetus	$2.2\ 10^6$

/164

planetocentric meteorites in the production phase of the regular satellite systems, because (i) the observed crater populations must have occurred during at least several hundred billion years (Smith et al. 1982) and (ii) the regular satellite systems must have formed in many shorter periods of time, if only because of the relatively short lifetime of particles in the region around Jupiter ($7 \cdot 10^6$ years) and Saturn (10^8 years).

On the basis of the argument of the short lifetime, therefore the observed crater populations must have occurred only by the impact of meteorites (comets) in heliocentric orbits. This may have also been the case for the Galileo satellites of Jupiter and the largest Saturn satellites (Rhea, Iapetus); these satellites are too large to be destroyed by comet cores striking against them, as was estimated by Smith et al., (1982) on the basis of the present impact frequencies by meteorites resembling comets.

The smaller satellites of Jupiter and Saturn may have even been destroyed several times by large comet cores (for the Saturn system compare Smith et al., 1982). However, it would be possible for the observed crater populations of the smaller Saturn and Jupiter satellites to have been produced predominantly by planetocentric particles, which were produced by destruction of the parent satellite through a large heliocentric comet. Such /166
a scenario would be supported by the observed crater frequencies on the Saturn satellite. It is apparent from Figure 65 that the theoretically derived crater frequencies for the Saturn satellites (from Table 7) would be much more consistent with the observed cumulative relative crater frequencies in the case of collisions with planetocentric meteorites rather than heliocentric meteorites (comets).

In Figure 67, the theoretical crater frequency standardized to values of Callisto is represented for the internal satellites of Jupiter. The observation data for Io and Europa are not available because of the geological activity of these satellites. The calculated variation of the cumulative crater frequency on Amalthea is about 400 (Figure 67), according to whether the craters are produced by heliocentric particles of eccentricity e=0.6 or by planetocentric particles of eccentricity 0.01. Future more exact observations of the crater frequency on Amalthea (size 270X165X150 km, Thomas and Veverka, 1982) might provide information as to whether the observed impacts on the Jupiter satellites have been caused by heliocentric or planetocentric projectiles. Because of their size the Galileo satellites of Jupiter (Io, Europa, Ganymede, Callisto) are certainly protected to a great extent against destruction, so that at least the craters on the large Jupiter satellites must have been caused by heliocentric particles (comet nuclei).

From the above, it is apparent that the oldest crater populations of the terrestrial planets were produced by bodies

in heliocentric orbits with the same or very similar mass spectrum. In the case of Jupiter satellites, some of the observations have theoretical arguments indicating clearly that the crater producing meteorites here were those with the same or very similar mass spectrum in planetocentric orbit; other arguments again, especially that of the short lifetime of planetocentric populations, are in favor of the bombardment by populations in heliocentric orbits. One solution might be that the bombardment of the Jupiter and Saturn moons took place in such a way that a primary population, whose own contribution is not apparent because of too low numbers, produced secondary meteorites by destruction of smaller satellites of the large planets, and this has given rise to the impression of planetocentric bombardment. /167

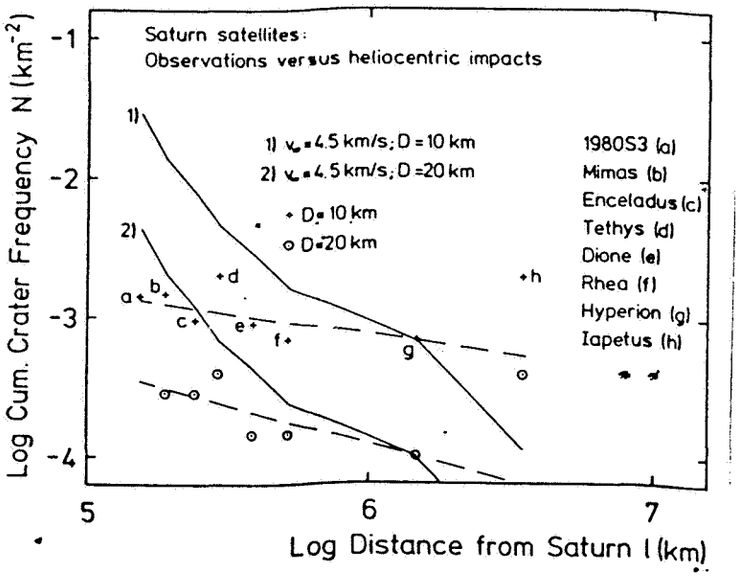

/168

Figure 65. Theoretical cumulative crater frequency N for the Saturn satellites from Table 7 for heliocentric projectiles of eccentricity e=0.6 for crater diameter D=10 km (curve 1) and D=20 km (curve 2). The symbol + corresponds to the observed N for D=10 km, ⊙ corresponds to the observed N for D=20 km.

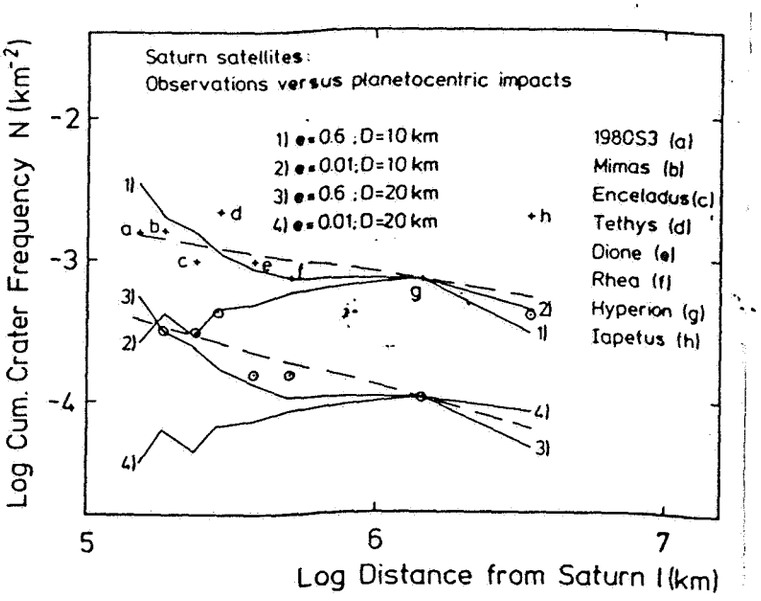

Figure 66. Theoretical crater frequencies as in Figure 65, but for planetocentric particle curves: curve 1 for e=0.6, D=10 km, curve 2 for e=0.1, D=10 km, curve 3 for e=0.6 D=20 km and curve 4 for e=0.01, D=20 km.

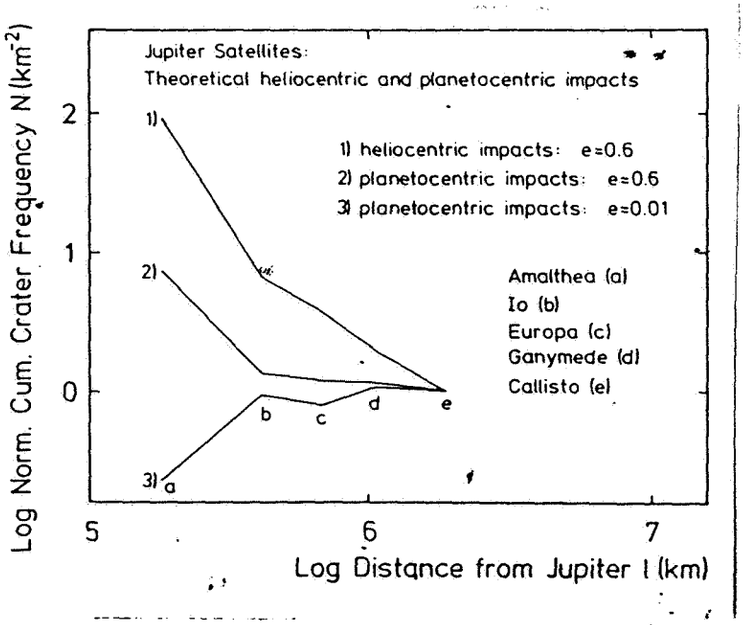

/169

Figure 67. Theoretical cumulative crater frequency for the Jupiter satellites (standardized for the values of Callisto).

X. SUMMARY

In this study for the first time a comprehensive description /170
has been given of the method of dating by measurement of the impact crater frequencies. The method was developed in its modern form in the last 15 years, especially on the basis of the data from the Apollo Moon Missions and the missions to the planet Mars (Mariner-9 and Viking). The improved technology and procedure of the relative and absolute dating was described in detail here. The method now makes it possible to obtain a good relative dating of the surface structures of the Earth's Moon, the planets Mercury and Mars and the moons of Jupiter and Saturn on the basis of photographic analyses. For the Earth's Moon, by correlation of the crater frequencies of the Apollo landing sites with the radiometric ages of the rock samples brought back, a cratering chronology (cumulative crater frequency as a function of age) was obtained for the period between oldest Moon crusts (4.3 to 4.4 billion years) and the present time. This empirical relationship makes it possible to achieve a good absolute dating of any areas of the Moon's surface by crater frequency analyses from photographic data with a time resolution of typically 30 million years for ages >3.5 billion years (because of the exponential dependence of the frequencies of the age) and about 20 to 30% of the age for ages <3.5 billion years (because of the linear dependence of the frequencies on the age).

An important element in the method of dating by crater frequency from photographic data is the recording of crater size distributions of the planetary crater population, in particular, the undisturbed images of the mass and velocity distributions of the meteorites, the production crater size distributions. By means of these distributions it is possible to compare crater frequencies from different diameter regions with regard to a reference diameter. The detailed investigations /171
carried out here for the Earth's Moon, the terrestrial planets Mercury and Mars and the moons of the large planets Jupiter and Saturn showed that:

a) the production crater size distributions cannot be approximated by simple power laws of crater frequencies as a function of the diameter over several orders of magnitude in D, but has a complicated structure:

b) the distributions do not show any apparent dependence on time over the studied diameter ranges 10 m<D<300 km and ages between more than 4 billion years and several hundred million years;

c) for the individual planets different production crater size distributions exist, whose differences, however, can be explained mainly by different impact velocities and different properties of the target material;

d) the crater producing meteorite populations were similar in their mass distribution.

It may be shown in particular that for the populations of the subkilometer craters of the Earth's Moon and the planets Mercury and Mars we are dealing basically not with secondary craters, but primary impact.

A detailed analysis of the crater frequencies of the older populations on the highlands (oldest crusts) of the planets shows that we are dealing with distributions in the production state and not with those in equilibrium between crater destruction and reproduction.

From the lunar crater chronology, it is possible to determine the lunar impact rate as the function of time. It is found that the impact rate in the early period between about 4.3 and 3 billion years ago decreased exponentially with a half life of about 100 million years on the average, but during the period between 3 billion years ago and today, remained on the average constant. Earlier interpretations, suggesting that the impact rate during the past about 600 million years may have been higher than on the average of the last 3 billion years, are not supported. /172

The radiometric age data of the Moon rocks show an accumulation about 4 billion years ago. One interpretation of this accumulation was that at that time there must have been a peak in the impact rate ("terminal cataclysm") with production of most ring basins of the front side of the Moon in the age period between 3.8 and 3.6 billions years (with corresponding impact metamorphoses of the highland rocks at that time). The analysis of the frequency size distributions of large craters and basins (D>20 km) and the stratigraphic data however, are against such a "terminal cataclysm" and in favor of a smooth decrease of the impact rate. The abrupt end of the production of the large basins (D>200 km), which marks a type of time horizon ("marker horizon") is produced by an exponential decrease of the impact rate combined with the special size distribution characteristics of the ring basins, which have a much flatter decrease in the region D>200 km than for smaller craters.

The distribution characteristics of the ring basins on Mars and Mercury are similar to that of the Moon. The observations are such that even on these planets the appearance of ring basins marks a time horizon. The crater frequencies of the younger basins determine the relative age of this "marker horizon". By means of these data and using the crater size distributions empirically determined for the corresponding planets and assuming a dependence of the impact rate on time, which corresponds to the lunar one, cratering chronologies may be derived for the planets Mercury and Mars. These cratering chronologies represent the basis for the determination of absolute age (crater retention age).

The application of the cratering chronology models on crater frequency measurements to different geological units and structures of the planet Mars show that Mars has undergone a very active early phase of geological activity, which was strongly marked by impact processes, but also volcanic and erosive processes. The vast geological activities of Mars, such as extrusion of highland lavas and formation of the northern deep plains (Planitiae) by volcanic processes, the large area erosion by melting of permafrost and by fluvial processes and the buildup of volcanoes in the highland and in the northern deep plains, all these activities took place at a time when the impact rate was still decreasing, that is, at least 1.5 billion years ago. Only the Tharsis region, the youngest large volcano complex with the powerful shield volcanoes, especially Olympus Mons, shows clear geological activity even recently until probably about 100 million years ago. /173

The application of the cratering chronology derived from Mercury shows that Mercury has a very old surface and all the previously studied units have ages of more than 3.85 billion years.

The advantage of determination of age through crater frequency is that a clear relative determination of the age is possible for the Moon, Mars and Mercury, and for the moons of the large planets, with application over the whole planet and the determination of the sequence of events. Moreover, through the empirically obtained relationships between radiometric ages and crater frequency absolute ages of geological units can be determined for the whole of the Earth's Moon with relatively high precision. For planets Mercury and Mars only a rough absolute determination of age (over the entire planet) is possible with uncertainties, which amount to 200 to 300 million years for ages >3.5 billion years; for younger ages the uncertainty is included in the cratering chronology model, and is of the order of a factor 2 to 3. This uncertainty can be possibly greatly reduced by better determination of the recent meteorite bombardments of Mars and Mercury through astronomical observations of the frequencies of the Apollo-Amor asteroids and short period comets and calculation of their impact rates. This seems to be an important object of research for the future, especially because probably the dating through crater frequencies in the next 15 to 20 years will be the only possibility of quantitative determination in time of the evolution of planets; since they cannot count in the immediate future on obtaining rock samples for radiometric dating. /174

The crater populations of the Jupiter and Saturn system show certain similarities in their crater size distribution with those of the internal Solar System. In particular, the populations in the oldest regions show characteristic features in their distributions in the region 50 to 100 km crater diameter. It seems possible that all the crater size distributions, even those of the moons of the large planets, are based on the same mass distribution of the meteorite populations, and the observed differences

are caused by differences in the impact velocities, target properties, surface gravitation etc. This explanation is however only possible for the Jupiter and Saturn systems, if we were dealing not with impact bodies in heliocentric, but in planetocentric orbits. Naturally, it seems difficult on the basis of the low survival times for such bodies to be expected theoretically, to obtain correctly the bombardment of Jupiter and Saturn satellites over several hundred millions of years, as is apparent from the observations. A solution might be that the bombardment of the Jupiter and Saturn moons occurred in such a way that a secondary planetocentric population of objects occurred through the destruction of smaller internal moons by a primary long-lived heliocentric population.

X. BIBLIOGRAPHY /175

Alexander, E. C., Jr., Bates, A., Coscio, M. R., Jr., Draggon, J. C., Murthy, V. R., Pepin, R. O. and Venkatesan, T. R. (1976) K/Ar dating of lunar soils II. Proc. Lunar Sci. Conf. 7th, 625-648.

Alvarez, L. W., Alvarez, W., Asaro F. and Michel, H. V. (1980) Extra-terrestrial cause for cretaceous-tertiary extinction. Science 208, 1095 - 1108.

Arvidson, R., Boyce, J., Chapman, C., Cintala M., Fulchignoni, M., Moore H., Neukum, G., Schultz, P., Soderblom, L., Strom, R., Woronow, A. and Young, R. (1978) Standard techniques for presentation and analysis of crater size-frequency data. Icarus 37, 467 - 474.

Arvidson, R., Drozd, R., Guiness, E., Hohenberg, C., Morgan, C., Morrison, R. and Oberbeck, V. (1976) Cosmic ray exposure ages of Apollo 17 samples and the age of Tycho. Proc. Lunar Sci. Conf. 7th, 2817 - 2832.

Arvidson, R., Goettel, K. A. and Hohenberg, C. M. (1980) A post-Viking view of martian geologic evolution. Rev. Geophys. and Space Phys. 18, 565 - 603.

Baldwin, R. B. (1949) The Face of the Moon. University of Chicago Press, Chicago.

Baldwin, R. B. (1963) The Measure of the Moon. Univ. of Chicago Press, Chicago.

Baldwin, R. B. (1964) Lunar crater counts. Astron. J. 69, 377 - 392.

Baldwin, R. B. (1968) Ranger VIII and gravity scaling of lunar craters. Science 159, 334.

Baldwin, R. B. (1971) On the history of lunar impact cratering: The absolute time scale and the origin of planetesimals. Icarus 14, 36 - 52.

Basaltic Volcanism Study Project (1981) Basaltic Volcanism on the Terrestrial Planets. Pergamon Press, New York, 1286 S.

Binder, A. B. (1974) On the origin of the moon by rotational fission. The Moon 11, 53 - 76.

Boyce, J. M., Dial, A. and Soderblom, L. (1974) Ages of the lunar nearside light plains and maria. Proc. Lunar Sci. Conf. 5th, 11 - 23.

Boyce, J. M. and Roddy, D. J. (1978) Martian rampart craters: Crater processes that may affect diameter-frequency distributions. Reports of Planetary Geology Program, 1977-1978, NASA Tech.Memo., TM 79729, 162 - 165.

Boyce, J. M. (1979) Diameter enlargement effects on crater populations resulting from impact into wet or icy targets. Reports of Planetary Geology Program, 1978-1979, NASA Tech. Memo., TM 80339, 119 - 122.

/176

Brinkmann, R. T. (1966) Lunar crater distribution from Ranger VI photographs. J. Geophys. Res. 71, 340 - 342.

Burghele, A., Dreibus, G., Palme, H., Rammensee, W., Spettel, B., Weckwerth, G. und Wänke, H. (1983) Chemistry of Shergottites and the Shergotty parent body (SPB): Further evidence for the two component model of planet formation. Lunar and Planet. Sci. Conf. XIV (exp. abstract) im Druck.

Cameron, W. S. and Vostreys, R. W. (1982) Data catalog series for space science and application flight missions. NSSDC/WDC-A-R&S 82-21.

Carr, M. H. (1981) The Surface of Mars. Yale Univ. Press, New Haven, London.

Chapman, C. R. and Haefner, R. R. (1967) A critique of methods for analysis of the diameter-frequency relation for craters with special aplication to the moon. J. Geophys. Res. 72; 549 - 557.

Chapman, C. R. (1976) Chronology of terrestrial planet evolution: The evidence from Mercury. Icarus 28, 523 - 536.

Condit, C. D. (1978) Distribution and relations of 4 to 10 km diameter craters to global geologic units of Mars. Icarus 34, 465 - 478.

Croft, S. K. (1977) Energies of formation for ejecta blankets of giant impacts. In D.J. Roddy, R. O. Pepin and R. B. Merrill (editors), Impact and explosion cratering, Pergamon Press, New York, 1279 - 1296.

Croft, S. K., Kieffer, S. W. and Ahrens, T. J. (1979) Low velocity impact craters in ice and permafrost with implications for Martian cratercount ages. NASA Conf. Publ. 2072, 18.

Dence, M. R., Grieve, R. A. F. and Robertson, P. B. (1977) Terrestrial impact structures: Principal characteristics and energy considerations. In D. J. Roddy, R. O. Pepin, and R. B. Merrill (editors), Impact and explosion cratering, Pergamon Press, New York, 247 - 275.

Drozd, R. K., Hohenberg, C. M., Morgan, C. J. and Ralston, C. E. (1974) Cosmic-ray exposure history at the Apollo 16 and other lunar sites: lunar surface dynamics. Geochim. Cosmochim. Acta 38, 1625 - 1642.

Eberhardt, P., Geiss, J., Grögler, J. and Stettler, A. (1973) How old is the crater Copernicus? The Moon 8, 104 - 114.

Fechtig, H., Gentner, W., Hartung, J.B., Nagel, K., Neukum, G., Schneider, E. and Storzer, D. (1975) Microcraters on lunar samples. Proceedings of the Soviet-American Conference on Cosmochemistry of the Moon and the Planets, Moscow, June 4-8, 1974 (in russisch) S. 453 - 472, auch als NASA SP-370 (1977). /177

Gault, D. E. (1970) Saturation and equilibrium conditions for impact cratering on the lunar surface: criteria and implications. Radio Science 5, 273.

Gault, D. E. (1974) Impact cratering. In R. Greeley, and P. Schultz (editors), A primer in lunar geology. NASA Ames, 137 - 175.

Gault, D. E., Guest, J. E., Murray, J. B., Dzurisin, D. and Malin, M. C. (1975) Some comparisons of impact craters on Mercury and the Moon. J. Geophys. Res. 80, 2444 - 2460.

Gault, D. E. and Wedekind, J. A. (1977) Experimental hypervelocity impact into quartz sand - II, Effects of gravitational acceluation. In D. J. Roddy, R. O. Pepin und R. B. Merrill (eds.), Impact and explosion cratering, Pergamon Press, New York, 1231 - 1244.

Gilbert, G. K. (1893) The Moon's face: A study of the origin of its features. Phil. Soc. Wash. Bull., 12, 241 - 292.

Goldreich, P. and Soter, S. (1966) Q in the solar system. Icarus 5, 375 - 389.

Greeley, R. and Gault, D. E. (1970) Precision size-frequency distributions of craters for 12 selected areas of the lunar surface. The Moon 2, 10 - 77.

Greeley, R. and Spudis, P.D. (1981) Volcanism on Mars. Rev. Geophys. and Space Phys. 19, 13 - 41.

Grieve, R. A. F. and Dence, M. (1979) The terrestrial cratering record II. The crater production rate. Icarus 38, 230 - 242.

Grieve, R. A. F. and Robertson, P. B. (1979) The terrestrial cratering record I. Current status of observations. Icarus 38, 212 - 229.

Grudewicz, E. B. (1973) Endogenic cratering distribution on the Moon. Nature 241, 186 - 187.

Grun, E. (1981) Physical and chemical properties of the interplanetary dust--measurements of micrometeorite experiments on helios phases. Thesis to obtain "Habilitation" (qualify as University lecturer, University of Heidelberg.

Guest, J. E. and Greeley, R. (1977) Geology on the Moon. Wykeham Publications, London.

Guiness, E. A. and Arvidson, R. E. (1977) On the constancy of the lunar cratering flux over the past 3.3×10^9 yr. Proc. Lunar Sci. Conf. 8th, 3475 - 3494.

Hartmann, W. K. (1965) Terrestrial and lunar flux of large meteorites in the last two billion years. Icarus 4, 157 - 165. /178

Hartmann, W. K. (1966a) Early lunar cratering. Icarus 5, 406 - 418.

Hartmann, W. K. (1966b) Martian cratering. Icarus 5, 565 - 576.

Hartmann, W. K. and Wood, C. A. (1971) Moon: origin and evolution of multi-ring basins. The Moon 3, 3 - 78.

Hartmann, W. K. (1972) Paleocratering of the Moon. Review of post-Apollo data. Astrophys. Space Sci. 17, 48 - 64.

Hartmann, W. K. (1973a) Ancient lunar mega-regolith and subsurface structure. Icarus 18, 634 - 636.

Hartmann, W. K. (1973b) Martian cratering 4. Mariner 9 initial analysis of cratering chronology. J. Geophys. Res. 78, 4096 - 4116.

Hartmann, W. K. (1977) Relative crater production rates on planets. Icarus 31, 260 - 276.

Hartmann, W. K. (1978) Martian cratering, V. Toward an empirical martian chronology, and its implications. Geophys. Res. Lett. 5, 450 - 452.

Head, J. W., Wood, C. A. and Mutch, T. A. (1977) Geologic evolution of the terrestrial planets. American Scientist 65, 21-29.

Hiller, K. (1979) Mars: Photogeological investigations of the Amenthes and bordering regions. Dissertation, University of Munich.

Hiller, K., Janle, P., Neukum, G., Guest, J. E. and Lopes, R. M. C. (1982) Mars: Stratigraphy and gravimetry of Olympus Mons and its aureole. J. Geophys. Res. 87, 9905 - 9915.

Hörz, F., Brownlee, D. E., Fechtig, H., Hartung, J. B., Morrison, D. A., Neukum, G., Schneider, E., Vedder, J. F. and Fault, D. E. (1974) Lunar microcraters: implications for the micrometeoroid complex. Planet. Space Sci. 23, 151 - 172.

Holsapple, K. A. and Schmidt, R. M. (1982) On the scaling of crater dimensions. 2. Impact processes. J. Geophys. Res. 87, 1849 - 1870.

Howard, K. A. (1973) Avalanche mode of motion - implication from lunar samples. Science 180, 1052 - 1055.

Howard, K. A. and Mühlberger, W. R. (1973) Lunar thrust faults in the Taurus-Littrow region. Apollo 17 Preliminary Science Report, NASA SP-330, 31 - 25.

Hulme, G. (1973) Turbulent lava flow and the formation of lunar sinuous rilles. Mod. Geol. 4, 107 - 117.

Jessberger, E. K., Kirsten, T. and Staudacher, Th. (1977) One rock and many ages - Further K-Ar data on consortium breccia 73215. Proc. Lunar Sci. Conf. 8th, 2567 - 2580. /179

Jessberger, E. K. (1981) Ar-Ar age determination technology: proiciple, development and application in cosmochronology. Thesis to obtain "Habilitation" (qualify as University lecturer), University of Heidelberg.

Kirsten, T. and Horn, P. (1974) Chronology of Taurus-Littrow region-III: ages of mare basalts and highland breccias and some remarks about the interpretation of lunar highland rock ages. Proc. Lunar Sci. Conf. 5th, 1451 - 1475.

Kittel, C., Knight, W. D., and Ruderman, M. A. (1973) Mechanics. McGraw-Hill Book Comp.

König, B. (1977) Study of primary and secondary impact structures of the Moon and laboratory experiments to study the ejection of seconday particles. Dissertation, University of Heidelberg.

Kresak, L. (1980) The flux of earth-crossing and moon-cratering interplanetary bodies. Vortrag, 23. Plenary Meeting, COSPAR, Budapest.

Lucchitta, B. K. and Sanchez, A. G. (1975) Crater studies in the Apollo 17 region. Proc. Lunar Sci. Conf. 6th, 2427 - 2441.

Marcus, A. H. (1964) A stochastic model of the formation and survival of lunar craters, 1. Icarus 3, 460 - 472.

Marcus, A. H. (1966) A stochastic model of the formation and survival of lunar craters, 2. Icarus 5, 165 - 177.

Marcus, A. H. (1970) Comparison of equilibrium size distributions for lunar craters. J. Geophys. Res., 75, 4977 - 4984.

Masursky, H., Eliason, E., Ford, P., McGill, G., Pettengill, H., Schaber, G. and Schubert, G. (1980) Pioneer radar results: altimetry and surface properties. J. Geophys. Res. 85, 8261 - 8270.

Maurer, P., Eberhardt, P., Geiss, J., Grögler, N., Stettler, A., Brown, G. M., Peckett, A. and Krähenbühl, U. (1978) Pre-Imbrian craters and basins: ages, compositions and excavation depths of Apollo 16 breccias. Geochim. Cosmochim. Acta 42, 1687 - 1720.

McElroy, M. B., Kong, T. Y. and Yung, Y. L. (1977) Photochemistry and evolution of Mars' atmosphere: A Viking perspective. J. Geophys. Res., 82, 4379 - 4388.

McGetchin, T. R., Settle, M. and Head, J. W. (1973) Radial thickness variation in impact crater ejecta: implications for lunar basin deposits. Earth Planet. Sci. Lett. 20, 226 - 236.

Meeus, J. and Combes, M. A. (1974) L'Astronomie et Bulletin de la Société Astronomique de France, 88e Année, 194 - 220.

Melosh, H. J. (1980) Cratering mechanics - observational, experimental, and theoretical. Ann. Rev. Earth Planet Sci. 8, 65 - 93. /180

Moore, H. J. (1964) Density of small craters on the Lunar Surface. US Geol. Surv. Astrogeol: Stud. Ann. Proj. Rep., Washington DC., 34 S.

Moore, H. J., Boyce, J. M. and Hahn, D. A. (1980) Small impact craters in the lunar regolith - their morphologies, relative ages and rates of formation. The Moon and the Planets 23, 231 - 252.

Mouginis-Mark, P. (1979) Martian fluidized crater morphology: Variations with crater size, latitude, altitude, and target material. J. Geophys. Res. 84, 8011 - 8022.

Mühlberger, W. R., Batson, R.M., Cernan, E.A., Freeman, V.L., Hait, M.H., Holt, H.E., Howard, K.A., Jackson, E.D., Larson, K.B., Reed, V.S., Rennilson, J.J., Schmitt, H.H., Scott, D.H., Sutton, R.L., Stuart-Alexander, D., Swann, G.A., Trask, N.J., Ulrich, G.E., Wilshire, H.G. and Wolfe, E.W. (1973) Preliminary geologic investigation of the Apollo 17 landing site. Apollo 17, Preliminary Science Report, NASA SP-330.

Mutch, T. A. (1972) Geology of the Moon. Princeton Univ. Press, Princeton, N. J.

Mutch, T. A., Arvidson, R. E., Head, III, J.W., Jones, K. L. and Saunders, R. S. (1976) The geology of Mars. Princeton Univ. Press, Princeton, N. J.

Ness, N.F., Acuna M.H., Lepping, R.P., Burlaga, L.F., Behannon, K.W. and Neubauer, F.M. (1979) Magnetic Field Studies at Jupiter by Voyager 1: Preliminary Results. Science 204, 982-987.

Neukum, G. (1971) Studies of impact craters of the Moon. Dissertation, University of Heidelberg.

Neukum, G. and Dietzel, H. (1971) On the development of the crater population on the moon with time under meteoroid and solar wind bombardment. Earth Planet. Sci. Lett. 12, 59 - 66.

Neukum, G., Hörz, F., Morrison, D. A. and Hartung, J. B. (1973) Crater populations on lunar rocks. Proc. Lunar Sci. Conf. 4th, 3255 - 3276.

Neukum, G. (1975) Cratering in the Earth-Moon system - Some comparison with other terrestrial planets. Proc. International Colloquium of Planetary Geology, Rome (exp. abstracts), 341.

Neukum, G., König, G. and Arkani-Hamed, J. (1975) A study of lunar impact crater size-distributions. The Moon 12, 201 - 229.

Neukum, G. and Horn, P. (1976) Effects of lava flows on lunar crater populations. The Moon 15, 205 - 222.

Neukum, G. and König, B. (1976) Dating of individual lunar craters. Proc. Lunar Sci. Conf. 7th, 2867 - 2881.

Neukum, G. and Wise, D. U. (1976) Mars: A standard crater curve and possible new time scale. Science 194, 1381 - 1387.

Neukum, G. (1977a) Lunar cratering. Phil. Trans. R. Soc. Lond. A. 285, 267 - 272.

Neukum, G. (1977b) Different ages of lunar light plains. The Moon 17, 383 - 393.

Neukum, G., Hiller, K., Henkel, J. and Bodechtel, J. (1978) Mars chronology. Reports of Planetary Geology Program 1977 - 1978, NASA TM 79729, 172 - 174.

Neukum, G. (1981) Surface history of the terrestrial-type planets. Proc. Alpbach Summer School, 1981, ESA SP-164, 129-137.

Neukum, G. and Hiller, K. (1981) Martian ages. J. Geophys. Res. 86, 3097 - 3121.

Neukum, G. and Wilhelms, D. E. (1982) Ancient lunar impact record. Lunar and Planetary Sci. Conf. 13th (exp. abstracts), Houston.

Neukum, G. (1983) Post-accretional cratering. In Vorbereitung.

Nyquist, L. E. (1982) Do oblique impacts produce martian meteorites? Lunar and Planetary Sci. Conf. 13th (exp. abstract), 602 - 603.

Oberbeck, V. R. and Morrison, R. H. (1973) On the formation of the lunar herring-bone pattern. Proc. Lunar Sci. Conf. 4th, 107 - 123.

Oberbeck, V. R., Hörz, F., Morrison, R. H., Quaide, W. L. and Gault, D. E. (1975) On the origin of the lunar smooth plains. The Moon 12, 19 - 54.

Oberbeck, V. R. and Aggarwal, H. (1977) Topographic analysis of lunar secondaries of Copernicus and implications. Proc. Lunar Sci. Conf. 8th, 3521 - 3537.

Öpik, E. J. (1960) The lunar surface as an impact counter. Mon. Not. Roy. Astr. Soc. 120, 404 - 411.

Öpik, E. J. (1966) The stray bodies in the solar system. Part II. The cometary origin of meteorites. Adv. Astron. Astrophys. 4, 301 - 336.

O'Keefe, J. D. and Ahrens, R. J. (1982) Cometary and meteorite swarm impact on planetary surfaces. J. Geophys. Res. 87, 6668-6680.

Peale, S. J. (1977) Rotation histories of the natural satellites. In Planetary Satellites (editor J.A. Burns) Univ. of Arizona Press, 87 - 112.

Peale, S. J., Cassen, P., Reynolds, R. T. ;979) Melting of Io by tidal dissipation. Science 203, 892 - 894. /182

Pike, R. J. (1967) Schroeter's rule and the modification of lunar crater impact morphology. J. Geophys. Res. 72, 2099 - 2106.

Pike, R. J. (1974) Ejecta from large craters on the Moon: Comments on the geometric model of McGetchin et al., 1973. Earth Planet. Sci. Lett. 23, 265 - 274.

Plescia, J. B. and Boyce, J. M. (1982) Crater densities and geological histories of Rhea, Dione, Mimas and Tethys. Nature 295, 285 - 290.

Pohl, J., Stöffler, D., Gall, H. and Ernstson, K. (1977) The Ries impact crater. In Impact and Explosion Cratering, Pergamon Press, New York.

Pohl, J. (1982) Impact crater formation in ice bodies. Lecture held at the DFG symposium "Exploration of the planets Jupiter and Saturn and their environments", Goslar, October 18-22, 1982.

Ringwood, A. E. (1960) Some aspects of the thermal evolution of the Earth. Geochem. Cosmochem. Acta 20, 241 - 249.

Ringwood, A. E. (1979) Origin of the Earth and Moon. Springer Verlag, New York.

Ross, H. P. (1968) A simplified mathematical model for lunar crater erosion. J. Geophys. Res. 73, 1343.

Runcorn, S. K. (1977) Early melting of the Moon. Proc. Lunar Sci. Conf. 8th, 463- 469.

Ryder, G. and Spudis, P. (1980) Volcanic rocks in the lunar highlands. Proc. Conf. Lunar Highlands Crust, 353 - 375.

Safronov, V. S. (1969) Evolution of the protoplanetary cloud and formation of the Earth and of the planets. Moscow, Nauka Press.

Shoemaker, E. M. (1965) Preliminary analysis of the fine structure of Mare Cognitum. JPL-TR-32-700, 75 S.

Shoemaker, E. M., Hackman, R. and Eggleton, R. (1962) Interplanetary correlation of geologic time. Advan. Astronaut. Sci. 8, 70 - 89.

Shoemaker, E. M. and Hackman, R. J. (1962) Stratigraphic basis for a lunar time scale. In Kopal and Mikhailov (editors), The Moon, Academic Press, London.

Shoemaker, E. M. (1963) Impact mechanics at Meteor Crater, Arizona. In The Moon, Meteorites, and Comets, Univ. of Chicago Press, Chicago.

Shoemaker, E. M. (1970) Origin of fragmental debris on the lunar surface and the history of bombardment of the Moon. Vortrag auf I Seminario de Geologia Lunar, Universität Barcelona, Mai 1970 (Rev. Januar 1971). /183

Shoemaker, E. M., Hait, M. H., Swann, G.A., Schleicher, D.L., Dahlem, D.H., Schaber, G.G. and Sutton, R. L. (1970a) Lunar regolith at Tranquillity Base. Science 167, 452.

Shoemaker, E. M., Batson, R. M., Bean, A. L., Conrad Jr., C., Dahlem, D. H., Goddard, E. N., Hart, M. H., Larson, K.B., Schaber, G. G., Schleicher, D. L., Sutton, R. L., Swann, G. A. and Waters, A. C. (1970b) Preliminary geologic investigation of the Apollo 12 landing site, Part A. Geology of the Apollo 12 landing site, Apollo 12 Preliminary Science Report NASA SP 235.

Shoemaker, E. M. (1977) Astronomically observable crater-forming projectiles. In Impact and Explosion Cratering (D.J. Roddy, R.O. Pepin und R.B. Merrill, eds.) 617 - 628, Pergamon, N.Y.

Shoemaker, E. M., Williams, J. G., Helin, E. F. and Wolfe, R. F. (1979) Earth-crossing asteroids: orbital classes, collision rates with Earth, and origin. In T. Gehrels (editor), Asteroids, University of Arizona Press, 253 - 282.

Shoemaker, E. M. and Wolfe, R. F. (1982) Cratering time scales for the galilean satellites. In D. Morrison (editor), Satellites of Jupiter, University of Arizona Press, 277 - 339.

Silver, L. T. (1971) U-Th-Pb isotopic systems in Apollo 11 and 12 regolith materials and a possible age for the Copernicus event. EOS (Trans.Am.Geophys. Union) 52, 534.

Smith, B. A., Soderblom, L.A., Beebe, R., Boyce, J., Briggs, G., Carr, M., Collings, S.A., Cook II, A.F., Danielson, G.E., Davies, M.E., Hunt, G.E., Ingersoll, A., Johnson, T.V., Masursky, H., McCauley, J., Morrison, D., Owen, T., Sagan, C., Shoemaker, E.M., Strom, R., Suomi, V.E. nd Veverka, J. (1979) The Galilean satellites and Jupiter: Voyager 2 imaging science results. Science 206, 927 - 950.

Smith, B. A., Soderblom, L.A., Beebe, R., Boyce, J., Briggs, G., Bunker, A., Collins, S.A., Hansen, C.J., Johnson, T.V., Mitchell, J.L., Terrile, R.J., Carr, M., Cook II, A.F., Cuzzi, J., Pollack, J.B., Danielson, G.E., Ingersoll, A., Davies, M.E., Hunt, G.E., Masursky, H., Shoemaker, E., Morrison, D., Owen, T., Sagan, C., Veverka, J., Strom, R., Suomi, V.E. (1981) Encounter with Saturn: Voyager 1 imaging science results. Science 212, 163 - 190.

Smith, B. A., Soderblom, L.A., Batson, R., Brdiges, P., Inge, J., Masursky, H., Shoemaker, E., Beebe, R., Boyce, J., Briggs, G., Bunker, A., Collins, S.A., Hansen, C. J., Johnson, T. V., Mitchell, J. L., Terrile, R. J., Cook II., A. F., Cuzzi, J., Pollack, J. B., Danielson, G. E., Ingersoll, A. P., Davies, M. E., Hunt, G. E., Morrison, D., Owen, T., Sagan, C., Veverka, J., Strom, R., Suomi, V.E., (1982) A new look at the Saturn system: The Voyager 2 images. Science, 215, 504 - 537.

Soderblom, L. A. (1970) A model for lunar impact erosion applied to the lunar surface. J. Geophys. Res. 75, 2655 - 2661. /184

Soderblom, L. A. and Boyce, J. M. (1972) Relative ages of some near-side and far-side terra plains based on Apollo 16 metric photography. Apollo 16 Preliminary Science Report, NASA Spec. Publ. SP-315, 29-3-29-6.

Soderblom, L. A., Condit, C. D., West, R. A., Herman, B. M. and Kreidler, T. J. (1974) Martian planetwide crater distributions: Implications for geologic history and surface processes. Icarus 22, 239 - 263.

Soderblom, L. A. (1977) Historical variations in the density and distribution of impacting debris in the inner solar system: Evidence from planetary imaging. In Impact and Explosion Cratering, Pergamon, New York, 629 - 633.

Solomon, S. C. and Chaiken, J. (1976) Thermal expansion and thermal stress in the moon and terrestrial planets: Clues to early thermal history. Proc. Lunar Sci. Conf., 7th, 3229 - 3243.

Solomon, S.C. and Head, J. W. (1982) Mechanisms for lithospheric heat transport on Venus: Implications for tectonic style and volcanism. J. Geophys. Res. 87, 9236 - 9246.

Schaber, G. G. (1973) Lava flows in Mare Imbrium: geologic evidence from Apollo orbital photography. Proc. Lunar Sci. Conf. 4th, 73 - 92.

Schaber, G. G. and Boyce, J. M. (1977) Probable distribution of large impact basins on Venus: Comparison with Mercury and the Moon. In Impact and Explosion Cratering, Pergamon Press, New York.

Schaeffer, O.A., Husain, L. and Schaeffer, G. A. (1976) Ages of highland rocks: the chronology of lunar basin formation revisited. Proc. Lunar Sci. Conf. 7th, 2067 - 2092.

Stöffler, D., Knöll, H.-D. and Maerz, U. (1979) Terrestrial and lunar impact breccias and the classification of lunar highland rocks. Proc. Lunar and Planet. Sci. Conf. 10th, Pergamon Press, New York.

Stöffler, D. (1981) Cratering mechanics: Data from terrestrial and experimental craters and implications for the Apollo 16 site. Lunar and Planetary Inst. LPI TR81-81, 132 - 141.

Strom, R. G. (1971) Lunar mare ridges, rings and volcanic complexes. Mod. Geol. 2, 133 - 157.

Strom, R. G. and Whitaker, E. A. (1976) Populations of impacting bodies in the inner solar system. NASA TX-3346.

Strom, R. G. (1977) Origin and relative age of lunar and mercurian inter-crater plains. Phys. Earth Planet. Inter. 15, 156-172.

Strom, R. G. (1979) Mercury: a post-Mariner 10 assessment. Space Sci. Rev. 24, 3 - 70.

Strom, R. G., Woronow, A. and Gurnis, M. (1981) Crater populations on Ganymede and Callisto. J. Geophys. Res. 86, 8659-8674. /185

Strom, R. G. and Woronow, A. (1982) Solar system cratering populations. Lunar and Planetary Sci. Conf. 13th (exp. abstr.) 782 - 783.

Taylor, S. R. (1975) Lunar Science: A Post-Apollo View. Pergamon Press, New York.

Taylor, S. R. (1982) Planetary Science: A Lunar Perspective. Lunar and Planetary Institute, Houston.

Tera, F. and Wasserburg, G. J. (1974) U-Th-Pb systematics on lunar rocks and inferences about lunar evolution and the age of the Moon. Proc. Lunar Sci. Conf. 5th, 1571 - 1599.

Tera, F., Papanastassiou, D. A. and Wasserburg, G. J. (1974) Isotopic evidence for a terminal lunar cataclysm. Earth Planet. Sci. Lett. 22, 1- 21.

Thomas, P. and Veverka, J. (1982) Amalthea. In D. Morrison (ed.), Satellites of Jupiter, University of Arizona Press, 147 - 173.

Trask, N. J. (1966) Size and spatial distribution of craters estimated from Ranger photographs. Jet Propul. Lab. Tech. Rep. 32-700, Pasadena, Cal., 252 S.

Turner, G. (1977) Potassium argon chronology of the Moon. Phys. Chem. Earth 10, 145 - 195.

Wänke, H. (1981) Constitution of terrestrial planets. Phil. Trans. R. Soc. Lond. A. 303, 287 - 302.

Wänke, H., Dreibus, G., Palme, H., Rammensee, W. and Weckwerth, G. (1983) Geochemical evidence for the formation of the Moon from material of the Earth's mantle. Lunar and Planetary Sci. Conf. 14th (im Druck).

Walker, E. H. (1967) Statistics of impact crater accumulation on the lunar surface exposed to a distribution of impacting bodies. Icarus 7, 233 - 243.

Wegener, A. (1920) Experiments on the accumulation theory of Moon craters. Nova Acta Abh. d. Leop. Carol. Deutsch. Akad. d. Naturf. 106, 107-117.

Wegener, A. (1921) Production of Moon craters. H. 55d. Collection of Vieweg Questions on Topics in Science and Technology. Fried. Vieweg u. Sohn, Braunschweig, 48 pp.

Wetherill, G. W. (1967) Collisions in the asteroid belt. J. Geophys. Res., 72, 2429- 2444.

Wetherill, G. W. (1975) Late heavy bombardment of the Moon and terrestrial planets. Proc. Lunar Sci. Conf. 6th, 1539 - 1561.

Wetherill, G. W. (1976) The role of large bodies in the formation of the earth and the moon. Proc. Lunar Sci. Conf. 7th, 3245-3257. /186

Wetherill, G. W. (1981) Nature and origin of basin-forming projectiles. In P. H. Schultz and R. B. Merrill (editors), Multi-ring basins, Proc. Lunar Planet. Sci., 12A, 1- 18.

Wilhelms, D. E. (1976) Secondary impact craters of lunar basins. Proc. Lunar Sci. Conf. 7th, 2883 - 2901.

Wilhelms, D. E., Oberbeck, V. and Aggarwal, H. (1978) Size-frequency distributions of primary and secondary lunar impact craters. Proc. Lunar Planet. Sci. Conf. 9th, 3735 - 3762.

Wilhelms, D. E. (1979) Relative ages of lunar basins. Rep. of Planetary Geol. Prog. 1978 - 1979, NASA TM 80339, 135 - 137.

Wilhelms, D. E. (1983) The geologic history of the Moon. NASA SP, im Druck.

Wise, D. U. (1966) Origin of the Moon by fission. In the Earth - Moon System, Plenum Press, New York.

Wise, D. U., Golombek, M. P. and McGill, G. E. (1979) Tectonic evolution of Mars. J. Geophys. Res. 84, 7934 - 7939.

Wolfe, E. W., Lucchitta, B. K., Reed, V.S., Ulrich, G.E. and Sanchez, A.G. (1975) Geology of the Taurus-Littrow valley floor. Proc. Lunar Sci. Conf. 6th, 2463 - 2482.

Womer, M. B., Greeley, G. and King, J. (1979) Pyroclastic valcanism of the Snake River Plain, Idaho: Implications for Mars. Rep. of Plan. Geology Program 1978 - 1979, NASA TM-80339, 265 - 267.

Wood, J. A., Dickey Jr., J.S., Marvin, U.B. and Powell, B. N. (1970) Lunar anorthosites and a geophysical model of the Moon. Proc. Apollo 11 Lunar Sci. Conf., 965 - 988.

Woronow, A. (1977) Crater saturation and equilibrium: A Monte Carlo simulation. J. Geophys. Res. 82, 2447 - 2451.

Woronow, A. (1978) A general cratering-history model and its implications for the lunar highlands. Icarus 34, 76 - 88.